

# UNCLASSIFIED

AD NUMBER
AD803668
NEW LIMITATION CHANGE
TO Approved for public release, distribution unlimited
FROM Distribution: DoD only: others to Advanced Research Projects Agency, Washington, D. C. 20301. Attn: AGILE
AUTHORITY
DARPA ltr, 20 Nov 2001

THIS PAGE IS UNCLASSIFIED

803668

# **FINAL TECHNICAL REPORT**

## **SAILWING WIND TUNNEL TEST PROGRAM**

### **ARPA ORDER NO. 879**

PROGRAM CODE NO. 6G20(23)

This report supplied by  
Fairchild Hiller Corporation, Hagerstown, Maryland  
in accordance with Contract AF 33(615)-5416

Report No. R540A-002, dated 30 September 1966,  
prepared by Messrs. T.E.Sweeney, R.A.Ormiston,  
and J.E.Mercer with the assistance of Mr. A.Jobst

Each transmittal of this document outside the  
Department of Defense must have prior approval of  
ARPA/ACILE

D D C  
DEC 16 1966  
A



# FOREWORD

The Fairchild Hiller Corporation and Princeton University are deeply appreciative of having had the opportunity to participate with NASA personnel in the full scale wind tunnel testing of the Princeton Sailwing Concept. Particular thanks are extended to the NASA full scale tunnel group, ARPA and the Air Force Systems Command. Without the excellent cooperation of these three groups it would have not been possible to accomplish this happy task.

## TABLE OF CONTENTS

	<u>Page</u>
SUMMARY	11
LIST OF SYMBOLS	1v
I INTRODUCTION	1
II MODELS	6
III INSTRUMENTATION	8
IV TESTS	12
V TEST RESULTS	15
VI AERODYNAMIC ANALYSIS	21
VII COMPARISON OF SAILWING TO OTHER WINGS	34
VIII COMMENTS ON THE SAILWING	39
IX CONCLUSIONS	42
X REFERENCES	45
XI FIGURES	45

### SUMMARY

The results, analysis and conclusions drawn from a full scale wind tunnel investigation of two Sailwings of different aspect ratio are presented. One model is of a complete Sailwing airplane incorporating an aspect ratio 11.5 wing while the other is a wing-alone rig of aspect ratio of 5.92.

Results show both wings to have high values of  $C_L$  max and  $L/D$  max equaling or exceeding comparative values for conventional wings and greatly exceeding other flexible wings insofar as lift/drag ratios are concerned.

Adequate lateral control with low stick forces are shown to exist by means of wing warping. Very high values of stick fixed longitudinal stability are indicated. Stall characteristics are unusually gentle and the initially steep lift curve slope decreases in a gradual manner over a wide range of angles of attack indicating the possibility of smooth normal flight in gusty weather. The dominant aerodynamic characteristics of the wing appears invariant with dynamic pressure for the range of  $q$ 's tested and the repeatability of the test results appears good.

Both lift and pitching moment curves pass through zero lift angles without discontinuity or other adverse effects. Properly rigged sailwings display no serious flutter, luffing or other sail misbehavior at any angle of attack tested. Internal and external structural loads appear to be less than anticipated and easily

within the limits of the simple type structures contemplated for the wing. Dacron Sailcloth seems to be, at least for presently anticipated applications, completely adequate, however little is known of its aging characteristics. Lateral stability for the case of zero dihedral angle appears slightly positive.

# LIST OF SYMBOLS

$C_L$	Lift Coefficient	
$C_D$	Drag Coefficient	
$C_m$	Pitching Moment Coefficient	
$C_l$	Rolling Moment Coefficient	
$C_n$	Yawing Moment Coefficient	
$C_Y$	Side Force Coefficient	
$L/D$	Lift/Drag ratio	
R.N.	Reynolds number	
$q$	Dynamic pressure	(lbs/ft <sup>2</sup> )
$\alpha$	Angle of attack	(Degrees)
$\beta$	Sideslip angle	(Degrees)
$\Gamma$	Dihedral angle	(Degrees)
$\delta_r$	Rudder angle	(Degrees)
$\delta_e$	Elevator angle	(Degrees)
$\delta_a$	Aileron angle	(Degrees)
$\delta_{aR}$	Right aileron angle	(Degrees)
$\delta_{aL}$	Left aileron angle	(Degrees)
$C_{m\alpha}$	$dC_m/d\alpha$	
$C_{l\alpha}$	$dC_l/d\alpha$	
$C_{l\delta_a}$	$dC_l/d\delta_a$	
$C_{l\beta}$	$dC_l/d\beta$	

# LIST C. SYMBOLS (continued)

$\dot{C}_{lp}$	Lateral Damping Derivative	
$\psi_{b/RV}$	Wing Tip Helix angle in roll	
$e$	Airplane efficiency factor	
$mac$	Mean Aerodynamic chord	(ft.)
$a_w$	Initial Slope of the lift curve	
$C_{HA}$	Aileron hinge moment Coefficient	
$C_{DT}$	Drag strut tension Coefficient	$\frac{\text{Force}}{qS}$
$C_{LT}$	Lift Strut tension Coefficient	$\frac{\text{Force}}{qS}$
$C_{Bi}$	Inboard Bridle tension Coefficient	$\frac{\text{Force}}{qS}$
$C_{Bc}$	Center Bridle tension Coefficient	$\frac{\text{Force}}{qS}$
$C_{ms}$	Spar Bending Moment Coefficient	$\frac{\text{Moment}}{qS(mac)}$ (sub number refers to spar station)
$C_{Rm}$	Spar Root moment (torque) Coefficient	$\frac{\text{Torque}}{qS(mac)}$
$C_{AL}$	Spar Root Lift Coefficient	$\frac{\text{Force}}{qS}$
$C_{RD}$	Spar Root Drag Coefficient	$\frac{\text{Force}}{qS}$
$C_{RC}$	Spar Root Compression Coefficient	$\frac{\text{Force}}{qS}$
$C_{Tt}$	Trailing edge Tension Coefficient	$\frac{\text{Force}}{qS}$
$C_{Tx}$	Trailing edge x - component Coefficient	$\frac{\text{Force}}{qS}$
$C_{Tz}$	Trailing edge z - component Coefficient	$\frac{\text{Force}}{qS}$



## 1 INTRODUCTION

### A. General Background

The Princeton Sailing while old in concept (approximately fifteen years) is rather new insofar as relatively little of its behavior has been thoroughly understood. Recent experiments conducted in the full scale wind tunnel at the NASA Langley Research Center have, however, revealed a considerable amount of new information about this highly unconventional wing - particularly so in regard to the limits of its performance and stability characteristics.

Early work at Princeton University was necessarily confined to the examination of only discreet portions of the device's overall performance and many deductions were made based upon these findings and upon theoretical predictions of the behavior of an optimized sailing. The work for many years, while a serious scientific pursuit, was confined to a "hobby" status and was, during this stage, completely unsupported financially.

In 1959 as part of the Princeton-TRECOM ALART Research program a modest amount of sponsored work was begun with the wing. In subsequent years Princeton University, and more recently Fairchild-Hiller, sponsorship has made it possible for a small group of graduate students to participate in a team effort (and also on an individual basis) to systematically study the sailing's many special characteristics. The work has been both

experimental and theoretical and has not been widely published. While on two occasions there have been magazine articles reporting the progress of the work, every effort has been made over the years to avoid publicity of any type. This has been done because the extreme structural simplicity of the sailwing might prematurely excite the interest of the amateur constructor to attempt to fly with a device not thoroughly understood even by its originators.

#### B. Technical Background

The Princeton Sailwing is, in concept, a single spar leading edge with a rigid tip and a wire cable trailing edge. About this structure a "double sheeted" sail is wrapped and laced to the trailing edge cable. The sail is designed to have a catenary curve along the trailing edge so that when tautly laced to the cable a chordwise tension is produced in the sail. This is schematically shown in Figure 1. Also shown in Figure 1 are typical loaded and unloaded profiles of the sailwing. The device is described in some detail in Reference 1. This Reference also points out some of the unique characteristics of the sailwing as understood at the time of publication and covers some of the subtleties associated with the techniques of rigging the wing.

Following the initial work reported in Reference 1 it was decided to undertake an analysis of the catenary and trailing edge tensions required to produce, as closely as possible, an elliptical span lift distribution. Reference 2 reports

this work and Reference 3 extends and refines the work of Reference 2. During this period experiments with a free flight sailing glider and small scale wind tunnel tests showed close agreement with theory insofar as the deformations of the wing under load are concerned. The wind tunnel work pointed out for the first time some of the unique lift and stability characteristics of the device. A photograph of this first free flight model (Sailwing I) of 12 feet in span is shown in Figure 2.

Following this work it was decided that realistic experiments could only be conducted if the model were near full scale. This decision was based upon the difficulty of scaling the flexible properties of the sail and to some extent the errors introduced by "out of scale" porosity of the sail. For this reason Sailwing II was constructed (see Figure 3). This is a 30 ft. span craft capable of carrying a pilot on runway skimming flights. A great deal of practical experience was accumulated with this towed glider - particularly in its later configurations which resulted in Sailwings IV and V. However, prior to these subsequent modifications Sailwing III was constructed. There were two purposes for this machine: First, its configuration was closely akin to the minimum airplane as previously designed by the Princeton group and it was felt that the translation of this design into hardware would provide a background toward the goal of a truly useful minimum aircraft. The second reason for Sailwing III was to gain some flight experience with a control-

lable sailwing. Although much had been learned from flights of Sailwing II, adequate lateral control had not been achieved. Rather than hold up other important studies and possibilities of application of the wing it was decided to equip Sailwing III with more or less conventional ailerons. This was accomplished by making the inboard two thirds of the span a sailwing with the outboard sections of conventional construction. This craft is shown in Figure 4. It will be noted that it is also a single place machine powered with a 45 HP Nelson engine. The span of this craft is 24 feet and its performance and control proved to be most satisfactory. It possesses a true STOL capability and continues to exist as a valuable research airplane. It was, however, not a true sailwing by virtue of the conventional tips and ailerons.

During this period a parallel program was undertaken aimed at optimizing the performance of the sailwing. The approach was both experimental and theoretical and was essentially aimed at combining the span camber distribution with the span angle of attack distribution to yield an elliptical span lift distribution. An intensive two-dimensional wind tunnel study was a vital part of this work in that it provided a basis for an analytical integration of sectional data into the three-dimensional wing. This work is reported in Reference 2. An extension of this research looking into the effect of a multipoint bridle system on the L/D of the optimized sailwing is reported in Reference 3.

As a result of many lateral control experiments conducted with the Sailwing II glider (and also as a result of a rigorous analysis of several systems) it was decided to modify the craft to include a wing warping system for control and to power the machine to eliminate the need for a tow vehicle and the accompanying hazards. This resulted in Sailwing IV shown in Figure 5. More than seventy-five flights were made during this program each one an experiment looking into one or another obscure point of lateral control and stability. This work is reported in Reference 4. Following the successful completion of the lateral control program the craft was immediately re-instrumented for a series of performance flight tests. Of particular interest was the maximum values of L/D attainable in free flight, (see Reference 5). At the conclusion of this program more than two hundred flights had been made with the airplane yielding valuable experiences in addition to the measurements made.

Very fortunately for the sailwing effort some interest in the device was displayed by ARPA, NASA Langley Research Center, and AFSC. This led to an agreement between those organizations and the Fairchild-Hiller Corporation (with Princeton University technical support) to examine in as much detail as possible the over-all performance, stability and control envelope of the concept in the full scale wind tunnel at Langley Field. The most recent flight article (Sailwing IV) was chosen as the basis for the wind tunnel model and substantial modifications were

made to the craft for this purpose. The resulting airplane designated Sailwing V is shown in Figure 6. It will be noted that the major modifications occurred to the fuselage in an effort to reduce the high values of tare drag associated with the very aerodynamically "dirty" Sailwing IV fuselage.

Sailwing VI was also constructed for testing in the full scale tunnel during the same program (it is shown pictorially in Figure 7). The reasons for this model are two-fold: of first consideration was the interest in determining the lateral stability characteristics of the sailwing alone without the substantial influence of a fuselage. The second reason for Sailwing VI was to obtain performance data on a more realistic planform and a much more simple spar configuration. It was felt that the work would be of more general interest, particularly regarding future applications of the device, if an aspect ratio 6 wing were tested in addition to the high aspect ratio wing on Sailwing V. It was also thought that a simple tubular spar with a leading edge fairing would be more compatible to the structural simplicity of the concept than the more elaborate and costly tapered D-spar of Sailwing V. Thus Sailwing VI was designed to have an aspect ratio of 6 and was equipped with the simple spar.

## II MODELS

### A. Sailwing V

This model was of a complete airplane and was evolved from the Sailwing IV flight article as previously described. A three

view drawing of the craft is shown in Figure 8. The longitudinal and directional stability and control features of the airplane were completely conventional as will be noted from the drawing. In the modifications for the wind tunnel tests, however, the rudder was fixed at  $\delta_r = 0^\circ$  and the gap between the rudder and fin completely sealed. Lateral control was achieved by wing warping (i.e. - hinged tips) which was, during the wind tunnel tests remotely accomplished by means of an electric actuator within the model. A similar arrangement was used to operate the elevators. Pertinent dimensions, areas and other significant aerodynamic parameters are shown tabulated below. In addition, Figure 9 schematically shows the spar cross-section and major dimensions of the mean aerodynamic chord.

#### Sailwing V - Physical Characteristics

Fuselage: Conventional steel tube, fabric covered except for the nose fairing which is rigid polyurathane, fabric covered - length = 19.29 ft. including rudder.

Fin and Rudder: Steel tube, fabric covered "slab type" surfaces.

Stabilizer and Elevators: Construction same as fin and rudder  $\delta_e$  range =  $\pm 30^\circ$ .

Wing: Princeton Sailwing type - single D-spar leading edge drooped  $8^\circ$  - rigid, hinged tips - wire cable trailing edge - sail material 4.2 oz. Dacron sailcloth with no additional treatment except paint stripes on starboard wing - span 30.5 ft. - root chord 4.75 ft. - tip chord 1.88 ft. - taper ratio = 0.4 - area =  $81 \text{ ft}^2$  - aspect ratio = 11.5 - section thickness @ mac = 16.5% mac. - mac = 2.66 ft. - wing warping through  $\pm 8^\circ$  at tip - each wing braced with single lift strut and single drag strut and three point bridle system.

## B. Sailwing VI

This model was a "wing alone" apparatus as shown in Figure 10. The wing differs from that used on the complete airplane model in the manner previously described in a general way. One of the differences, the spar design, is shown in Figure 9 while other pertinent dimensions and parameters are tabulated below:

### Sailwing VI - Physical Characteristics

Wing: Type - Princeton Sailwing - single tubular spar with leading edge fairing drooped  $15^\circ$  - rigid tips - wire cable trailing edge - sail material 4.2 oz. Dacron Sailcloth with no additional treatment except paint stripes for contour visualization - Span = 23.30 ft., root chord = 6.0 ft., tip chord = 3.0 ft., taper ratio = 0.5, area = 92 ft.<sup>2</sup>, aspect ratio = 5.92, section thickness @ mac = 9.4% mac - mac = 3.92 ft., each wing braced with single lift strut and single drag cable and fitted with a two point bridle system.

Supporting Frame: This structure was designed to attach the wing and its external rigging to the three point wind tunnel balance system. It consists of tubular aluminium and steel components with wire rigging for stiffening the frame.

## III INSTRUMENTATION

The instrumentation for the tests consisted of the wind tunnel balance, the tunnel "q" manometer, barometer, hygrometer, strain gauge bridges with read out meters, and control surface position indicators; the latter two devices were employed only on Sailwing V tests.

Force measurements were accomplished by recording data from seven scales. Four of the scales were used to measure lift force, two to measure side force, and the remaining one to measure drag force. By measuring the forces in this manner it was possible to



obtain rolling, sawing, and stretching, etc. The scales were mass balanced and had a recording device which stamped the force reading onto a paper tape. The readings were taken at each test point and then averaged.

Tunnel "q" was measured using a probe located in the flow so as to give a representative reading; this probe was connected to a sensitive inclined manometer. Readings were recorded by hand for each scale reading. Also pressure, temperature, and humidity in the test section were recorded for each tunnel "q" using a mercury barometer and a wet and dry bulb hygrometer. Knowing these properties the density and wind speed can be computed.

Strain gauge instrumentation was comprised of 120 ohm, SR - 4, A - 7, Baldwin Lima Hamilton paper gauges with B-4 servo read-out meters. The gauges were arranged in a conventional wheatstone bridge with all gauges matched to within one tenth of an ohm. In this configuration the bridge is temperature compensated thereby eliminating the problem of thermal drift.

Two types of bridges were employed, one with all four gauges acting as active strain elements, the other with two active elements and two purely temperature compensating elements. Where the strain in the material being monitored was a bending moment or a torsion, the former bridge was attached, and the latter for a tension strain. A moment caused two gauges in the bridge to be compressed and the other two to be stretched, but for tension two of the gauges were cemented transverse to the strain so that they

would not be strained. Tension in all four gauges would produce no unbalance in the bridge. Where ever possible bridges were designed to place all gauges under stress to increase the sensitivity of the system.

All the moment bridges were made by cementing two gauges to one side of the beam and the remaining two to the opposite side. The torsion bridge was made by cementing two gauges on the rod at a five degree angle to centerline and the other two at a right angle to the first two. This arrangement places all four gauges under strain when there is torsion on the rod unbalancing the bridge, but when other forces are applied the strains produce no unbalance. Isolation of forces was designed into all bridges so that data reduction would be as simple as possible.

The B-4 servo output instrument supplied the voltage (10v) to the bridge and presented the amount of unbalance on a dial with a servo operated pointer. There was also a counter associated with the dial; the first three digits were read from the counter and the last from the dial. One count corresponded to one millivolt of unbalance; this information is necessary to convert readings back to strain knowing the strain gauge factor. Calibration was used to convert readings to stress.

Control surface deflections were accomplished by means of a remote control panel connected to actuators in the model. Ailerons and the elevator were the only surfaces deflected. Linear potentiometers were connected to the cables at each aileron

and at the push rod to the elevator. The potentiometers were supplied by a regulated power source and connected to sensitive micro-ammeters located on the same panel as the actuator switches. Associated with the meters were potentiometers to adjust meter zero and sensitivity.

Before the tests all bridges and control surface monitors were calibrated. The tension measuring bridges were calibrated by securing one end and hanging weights onto the other. The lift and drag strut, bridle cable trailing edge tension and wing root normal force bridges were calibrated in this manner. Bending moment bridges to measure wing root drag and lift, trailing edge drag and lift, aileron hinge moment, and wing root torsion were calibrated using weights as before and measuring the moment arm.

The spar moment bridges were calibrated by disconnecting the struts, suspending the spar at the ends, and then hanging weights from the strut fittings. By knowing the distances and weights the moment at each bridge can be computed.

All calibration data were plotted to obtain the relationship between the B-4 reading and the force or moment. These data showed the relationship to be linear as expected and also to have very little scatter. Curves were also plotted for the control surface deflections using a propeller protractor. The aileron curves were linear, but the elevator curve was not, due to the attachment of the potentiometer. The data for all three curves were repeatable.

#### IV TESTS

The wind tunnel test program was divided into two major sections: The first of these was the examination of the complete airplane (Sailwing V, aspect ratio 11.5) and the second the investigation of a wing alone (Sailwing VI, aspect ratio = 5.92).

The philosophy of these separate approaches was evolved by consideration of the goals of the program which were first and foremost the determination, within time limitations, of the fundamental characteristics of the sailwing itself. Secondly the characteristics of the sailwing when mated to a fuselage and empennage uniquely suited to the structural requirements of the sailwing. This is not to say that the configuration of the Sailwing V airplane is necessarily the most desirable shape for the sailwing. It does however, offer sufficient fuselage depth for simple, lightweight external bracing and the tail of the fuselage is low enough relative to the wing for effective bridle angles. Such a test program should be and indeed did prove to be, an excellent educational opportunity.

Tests of both models continuously occupied the wind tunnel for two shifts during an entire week. The models had been planned to be as versatile as possible so that only a minimum of "down time" would be required to change configurations for the large number of test runs contemplated. Fifteen separate tests were conducted, many of which required multiple test runs - in some cases as

many as six runs per test. In addition many calibration and tare value runs were made. The range of variables investigated are listed below:

Angle of attack:	-10° to +20°
Dynamic Pressure:	1.66 to 10.03 lbs/ft <sup>2</sup>
Sideslip angles:	-5° , 0° , +5°
Dihedral angles:	0° and +5°
Aileron angles:	-8° through +8°
Elevator angles:	0° and +20°

The systematic pursuit of the effect of these variables resulted in the following tests:

#### A. Aerodynamic Tests

##### Sailwing V

- Test No. 1. Effect of Reynolds number on the Longitudinal Characteristics of the airplane. (Figure 11)
2. Effect of Elevator Deflections of the Longitudinal Characteristics of the airplane (including horizontal tail removed). (Figure 12)
3. Effect of Bridle Wires on the Longitudinal Characteristics of the Airplane. (Figure 13)
4. Longitudinal Characteristics of the Fuselage. (Figure 14)
5. Effect of Sideslip on the Basic Airplane Configuration. (Figure 15)
6. Effect of Dynamic Pressure on Lateral Characteristics with Ailerons Deflected. (Figure 16)
7. Effect of Sideslip on the Lateral Characteristics of the Airplane with Ailerons Deflected. (Figure 17)
8. Aileron Effectiveness on the Lateral Characteristics of the airplane at several angles of attack. (Figure 18)

##### Sailwing VI

- Test No. 1. Effect of dynamic pressure and sideslip on the characteristics of the Wing with 5° Dihedral. (Figure 19)

2. Effect of Dynamic Pressure on the Lateral Characteristics of the Wing with Sideslip for  $5^\circ$  Dihedral. (Figure 20)
3. Effect of R.N. on the Longitudinal Characteristics of the Wing with  $0^\circ$  Dihedral. (Figure 21)
4. Effect of Sideslip on the Characteristics of the wing with  $0^\circ$  Dihedral. (Figure 22)
5. Effect of Dihedral on the Characteristics of the Wing for  $\phi = 0^\circ$ . (Figure 23)
6. Effect of Dihedral on the Characteristics of the Wing for  $\phi = -5^\circ$ . (Figure 24)
7. Effect of Dihedral on the Characteristics of the Wing for  $\phi = 5^\circ$ . (Figure 25)

It is considered to be of substantial importance to point out that early in the Sailwing VI test program an improperly designed fitting on the drag cable partially failed (at the highest test velocity) which resulted in greatly diminished preloads which had been rigged into the wing. Proper cable tensions in the initial rigging stage are necessary to achieve the maximum performance of the Sailwing. By the time that it was discovered that this mis-hap had occurred, considerable testing had already been accomplished. The failure was remedied, however, and some of the best sailwing test data was obtained subsequent to the "fix". The behavior of the wing during the period where rigging tension had been lost is discussed fully in a following section and all the plots affected by this condition are clearly identified in the Figure section of this report.

#### B. Structural Tests

All structural tests were confined to the complete airplane

(Sailwing V) since it was the only one of the two models instrumented with strategically placed strain gage bridges. These tests were made to check the internal loadings assumed to exist in the sailwing and its rigging and to provide a basis for future sailwing structural design.

The following tests were systematically run in parallel with the aerodynamic tests:

1. Drag strut tensions as a function of  $\alpha$  ,  $q$  and  $\phi$
2. Lift strut tensions as a function of  $\alpha$  ,  $q$  and  $\phi$
3. Port wing bending moments (four discreet points) as a function of  $\alpha$  ,  $q$  and  $\phi$
4. Trailing edge cable tensions as a function of  $\alpha$  ,  $q$  , and  $\phi$
5. Trailing edge cable root angles as a function of  $\alpha$  ,  $q$  and  $\phi$
6. Aileron (wing warping) hinge moments as a function of  $\alpha$  ,  $q$  ,  $\phi$  and  $\delta_a$
7. Spar root lift, drag, pitching moment and side force as a function of  $\alpha$  ,  $q$  ,  $\phi$  and  $\delta_a$

A map of the exact location of each strain gage bridge appears in the Figure section and the structural tests are discussed in detail in the next section.

## V TEST RESULTS

### A. Aerodynamic Results

The results of the series of aerodynamic tests with Sailwing

V are shown in graphical form in Figures 11 through 18 while those for Sailing VI are presented in Figures 19 through 25. In the latter group of figures notations have been made to each of the curves affected by the loss in cable tension discussed in the preceding section. These notations are the only changes made in the data as received from NASA and are exclusively confined to those tests of the 5° dihedral angle configuration.

#### B. Structural Test Results

In addition to determining the aerodynamic characteristics of the sailing, the tests revealed some of the more important structural characteristics that must be considered in the design. Data from the tests were first reduced to coefficient form using tunnel "q", model wing area, and mean chord. All data were then plotted using angle of attack as the independent variable and "q" as a parameter. To further discuss the results of the testing, the data are presented for each member of the wing separately. The locations of the individual strain gage bridges are shown in Figure 8.

##### Drag Strut:

Because of a malfunction in either the indicator or the bridge itself considerable scatter appears in the drag strut data - enough so that the results were not directly useable. Drag strut loadings can, however, be extrapolated from the other bridge data. These data are shown in Figure 26. A careful analysis of data and strut locations indicates that for very large negative



angles of attack the force in the drag strut would be tension as it is for positive angles of attack. This change from tension to compression back to tension is a function of the lift strut angle which can be positioned so that the force in the drag strut is always tension for normal operation. If the drag strut were replaced by a cable which cannot support compression then the trailing edge wire would have to support the loads where a strut would be in compression.

#### Lift Strut:

Tension loads in the lift struts exist throughout most of the positive lift region. Near zero lift the loads become compressive due to the drag strut. At the spar location selected for the strut connections the maximum lift strut tension coefficient was slightly over 0.5 for the two "q's" plotted (Figure 27). This member limits the negative loads that the wing is capable of sustaining; if a greater negative load were desired a strut of lower slenderness ratio would be required.

#### Bridle:

The bridle makes it possible to reduce trailing edge wire tension while maintaining high chord-wise tension. As a result, the bridle tensions are greatly affected by both loading and the number of wires. Due to a strain gage bridge malfunction on one bridle cable data on only the center and inboard segments are available. Data from two wires are plotted in Figures 28 and 29. Figure 28 shows the tension coefficient as function of angle

of attack for the inside bridle while Figure 29 shows the tension coefficient for the center bridle with all three wires connected and also with only the center one connected. As can be seen from Figure 29, with only one bridle the tension in that wire is much higher than with all three since the one wire must support the entire load.

From the plots it will also be noted that the inboard bridle sustains higher tensions than the center bridle because the lift is greater toward the wing root. It will further be noted that these two wires maintain approximately the same ratio of tensions throughout the angle of attack range. This would tend to indicate that the lift distribution across the span remains the same and changes only in magnitude even through maximum lift coefficient. Also the regions between  $-40^\circ$  and  $+40^\circ$  on the plots are nearly linear which coincides with the linear region of the lift curve; an indication that the bridle tension is dependent on lift coefficient and again that the lift distribution does not change.

#### Aileron Hinge:

Figures 30, 31 and 32 show the aileron hinge moment coefficient variations as functions of angle of attack, aileron deflection, and dynamic pressure. A static plot of hinge moment versus deflection angle (Figure 33) shows the hysteresis moment due to sliding the sail cloth across the spar. The hinge on the aileron is arranged so that there is virtually no tendency for the trailing wire to be stretched, thus reducing the static forces considerably.

From Figure 32 it can be seen that there is a change in the moment coefficient due to dynamic pressure. A reasonable explanation is that at high speeds the camber of the wing increases slightly tending to produce a higher lift coefficient at high speeds than at low speeds for the same angle of attack. With right stick (left aileron at a high angle of attack) the hinge moment is greater than with left stick; this would tend to confirm the effect due to speed. On one curve the left stick coefficients are higher than these for the right stick. This is probably due to a zero shift after the test began. The shift most likely occurred when the sail oriented itself on the spar.

In general all the hinge moment coefficients were small, meaning light control forces. These small forces mean also that the wing tip structure can be made from light materials and still be adequately strong.

#### Spar Moment:

Data from the four spar bridges are presented in Figures 34 through 38 as functions of angle of attack and station. Plots of the actual moment along the span are shown with the theoretical moment for an elliptical lift distribution assuming various percentages of the total lift to be carried by the spars. The slope of the curve at the origin was obtained from the root lift bridge; and the slope at the tip from the hinge moment bridge. As can be seen, the experimental curve compares favorably with the theoretical one which helps to explain the very high lift to

drag ratios and the close resemblance to hard wing performance.

From these results it is evident that a majority of the lift is carried by the spar. The spar is structurally a better member to carry high loads than the trailing wire since large forces in the latter member would mean that the tip structure would have to be built stronger.

#### Root Forces:

Root lift, drag, compression, and torsion forces are plotted versus angle of attack in Figures 39, 40, 41, 42 and 43. The highest force at the root was due to compression. This was caused by the lift and drag struts mainly, since the trailing wire tension did not change much, as will be seen later. The lift and drag forces remain small, largely because of the location of the struts near the center of lift. If the struts were moved inward the compression force would be reduced but the lift and drag forces would be increased. The root fitting must be designed to match the strut location.

The plots of torsion versus angle of attack and lift coefficient (Figures 42 and 43) show that the torsion moment is small throughout the range. In general for the configuration tested the principle load in the root fitting is from compression in the spar.

#### Trailing Wire:

Data shown in Figures 44, 45 and 46 are for the trailing wire. Throughout the tests the tension changes remained less than the pre-set force of about 160 pounds. The bridges helped considerably

to reduce the tension with one bridle reducing the change to less than half of that with no bridles. The X and Z components of the trailing wire force were very small indicating that the angle that the trailing wire makes with the root did not change more than a few degrees, and that very little of the lift and drag is transmitted through the trailing wire root fitting.

## VI AERODYNAMIC ANALYSIS

The particular feature of the Sailwing responsible for its unique aerodynamic characteristics lies in the use of a flexible member for the lifting surface. A major result of the tests performed is the ability to examine the extent of this influence on the aerodynamics of the Sailwing. The listing in the previous section describing the various tests undertaken in the wind tunnel and the corresponding figures of basic lift, drag, pitching moment and lateral directional characteristics indicate some of the important features of the device. In this section these data will be analysed for additional facts in order to reveal other pertinent points.

For each model tested, the analysis will be roughly divided into three areas, first; consideration of basic performance characteristics, second; longitudinal stability and control, and third; lateral stability. In each case it may be necessary to point out effects which were only the result of the accelerated testing program and would not have existed had more time been available.

#### A. Performance Data

##### 1. Sailwing V

The aerodynamic characteristics of the Sailwing are directly related to the deformation of the lifting surface which itself is the result of both external aerodynamic loads and the internal stress system.

For a rigid subsonic aircraft, and a given propulsion system, the performance can be completely determined from a unique relationship of lift and drag commonly presented in the form of a drag polar. Normally this can be closely approximated by a parabolic variation in drag with lift. The defining properties of this curve are the zero lift drag coefficient and the span efficiency factor,  $e$ . Due to the flexible nature of the Sailwing, such a simple relationship does not exist and lift and drag coefficients become functions of the dynamic pressure. One of the results of the present tests however, indicates that the variation of aerodynamic coefficients with dynamic pressure for the speeds tested and the rigging tensions used is small and in some cases negligible.

For complete accuracy in the use of data dependent on dynamic pressure this effect should be taken into account for consideration of standard aerodynamic characteristics. Lift to drag curves versus angle of attack and static stability characteristics for rigid aircraft are primarily used for level flight conditions, i.e. one g flight. This would be accomplished with the Sailwing data by plotting coefficient data for constant values of dynamic

pressure times lift coefficient. Since, as mentioned, these variations are small, no benefit was to be obtained by such additional calculations for the purpose of carrying out the following analysis.

An attempt was made to determine the span efficiency factor,  $e$ , for the complete airplane. A linearized polar is presented in Figure 47 for the complete airplane at  $q = 3.26$ . Since no linear portion existed an  $e$  could not be computed. However when the large tail and fuselage contributions were subtracted a roughly linear curve resulted. The corresponding span efficiency was approximately 1.3. Although this would be impossibly high for a conventional wing it can be partially explained by the high camber of the sailwing and the resultant high section profile drag at zero lift. As the lift coefficient increases and the airfoil assumes a more ideal contour the drag is seen to decrease to a minimum near a relatively high lift coefficient of .55. Thus the reduction of profile drag partially compensates for the increasing induced drag resulting in an artificially high value of  $e$ . If an ideal induced drag ( $e = 1.0$ ) is subtracted from the wing drag a rough estimate of the minimum profile drag of the wing can be obtained. This value turns out to be approximately  $C_{dp \text{ min}} = 0.009$  occurring at  $C_L = 1.15$ . Since, for highly cambered wings in general, and Sailwings in particular, the linearized drag polar is not linear for a large range of lift coefficients and the minimum drag and drag at zero lift are quite different,

the concept of spanwise efficiency does not appear to be useful. For this reason and also the fact that the horizontal stabilizer drag contribution is difficult to separate from the total drag, values of  $e$  for the other  $q$ 's and the bridle off configuration were not evaluated.

Probably the most important performance parameter for subsonic aircraft is the lift to drag ratio. In Figure 48, the values of  $L/D$  max for the various  $q$ 's tested are plotted. This variation of  $L/D$  max does not appear to reveal any major trends, the maximum deviation being approximately 10% from the average.

A brief look at the effect of the bridle on the wing aerodynamics was had by removing it in two steps at a single value of  $q$ . Although other parameters were more significantly affected, it appears that the reduction in  $L/D$  max using a single point bridle as opposed to a three point type is not large. However, for the bridle off configuration, the degradation of the wing contour produced a more serious decrease even though only about 10%. On this basis it may possibly be concluded that a one or two point bridle represents the best tradeoff between performance and simplicity.

Another important characteristic investigated was the maximum lift capability of the sailwing. Figure 49 shows the variation of  $C_L$  max with  $q$  for Sailwing V. Here it is seen that a uniform increase of  $C_L$  max exists with an increase in  $q$ , amounting to about 10% over the range tested. As would be expected from previous



Sailwing experience the bridle off configurations produced a similar increase in  $C_L$  max.

## 2. Sailwing VI

An attempt was made to evaluate span efficiencies for Sailwing VI and resulted in values of approximately 1.55 at  $q$ 's of 3.29 and 6.86. There appears to be no adequate explanation for these very high values and in fact at higher lift coefficients the total wing drag is considerably less than the minimum induced drag for an elliptical lift distribution. Because of this and since NASA officials emphasize these data are to be considered preliminary, it is felt that the high values of  $L/D$  for Sailwing VI are overly optimistic by a significant amount. Since certain other characteristics of interest are not dependent on absolute values of the data, but rather the general appearance of the curves, useful conclusions therefore can be drawn from Sailwing VI tests. Included in Figure 48 are the values of  $L/D$  max for the range of  $q$ 's tested. It is seen that for the  $5^\circ$  dihedral configuration a large reduction in  $L/D$  occurs with  $q$  but the  $0^\circ$  dihedral configuration is unaffected. The discrepancy here is accounted for in the description of the Sailwing VI tests in part IV. The slackening of the rigging cables appears to have progressed uniformly with increasing dynamic pressure. Its effects are apparent also in the NASA lift and moment data. The angle of attack runs were begun at the lowest angle of attack which was then increased to the stall angle. At the higher  $q$ 's where rigging

tension was lost, the sail was markedly undercambered at the start of the run and reverted to the normal contour only at a fairly high angle of attack.

As this transition occurred rapidly, usually between angle of attack changes, it is readily apparent in the lift and moment curves, and also accounts for the lowered values of L/D. Since the sail rigging was considerably improved when the model was modified to the  $0^\circ$  dihedral configuration these unusual camber changes did not occur and the L/D variation with  $q$  is not significant for the  $q$  range tested. This concurs with the conclusion drawn for the Sailwing V model.

Comparing maximum lift coefficients of Sailwing V and VI in Figure 49 it can be seen that the lower aspect ratio wing is lower by approximately 3%. Indeed, considering the differences in rigging and airfoil shape, this close agreement would not normally be expected. The scatter in the data for Sailwing VI is partly due to loss of rigging tension as explained previously.

## B. Longitudinal Stability

### 1. Sailwing V

Here will be discussed longitudinal stability characteristics of Sailwing V, including lift curve slopes and pitching moment data for various dynamic pressures and the three bridle configurations. Special consideration will also be given to qualitative discussion of various interesting results revealed by the tests.

A well known characteristic of Sailwings is the nonlinear

shape of the lift curve and its relatively high slope. The values given in Figure 50 were computed by constructing the reasonable tangent to the lift curve in the low angle of attack region. The variation with dynamic pressure cannot therefore be taken as too significant. The approximate average lift curve slope is about 25% higher than for a comparable hard wing (Reference 6). The explanation for this effect is that the lift reduction due to local angle of attack reduction is more than compensated for by an increase in camber in that region, as the wing surface deforms under load. More simply stated this means the local section angle of zero lift decreases with increasing wing angle of attack. As the bridle was removed, the loss of its stabilizing effect on the wing deformation caused the increase in lift curve slope also shown in Figure 50.

It must be remarked that lift curves in Figure 11 of the NASA data for six values of dynamic pressure, indicate that very consistent results can be expected from a properly rigged Sailwing model. This was not entirely foreseen considering the flexible nature of the Sailwing's construction.

Another point of particular interest concerns the behavior of the lift curve in the region of zero lift. Apparently the static rigging tensions were sufficient to preclude any sail vibration, or flutter at the trailing edge. In addition no abrupt camber reversal or "luff'ng" occurred in this low lift region. Visual observations indicated that the transition from positive

camber to zero camber at zero lift was gradual and occurred over a wide angle of attack range. Indeed, even at the lowest angle tested,  $-10^{\circ}$ , the camber had not completely reversed. With the bridle removed however, the wing surface was not as well behaved, with reverse camber occurring at the low angles of attack, and its variations becoming more pronounced. Any hysteresis that may have occurred as a result of this condition was not revealed since all runs were made while angle of attack was increased.

The last feature to be noted in connection with the lift curves of the Sailwing V model is the character of the stall. For all  $q$ 's tested, the NASA plots show excellent behavior and no large or abrupt loss of lift even at the highest angles tested.

Basic static stability data for the Sailwing is provided by pitching moment curves of the NASA data. Since the moment reference point and horizontal tail alignment were arbitrary these moments do not indicate absolute trim angles of attack or stability levels. For a rigid airplane, both the lift and pitching moment curves are linear with angle of attack and together define the neutral point of the airplane configuration. For the present tests linear approximations to the moment curves were constructed and static stability levels determined as given in Figure 51. Combined with the linearized estimates, for lift curve slope neutral point locations for the range of dynamic pressures can be determined. These are given in Figure 52. Due to the nature of the calculation these values can be regarded as only estimates and appear

not too dependent on dynamic pressure. The basic sailing characteristic brought out by these results is the very high level of static stability, or  $C_{M\alpha}$ . The tail off tests indicated a contribution to the neutral point location of 41.5% of the mean chord, compared with neutral points at 88% with tail on. This indicates an aerodynamic center location at 46.5% of the mean chord. The mechanism responsible for this rearward aerodynamic center location is the camber change with angle of attack. Probably the most significant result of the pitching moment data is the variation in  $C_m$  with angle of attack, especially in the region of zero lift coefficient. At this point the effect of sail camber changes would be expected to be largest. The lack of any large changes in the moment curves show the sail behavior to be free of any disturbing characteristics. Since, however, the pitching moment curves are nonlinear, the center of gravity position of a complete aircraft would have to be placed such that positive stability existed at all angles of attack.

Since all tests with the Sailing V model except one were made including the horizontal tail installed, the majority of data includes the pitching moment contribution of the tail. It appears from a comparison of tail on and tail off lift curves (at  $q = 3.28$ ) that the tail may have been stalled at low angles of attack. This effect would explain the decrease in  $C_m$  at low angles of attack exhibited by the rounding off in slope of the pitching moment curves (Figure 11).

A last point of interest for the Sailwing V model tests is the effect of bridle removal on the pitching moment curves. No large effect is uncovered by these tests; even though more deformation was indicated by the lift curves and by visual observations.

## 2. Sailwing VI

Many of the above remarks will also apply to the Sailwing VI model tests, though the scope here is not as broad. As the test schedule was set up, only the effect of dynamic pressure on pitching moments was to be investigated. Since the tests for the two dihedral angles were made for differently rigged conditions the effect of an additional variable has been made apparent. Referred to here is the gradual slackening of the rigging as the initial tests progressed upward in dynamic pressure. Re-rigging was accomplished when the dihedral was reduced to zero degrees.

Figure 19 includes lift curves for various dynamic pressures, the deviations at higher values being caused by camber reverting to its normal shape as a result of progressive slackening in the rigging. Included in Figure 50 are approximate values for lift curve slopes. It must be realized that they are representative only - due to the nonlinear nature of the lift curves. At the lower dynamic pressures the stall is somewhat less gentle than for Sailwing V. The effect of re-rigging the model for the zero degree dihedral configuration improved the shape of the lift curves, even at the highest  $q$ . Lift curve slopes are given in Figure 50.

Considerations of pitching stability will be inferred only

from the NASA data plotted in Figures 19 and 21. In each case ( $\Gamma = 0^\circ$ , and  $\Gamma = 50^\circ$ ) there are angles of attack for which the slope of the pitching moment curve is zero and the aerodynamic center is at the quarter chord, in contrast to the results for Sailwing V. In addition, however, at low angles of attack there is a stable portion of the curve indicating aerodynamic centers of approximately 40% and 45% respectively for the poorly rigged and improved conditions. This would be an effective neutral point shift with angle of attack change.

### C. Lateral Stability and Control

#### 1. Sailwing V

Figure 15 shows lateral directional aerodynamics of the complete Sailwing airplane. Since side forces and yawing moments are mainly dependent on fuselage and vertical tail configurations this analysis will concern itself primarily with roll data. This figure includes roll moment data for the complete angle of attack range for two sideslip angles. An immediate characteristic is the increased data scatter compared to the longitudinal data and the roll moment variation with angle of attack for zero sideslip. These two effects must be explained partly because of inherent flexibility of the sailwing, and also unsymmetrical static rigging of the aircraft. Although the dihedral effect is of a stable sense and approximately  $C_{l\beta} = -0.004/\text{deg}$  at most, it is not produced entirely by the wing due to the effect of the fuselage.

Figure 16 includes the effect of dynamic pressure and angle

of attack on roll moments for full aileron control deflection. The effect of dynamic pressure is seen to be small and random, but there exists a large variation with angle of attack. There are two possibilities for this effect. One would be stalling of the wing on the side of the downward deflected aileron, although it would be expected that this effect would not be apparent at low angles of attack. Rather it would occur more abruptly at an angle close to the stall. Another possibility is flexibility of the wing structure and aileron rigging. It must be mentioned that inaccuracies in the aileron hookup and its associated instrumentation did not allow precise determination of aileron deflection and aeroelastic effects during the tests. This somewhat accounts for unequal aileron deflections and asymmetries of the data.

Figure 17 shows that the effects of aileron deflection and sideslip combine in an essentially independent manner. In other words, the data of Figures 15 and 16 taken together are equivalent to Figure 17.

Figure 18 is a plot of aileron effectiveness at three angles of attack. When these data are compared to those of Figure 16, it is seen to yield higher control effectiveness at given angles of attack. The data for these two tests were obtained in two different ways, for the first, the ailerons were run to maximum deflection and not varied during the tests; for the second, Figure 18, the ailerons were adjusted continually during the tests. The difference would be that loss of effectiveness in the second



case would only be the result of spar torsion and deflection of the aileron beam whereas the data for Figure 16 contains the additional effect of cable stretch. It is not possible to estimate these effects quantitatively but only to point out that they exist.

An estimate of the slope of the roll moment curve in Figure 18 yields  $C_{l_{\delta_a}} = 0.25/\text{rad}$  where  $\delta_a$  is here considered the deflection of one aileron. An estimate of roll damping (from Reference 7) is  $C_{l_p} = 0.53$ . Combining these two estimates for an aileron deflection of  $8.15^\circ$  yields for the non-dimensional roll rate parameter  $p b/2v$  a value of 0.0735.

For all the data thus far considered the adverse aileron yaw has been of conventional sign i.e.,  $C_{n_{\delta_a}}$  positive.

As a concluding note on roll performance many possibilities exists for improvement on the existing results. Increasing total deflection and differential rigging would improve roll performance in general and also at higher angles of attack. In addition use "wash-out" would provide increased control at higher angles of attack and even through stall, for an aircraft configuration similar to that tested.

Of considerable importance for a piloted aircraft is an estimate of pilot control forces. The longitudinal axis presents no unusual problems, but the unique wing warping control system indicated the necessity for determining control forces. The results of a single test evaluation are shown in Figure 53 which includes forces corresponding to the aileron control data of

Figure 18. The hinge moment results show that their low level would present no problem for pilot control and are in fact predominantly made up of static friction in the control system for the dynamic pressure tested.

## 2. Sailwing VI

No analysis of the lateral data for the Sailwing VI model will be undertaken, for reasons indicated previously concerning the rigging problems. However, inspection of these data indicates that stable dihedral effect exists for both configuration tested i.e., at  $\Gamma = 5^\circ$  and  $\Gamma = 0^\circ$  although in the latter case it is nearly negligible.

## VII COMPARISON OF THE SAILWING TO OTHER WINGS

Because of the many geometric parameters influencing the aerodynamic behavior of any wing it is most difficult to draw valid comparisons between one wing and another, and even more so when one of the wings is highly unconventional. Since the Sailwing belongs to the same semi-rigid wing family as the Flex-wing and the Parawing, comparisons with these devices are in order. Also to provide a basis for a more absolute evaluation pertinent characteristics of conventional "hard wings" are of interest. For these reasons the two sailwings tested are compared with full scale wind tunnel results of the Flexible Wing Manned Test Vehicle, conventional wings of approximately the same planform as the sailwings and, to be most fair, to the best configuration of the cylindrical Parawing known to the authors.

In addition, the longitudinal stability characteristics of the Sailwing airplane are compared to those of the Navion airplane. The Navion was selected because of the large amount of flight research done with this type at Princeton University and because it is highly respected for its strong longitudinal stability. Comments are included comparing the lateral control characteristics of the Sailwing with those normally accepted as adequate.

#### A. Lift and Drag Comparisons

The results of full scale wind tunnel tests of the Flexible Wing Manned Test Vehicle as reported in Reference 8 is the basis for the comparisons with the Sailwing airplane shown in Figure 54. There are, of course, great differences between the two craft - the Sailwing airplane exhibiting a much higher lift curve slope, a substantially higher maximum lift coefficient and a much greater value of maximum lift/drag ratio than does the flexible wing vehicle. These differences are partially due to the difference in aspect ratio of the two airplanes and partially to the parasite drag differences of the two configurations. In order to make a more valid comparison of the concepts the measured fuselage (and empennage) characteristics were subtracted from those of the total airplane to construct the curves shown in Figure 55. This figure further emphasizes the difference in the lift/drag characteristics of the two wings. While it would not be normally fair to compare two wings of greatly different aspect ratios it is done here because the two concepts are many times considered to be somewhat competitive.

Figures 56 and 57 offer a much more valid indication of the performance potential of the Sailwing in comparison to that of other wings. Figure 56 compares the wing-alone characteristics of Sailwing V with those of a polished metal conventional wing as reported in Reference 6. This conventional wing was selected because its aspect ratio, taper ratio and thickness is approximately similar to those geometric characteristics of Sailwing V. It will be noted that the maximum values of the lift/drag ratios are approximately identical and that the sailwing exhibits a somewhat higher value of maximum lift coefficient. Also, clearly evident, is the characteristically higher lift curve slope of the sailwing. Beginning at  $+1^{\circ}$  angle of attack, however, the Sailwing lift curve slope constantly diminishes through a  $12^{\circ}$  range before maximum  $C_L$  is achieved. The possible ramifications of this are discussed in a later section.

Figure 57 compares the Sailwing VI wing with the cylindrical Parawing (Reference 9) and with a conventional wing of similar geometry (Reference 6). In this comparison all three wings are of approximately the same aspect ratio. The Sailwing appears to have a slightly higher lift curve slope than does the conventional wing. The Parawing on the otherhand has a much lower value of initial slope of the lift curve. All three wings have nearly the same value of maximum lift coefficient - the Parawing being only slightly lower than the other two. Insofar as the maximum values of lift/drag ratios are concerned the Parawing is 25% less than the

conventional wing while the Sailwing appears to be approximately 25% greater than the conventional wing. It is to be remembered, however, that these Sailwing data are, at the present time, considered preliminary by NASA.

#### B. Longitudinal Stability Comparisons

The inherent static longitudinal stability characteristics of the Sailwing are compared to those of the Navion airplane in Figure 58. From an inspection of this figure it is seen that the Sailwing V airplane is somewhat more stable than the Navion Airplane up to  $C_L = 1.0$ . This yields a stick fixed neutral point of 65% for the Sailwing airplane as compared to 55% for the Navion. Above  $C_L = 1.0$  the Sailwing craft has even stronger positive stability characteristics but not so strong as to require more than average proportions of stabilizer and elevator areas to trim to  $C_L$  max. This has been proven by flight tests of the Sailwing IV airplane (Reference 5).

Also shown in Figure 58 is a comparison of the Flexible Wing Manned Test Vehicle longitudinal stability about its center of gravity with those characteristics of the Sailwing airplane about its center of gravity. The plots indicate the same strong static stability mentioned above for the sailwing airplane and in the case of the flexwing an essentially neutral stability is shown.

It will be noted that the stability curves for the Sailwing airplane appearing in Figure 58 are linearized in a manner somewhat different than discussed in the preceding section. This has

been done to yield a more conservative estimate of the longitudinal stability characteristics through a major portion of its flight regime.

### C. Lateral Control Comparisons

In order to compare the Sailwing airplane lateral control characteristics to those traditionally acceptable it was decided to determine the maximum achievable value of  $pb/2v$  for the Sailwing. Figure 18 shows the relationship of  $C_L$  to aileron angle for several values of angle of attack. The straight dashed line shown in this figure is the approximate average of the curves for  $\alpha = 0^\circ$  and  $\alpha = 4.9^\circ$  shifted to account for the  $\delta_p = 0$  rolling moment. This residual moment was undoubtedly caused by asymmetries in the rigging of the system and it appears valid to arbitrarily pass the approximate average curve through zero. Since the craft had a total aileron angle of 16.3 degrees (half up and half down) the extension of the linear average curve to  $\pm 8.15^\circ$  indicates the maximum rolling moment coefficient to be .039. By following conventional procedures (outlined in Reference 7) the lateral damping derivative for Sailwing V was determined to be 0.53 and the resulting value of  $pb/2v$  for full aileron deflection to be .0735. This is slightly in excess of the traditional military requirements for cargo type aircraft which specify a full aileron  $pb/2v$  of .07.

Referring again to Figure 18 it is pointed out that the rolling moment coefficient versus aileron angle curve for  $\alpha = 14.6^\circ$  was not considered in the fairing of the approximate average curve.

This is because  $\alpha = 14.6$  is beyond the stall angle of Sailwing V. It is believed to be valid to assume that the rolling characteristics as deduced above can be maintained up to near the stall before deterioration in roll control occurs. This could be accomplished by removing some of the excess wash-in rigged into the wing.

#### VIII COMMENTS ON THE SAILWING

This report has been written to be as fair and honest an appraisal of the Sailwing as is possible. To do so it has been necessary to restrain a certain amount of natural enthusiasm over a well rigged Sailwing's obvious well behaved and very efficient characteristics. While continuing to recognize the wisdom of cautious optimism it is deemed fair and necessary to emphasize certain sailwing performance and stability characteristics that are of major importance to future applications of the device. These are listed below:

##### A. Nature of the Stall

Over the many years of testing at Princeton University there has never been experienced an abrupt sailwing stall either in the wind tunnel or in free flight. The test results reported upon herein confirm and define these results to a remarkable degree. The gentleness and symmetry of this maneuver is indeed a dominant characteristic of the wing and is an important point in its favor, particularly in the hands of amateur pilots.

#### B. Lift Curve Slope in Vicinity of Stall

As the stall angle is approached and exceeded there is, of course, an increase in drag and therefore in power required for level flight. However, with sufficient power available (probably no more than required for good take-off and climb-out capabilities) normal flight in the region of the stall seems to be a practicable maneuver. Considering the very gradual diminishment of the lift curve slope prior to the stall, and the gentleness of the stall itself if this angle is inadvertently reached, it appears that almost any gust sensitivity is within the pilots ability to select. Thus, in gusty air conditions it would be only necessary to slow the airplane to achieve the desired value of  $CL_{\alpha}$  for smooth flight.

#### C. Longitudinal Stability Considerations

Because of the high degree of longitudinal stability inherent in the Sailwing concept it appears there is only a minimal requirement for the normal stabilizer on the airplane. Because, however, of the need for substantial elevator power to trim to the highest attainable lift coefficient it is suggested that a controllable incidence stabilizer be used instead of a conventional stabilizer and elevator system.

#### D. Lift/Drag Ratio

From the data presented in this report it is obvious that one of the most outstanding aerodynamic characteristics of the wing is the very high values of lift/drag that can be achieved. While even



the "dirtiest" of aircraft can be improved with a good wing it is important to keep in mind that the fullest advantage can be made of the Sailwing by mating it to a relatively "clean fuselage". This does not mean that the fuselage must be sophisticated in either design or construction but it does suggest that reasonable attention to its aerodynamic shape is recommended in the design stage.

#### E. Lateral Control

Both flight test and the wind tunnel results indicate adequate lateral control by means of wing warping. This can be improved by increasing warping angles, reducing "wash-in" and by differential rigging. Alternate schemes are presently being studied which would take advantage of the effect of asymmetric ram air inflation and the use of differential bridle tensions as lateral control devices.

#### F. Flap Effect Possibilities

The bridle system used on Sailwing V while to a significant extent responsible for the "good" behavior of the wing limited  $C_L$  max to approximately 1.5. The same wing used on the Sailwing IV airplane produced a maximum lift coefficient in excess of 2.0 - this however was without a bridle system. Thus, it appears that a controllable bridle tension device would simulate the effect of flaps in increasing maximum lift coefficient.

#### G. Behavior of Sailwing Near Zero Lift

One of the most important results of the wind tunnel results

reported upon herein is the demonstrated ability of the Sailwing to pass through zero lift without displaying any discontinuity in lift, drag or pitching moment. This indicates that the design of a sailwing airplane can be accomplished with no special consideration for these vital characteristics of behavior.

#### IX CONCLUSIONS

From the results of this wind tunnel study it is possible to draw a series of important conclusions, some of which are beyond the original hopes of the Princeton - Fairchild group:

1. Previous findings of high lift curve slopes were confirmed as were the gradual reduction in slope prior to the stall and the excellent behavior through the stall range of angle of attack.

2. Values of  $C_L$  max are generally equal to or higher than those for comparable conventional wings and higher than other flexible wings.

3. Values of  $L/D$  max are equal to or higher than those for conventional wings and significantly greater than those values for other flexible wings of the same aspect ratio.

4. The variation of the significant aerodynamic parameters seems largely independent of dynamic pressure (at least for the range of  $q$ 's tested).

5. Repeatability of test results is excellent.
6. While the bridle appears necessary to achieve performance equal to or better than a conventional wing - the lack of its use causes a much smaller decrement in performance than had been anticipated.
7. The lift curves pass without discontinuity or other adverse results through zero lift in a completely acceptable manner. The same statement can be made for the pitching moment curve.
8. A properly rigged sailwing displays no serious flutter, luffing or other sail misbehavior at any angle of attack tested ( $\alpha - 10^\circ$  through  $\alpha = +20^\circ$ )
9. The non-linear portion of the lift curve appears to be through a range of angles great enough to permit normal flight in gusty weather. This is possible because of the very gradual reduction in slope over a wide range of angles of attack and is also enhanced by the excellent stall characteristics if that angle should be inadvertently exceeded.
10. The Sailwing appears to be exceptionally stable longitudinally. This characteristic would seem to require more elevator power but less stabilizer than normally designed into conventional aircraft. This feature also permits a wider range of c.g. travel than would a conventional wing.
11. Lateral control by means of wing warping seems to be an acceptable method. Adequate values of  $\rho b/2v$  were achieved and these seem easily improvable by greater warp angles, less wash-in and by differential rigging.

12. Structural loads in both the internal and external systems appear to be less than anticipated. There appears to be no reason why a full cantilever sailwing would not only be aerodynamically efficient but structurally so as well.

13. The unusually favorable aerodynamic results of Sailwing VI indicate that the very simple tubular spar with a leading edge fairing is a highly effective method of designing the wing. In fact, the results are such as to lead one to the thought that the leading edge fairing may not be necessary to achieve reasonably high values of L/D.

14. So far as has been experienced, the use of Dacron Sailcloth seems entirely acceptable as far as aerodynamic and structural considerations are concerned. It remains to be seen, however, how the material will age under tension, sunlight and normal useage.

15. Lateral stability for the case of zero dihedral angle appears to be slightly positive.

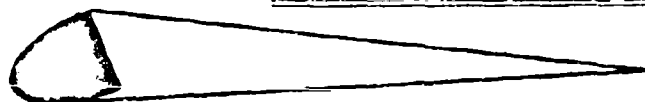
## X REFERENCES

1. Sweeney, T. E., Exploratory Sailwing Research at Princeton, Princeton University Report No. 578, December 1961.
2. Ormiston, R. A., The Effects of Deformation on the Aerodynamic Characteristics of a Sailwing, Princeton University, May 1964.
3. Ormiston, R. A., Additional Studies of the Effects of Deformation on the Aerodynamic Characteristics of a Sailwing, Princeton University Report No. 704, August 1964.
4. Condit, P. M., Lateral Control of the Sailwing, Princeton University Report No. 734, May 1965.
5. Sibert, G. W., A Flight Test Study of the Lift and Drag Characteristics of Sailwing IV, Princeton University Report No. 780, May 1966.
6. Anderson, R. F., The Experimental and Calculated Characteristics of 22 Tapered Wings, NACA Report No. 627, 1938.
7. Perkins & Hage, Airplane Performance Stability and Control.
8. Johnson, J.L., Jr., Hassell, J.L., Jr., Full Scale Wind Tunnel Investigation of a Flexible-Wing Manned Test Vehicle, NASA TN d-1946, August 1963.
9. Bugg, F. M., Effects of Aspect Ratio and Canopy Shape on Low-Speed Aerodynamic Characteristics of 50° Swept Parawings, NASA TN D2922, July 1965.

## XI FIGURES

The figures presented in the following pages are of both NASA and Princeton University origin. Figures 6 and 7 are official NACA photographs. Also Figures 8, 10 and 11 through 25 are NASA supplied data plots. The only changes made to the NASA figures have been the addition of figure numbers to fit the sequence of this report and the clearly identified notations added by the Princeton staff. All other figures originated at Princeton as an aid in interpretation and analysis of the wind tunnel results.

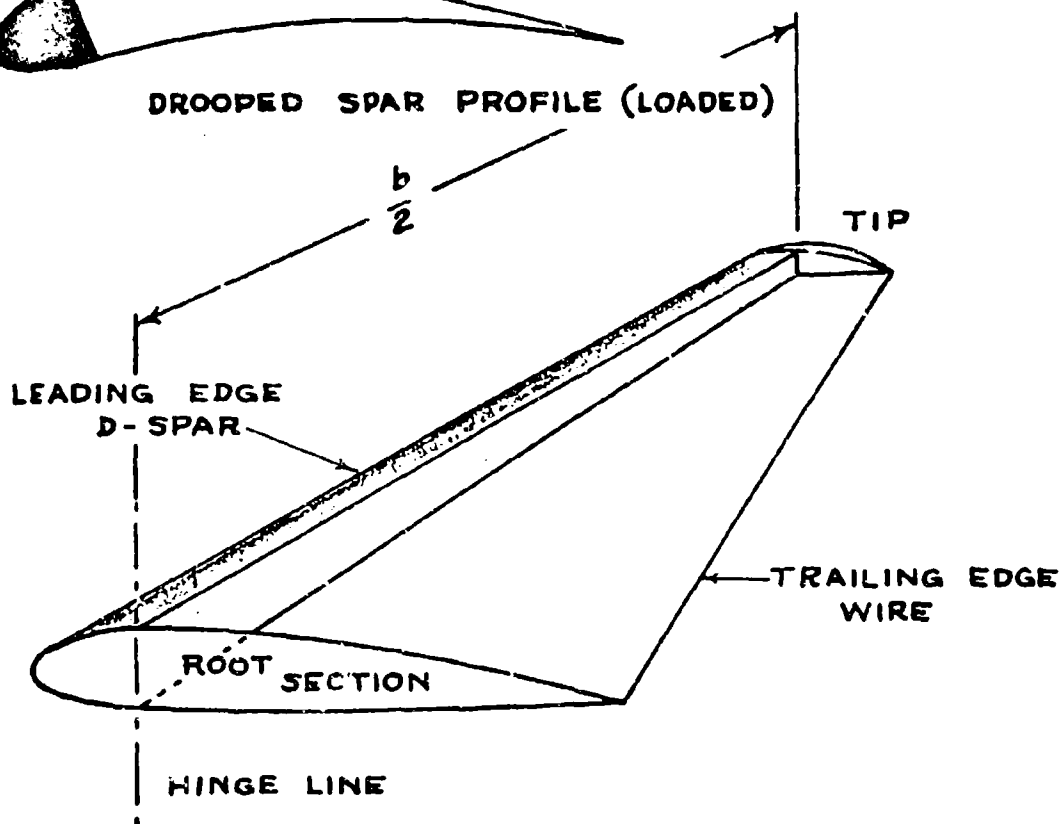
# BASIC SAILWING STRUCTURE



DROOPED SPAR (UNLOADED)

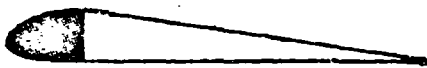


DROOPED SPAR PROFILE (LOADED)

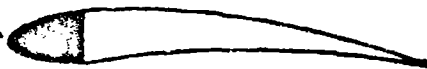


STRUCTURE COVERED TOP AND BOTTOM  
WITH FLEXIBLE CLOTH

TYPICAL  
SECTIONS



UNLOADED  
(AT REST)



LOADED  
(FORWARD  
FLIGHT)

Figure 1 SCHEMATIC REPRESENTATION OF THE SAILWING



Figure 2 SAILWING I - A TWELVE FOOT SPAN FREE FLIGHT MODEL

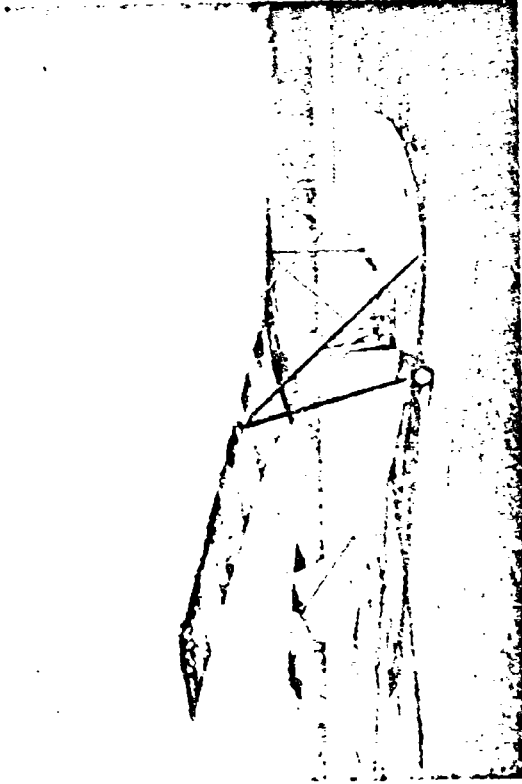
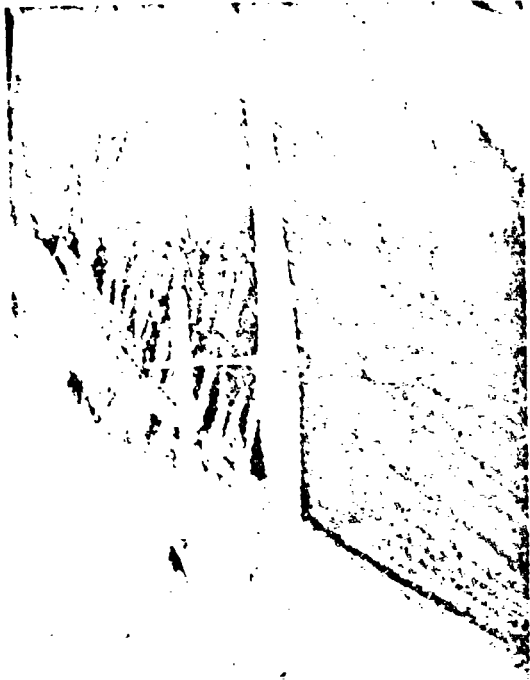
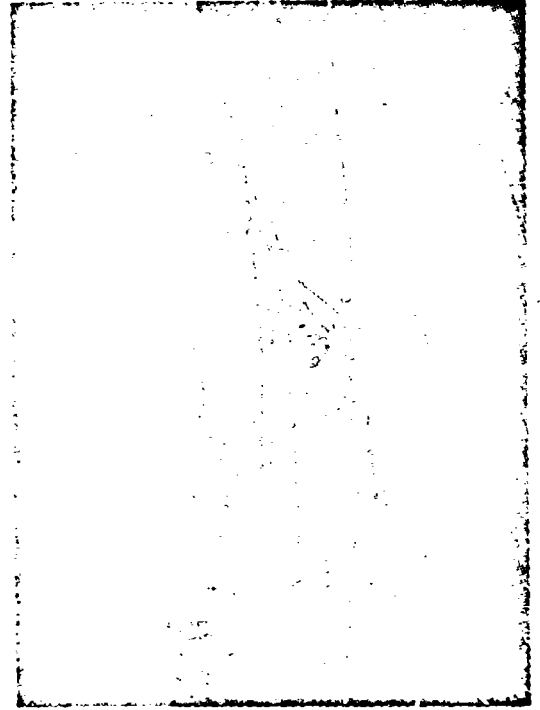


Figure 3 SAILWING II - A THIRTY FOOT SPAN MANNED GLIDER





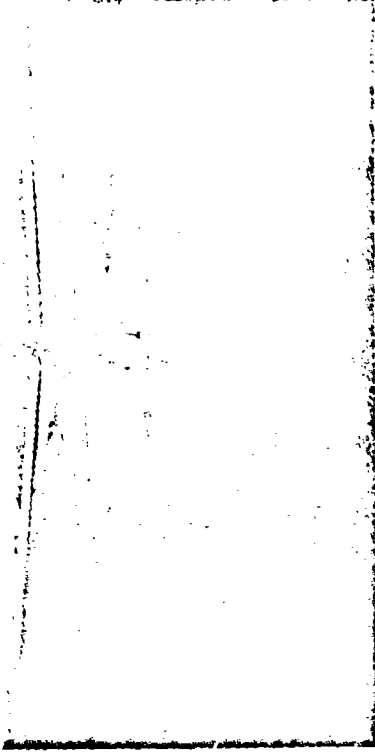
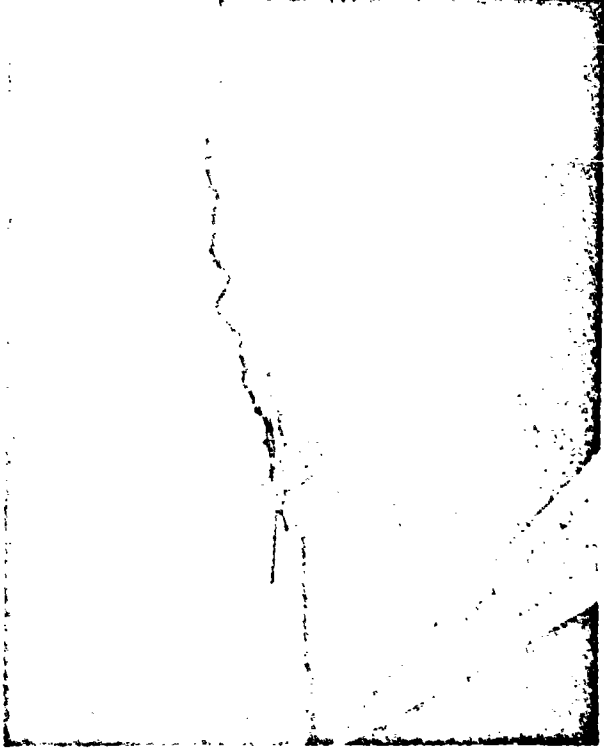
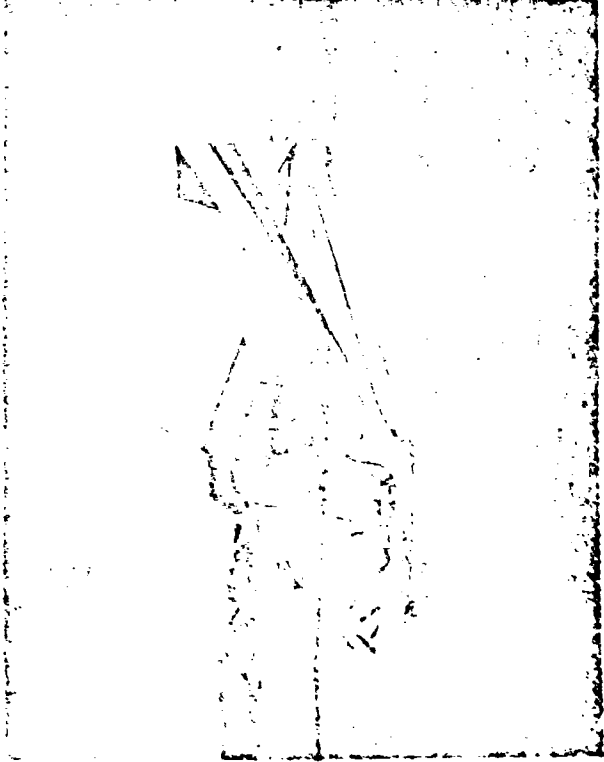


Figure 4 SAILING III - SINGLE PLACE POWERED AIRPLANE



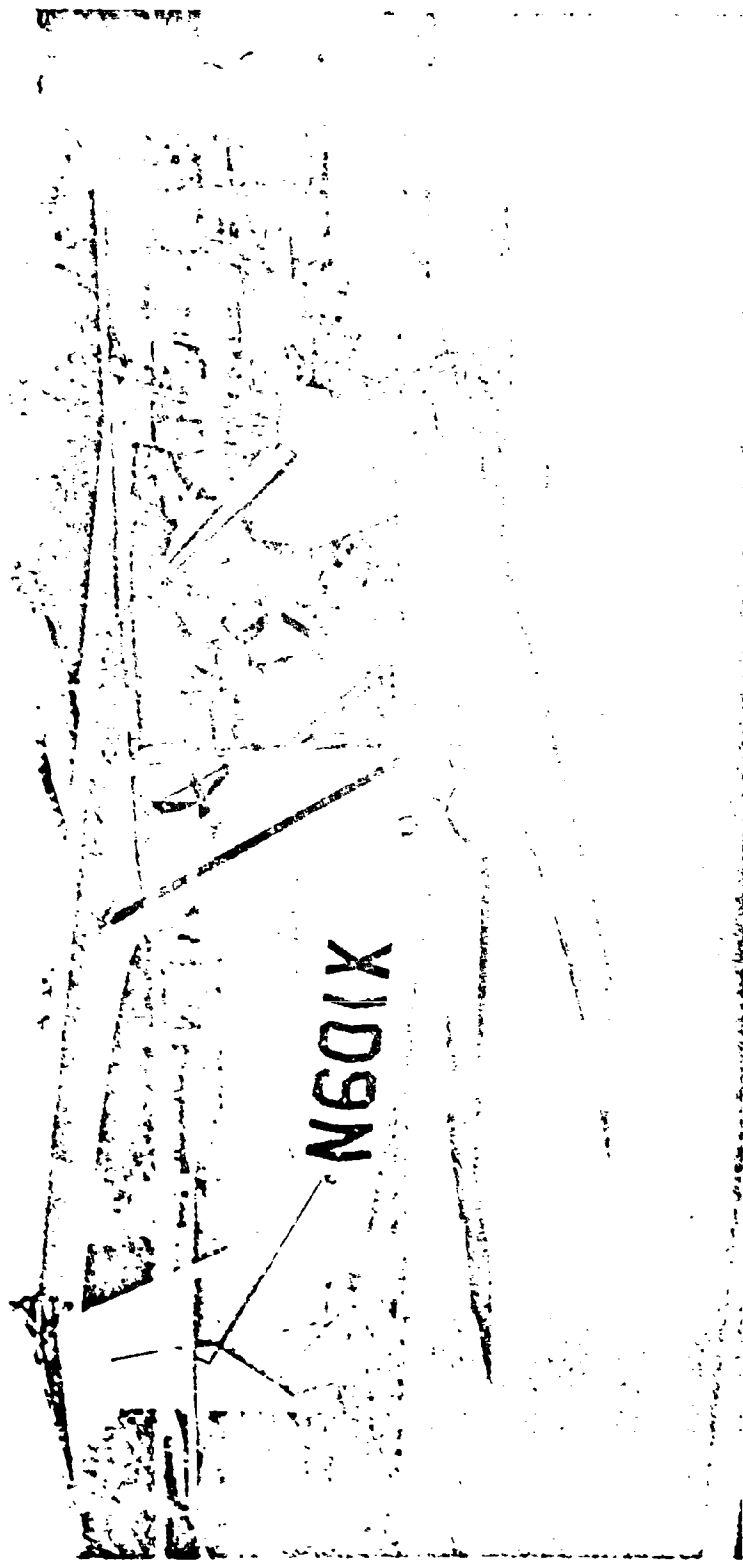


Figure 5 SAILING IV - SINGLE PLACE POWERED RESEARCH AIRPLANE

NASA  
L-60-4740

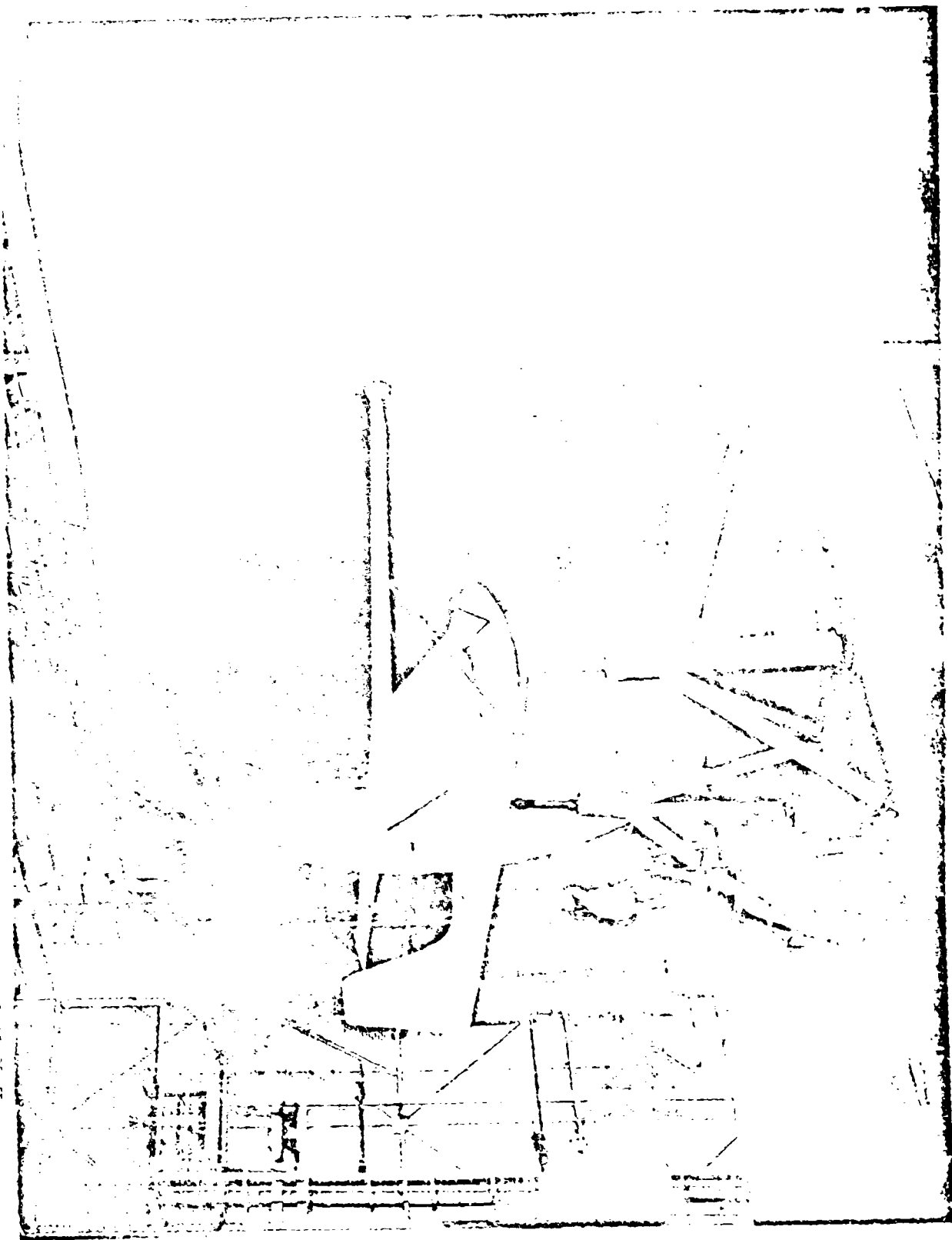


Figure 6 SAILING V - FULL SCALE WIND TUNNEL MODEL

NASA  
T.O. 2004

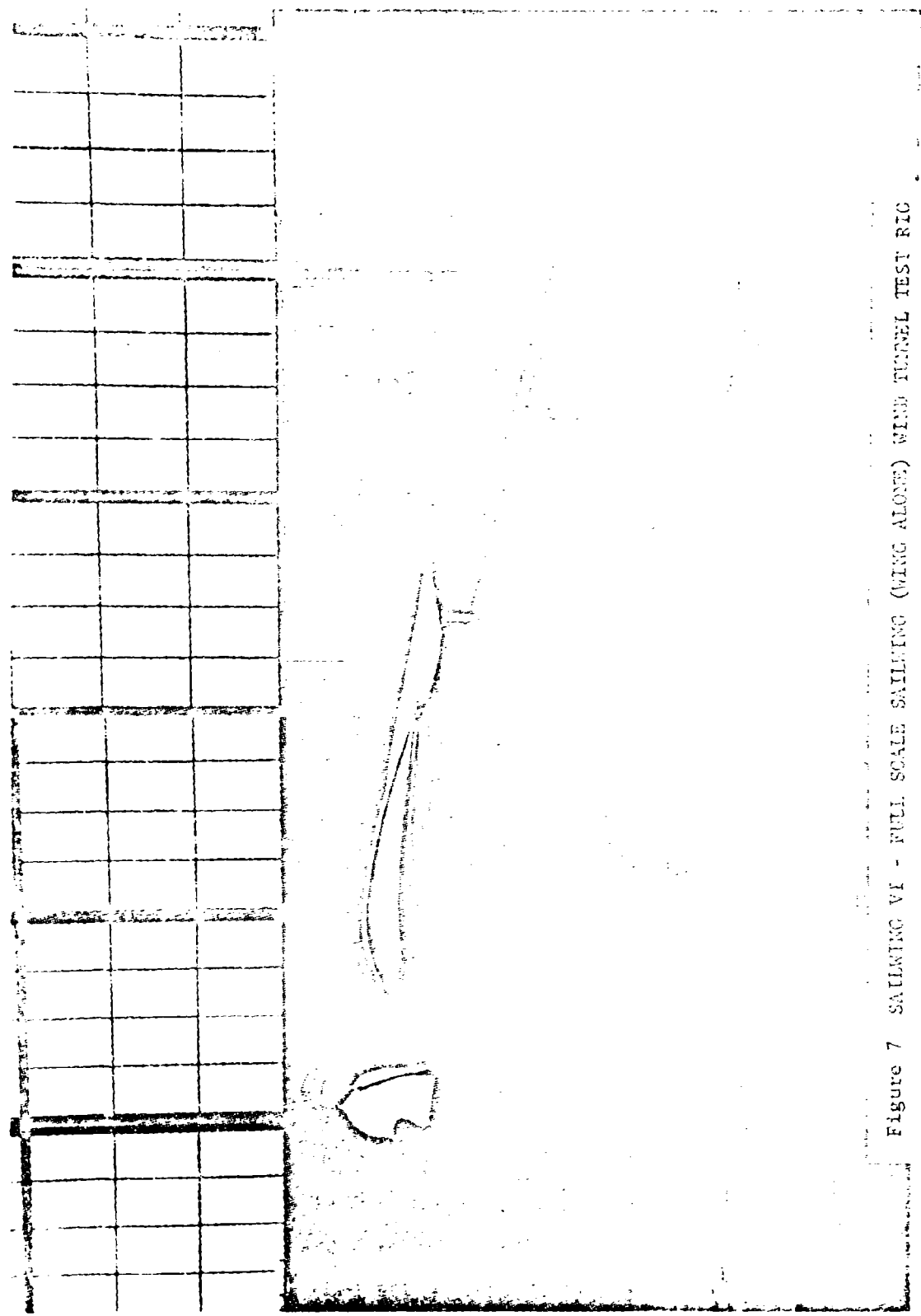
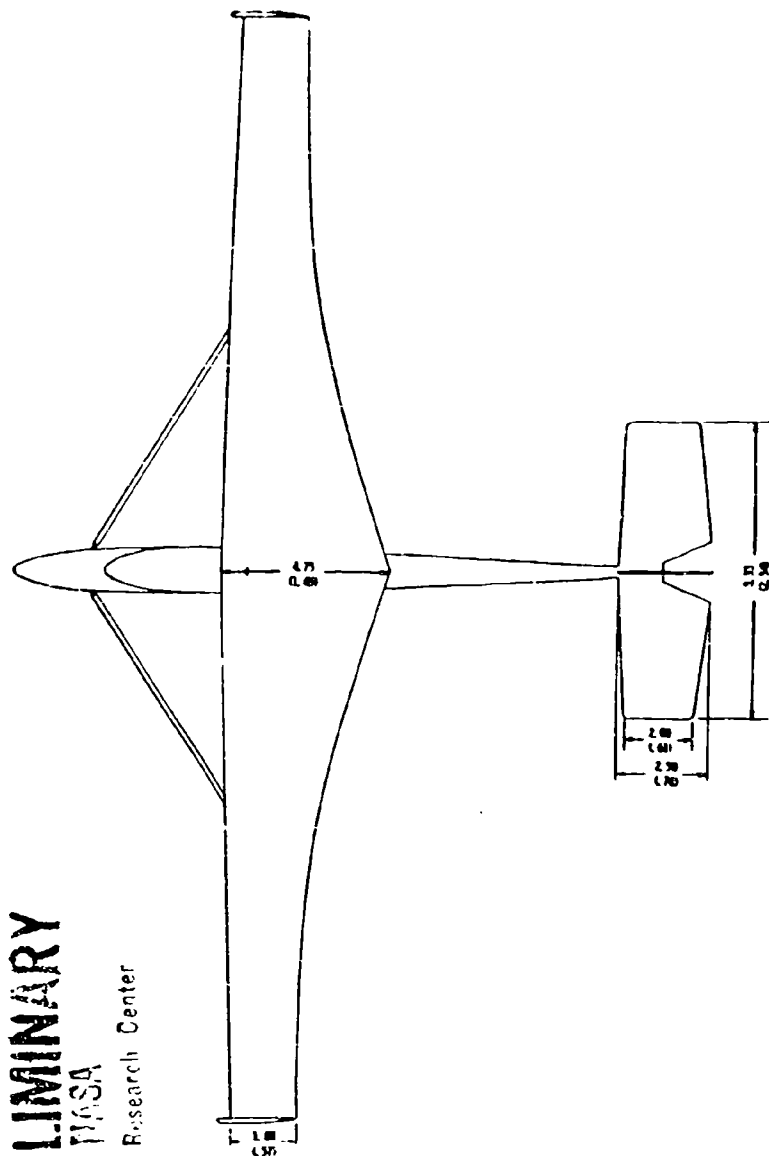


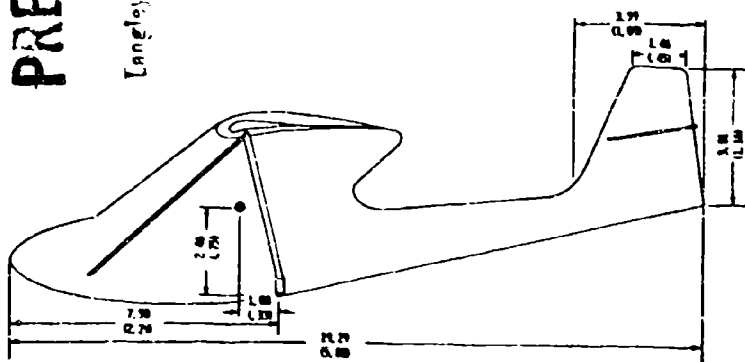
Figure 7 SAILWING VI - FULL SCALE SAILWING (WING ALONE) WIND TUNNEL TEST RIG



**PRELIMINARY**

**USA**

Language Research Center





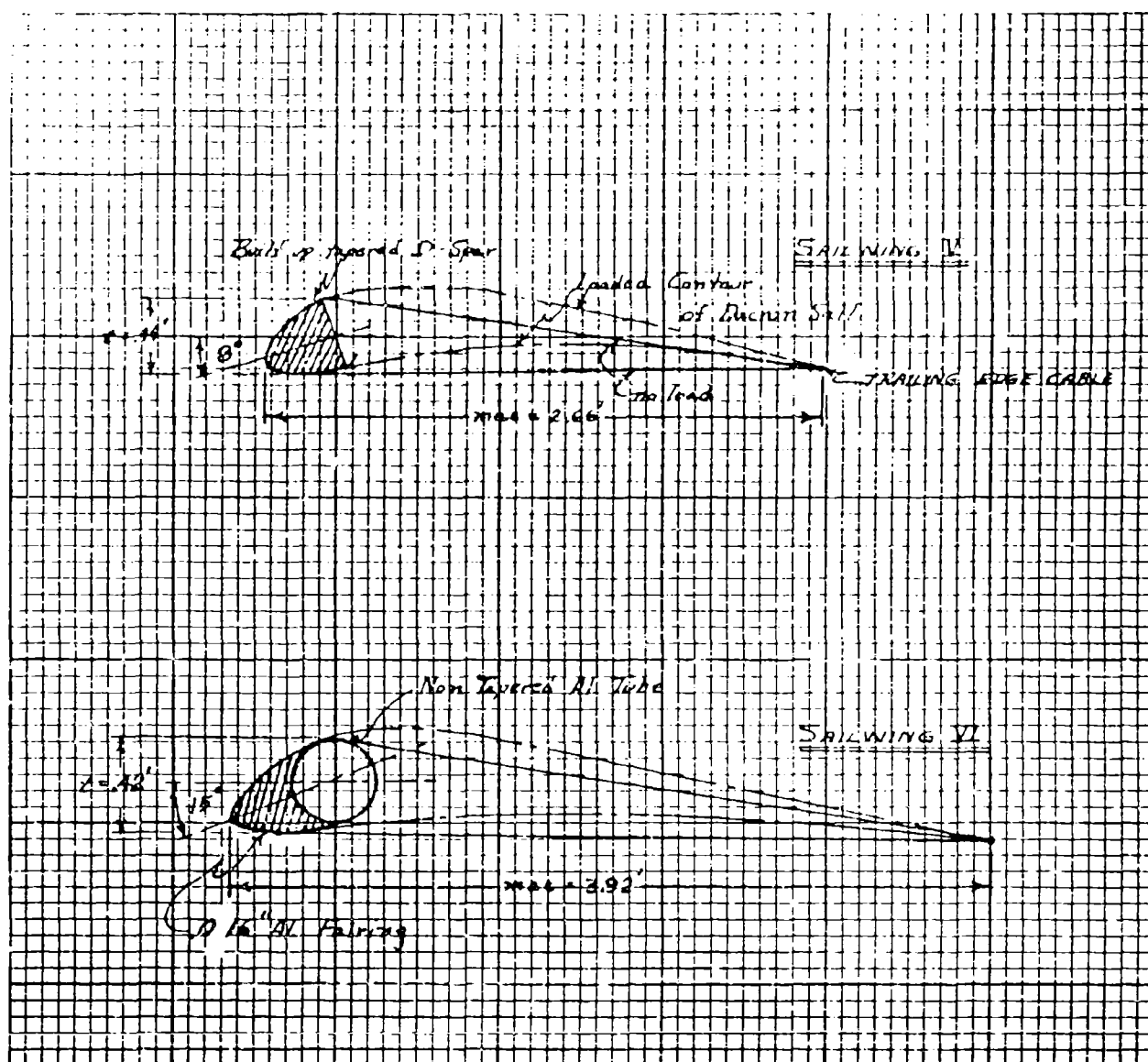
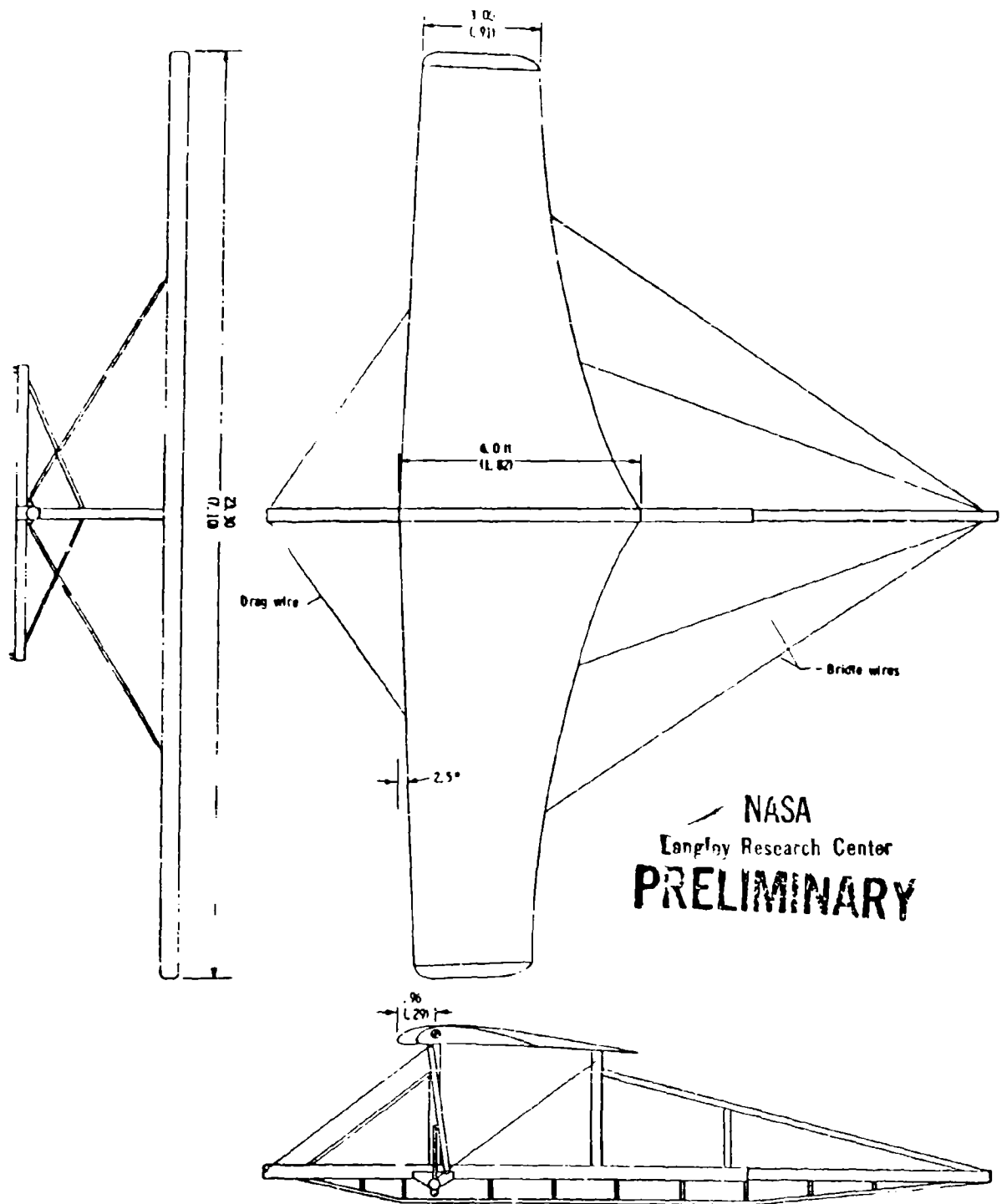


Figure 9 SCHEMATIC REPRESENTATION OF SECTION GEOMETRY OF SAILWINGS V AND VI



Wing alone apparatus

Figure 10



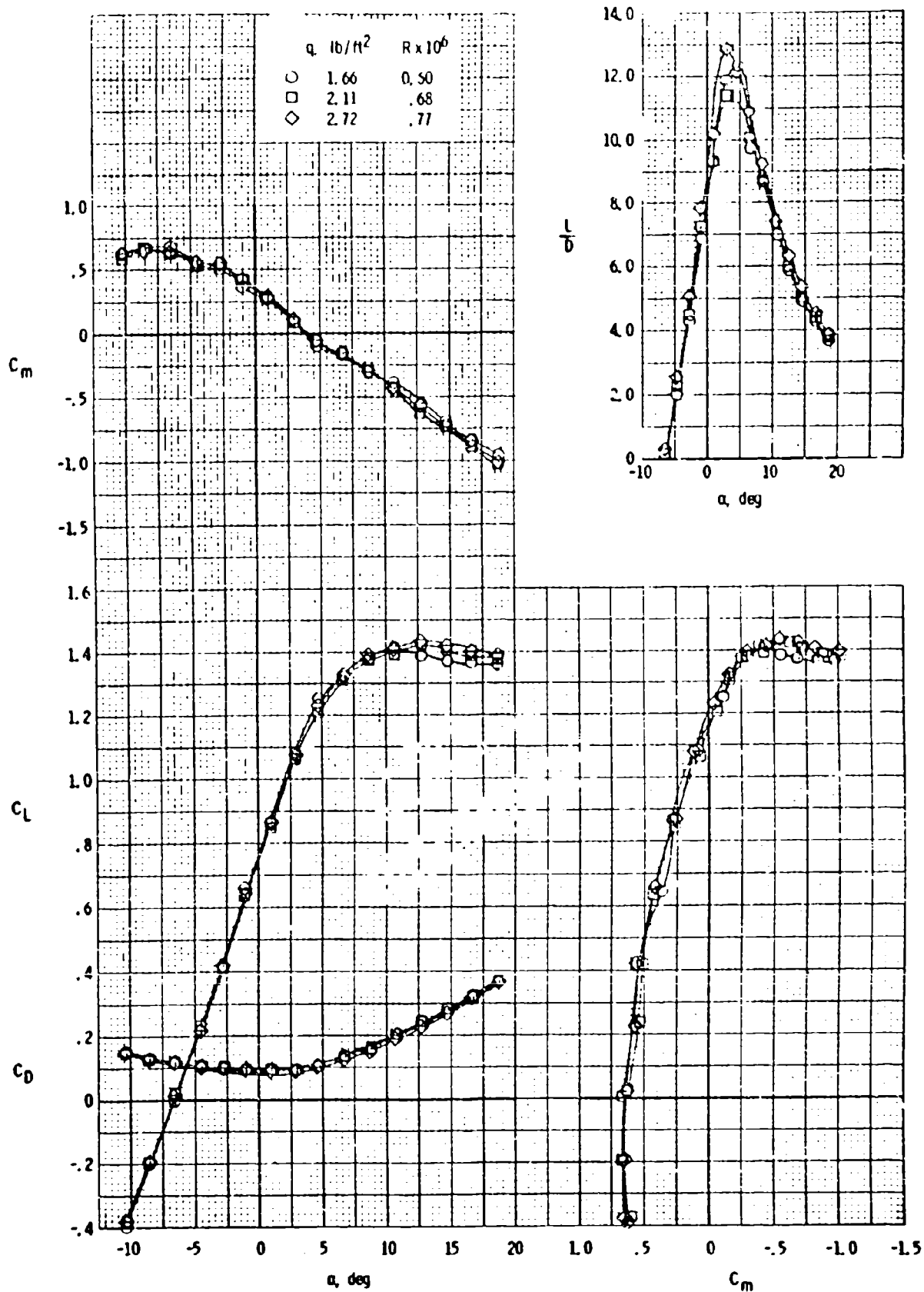


Figure 11 Effect of Reynolds number on the longitudinal characteristics of the airplane.

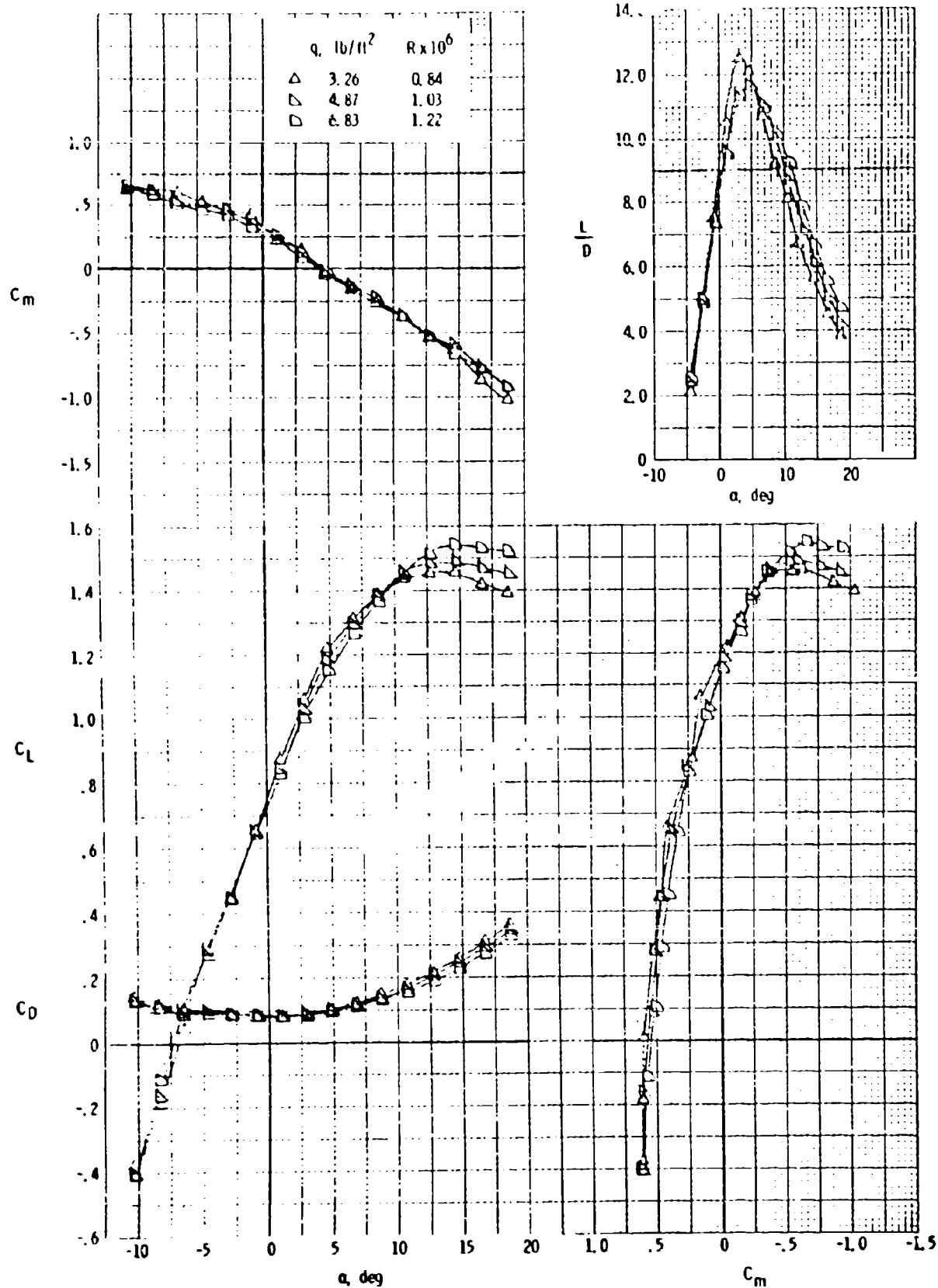


Figure 11 Concluded

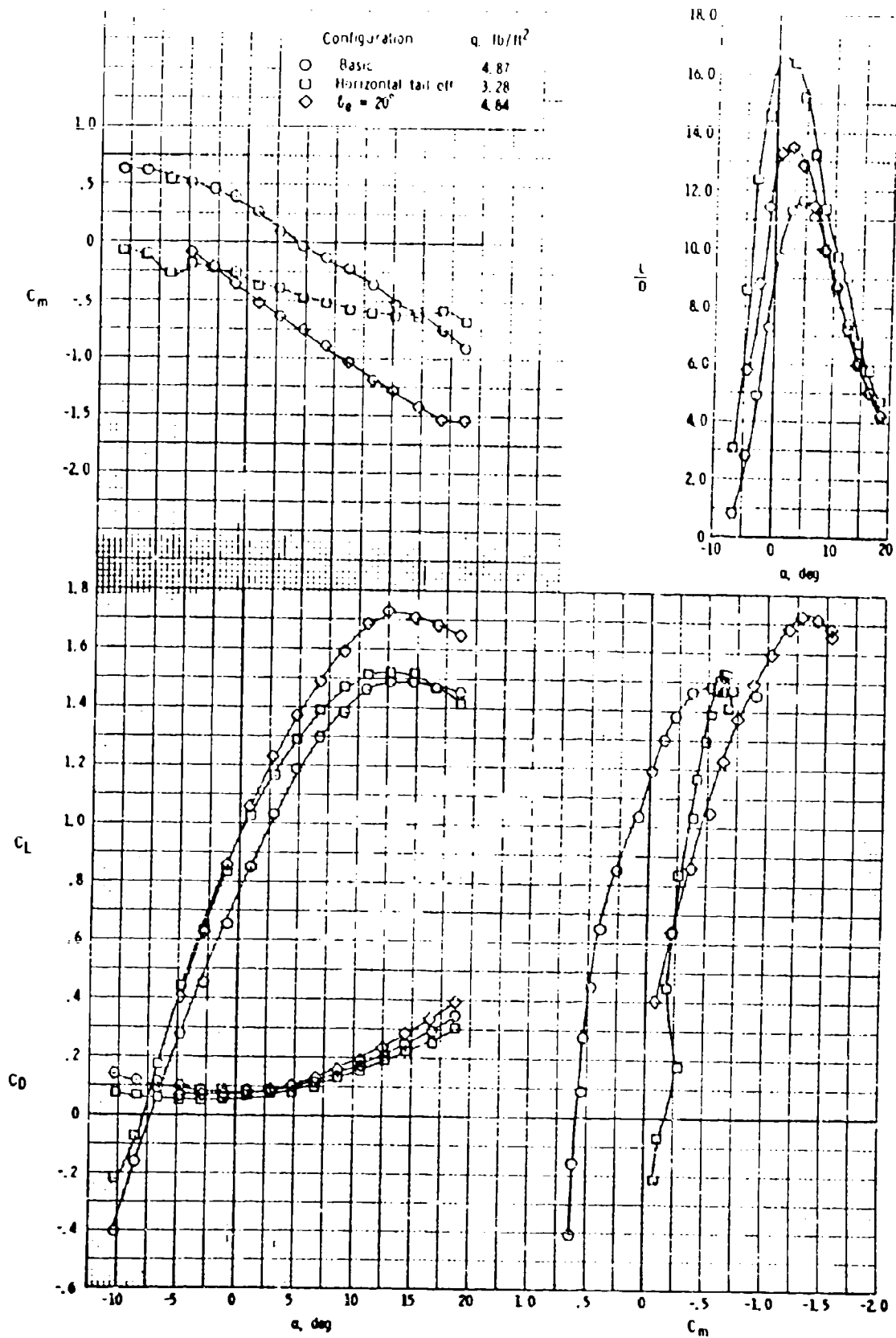


Figure 12 Effect of elevator deflection on the longitudinal characteristics of the airplane.

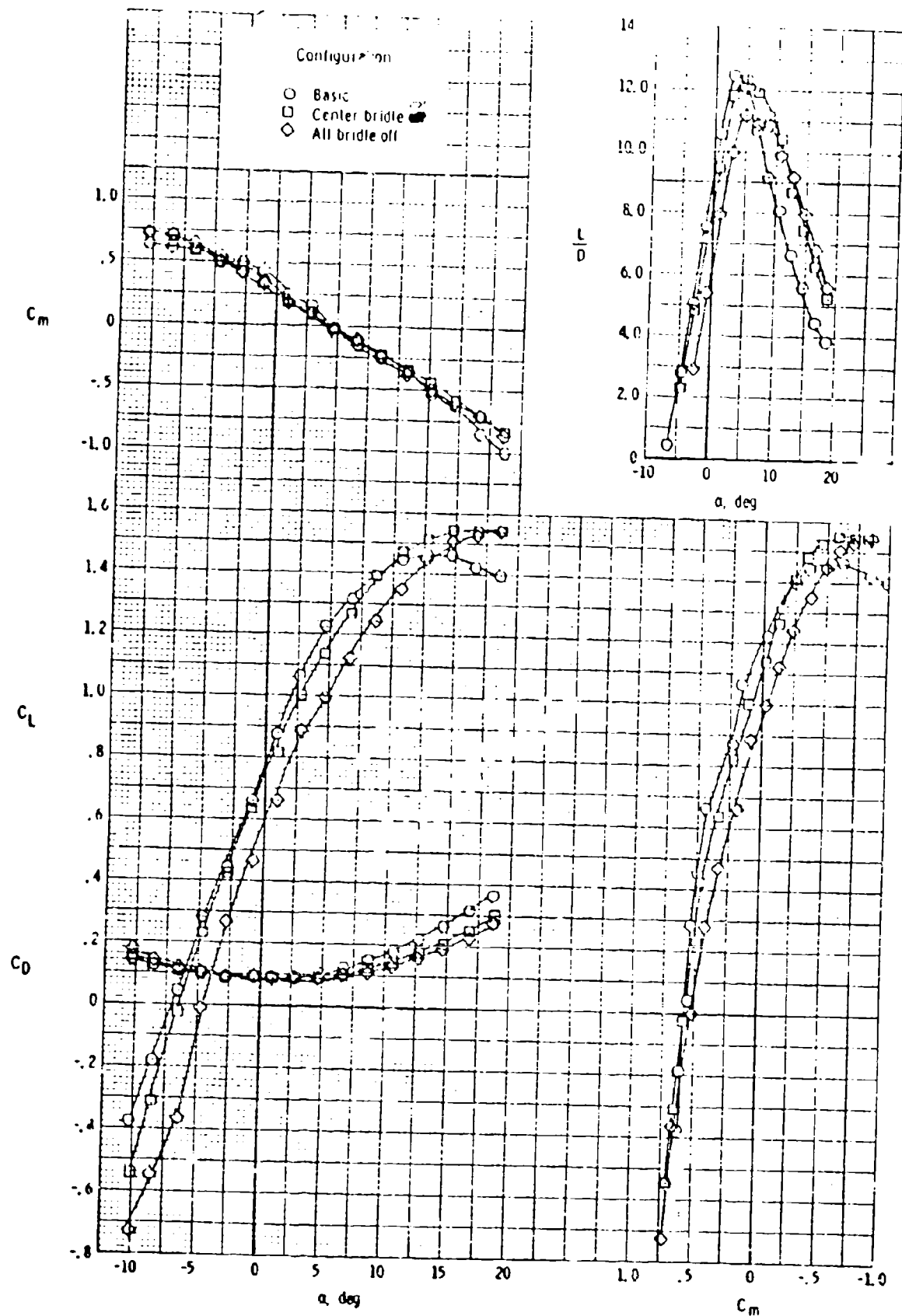


Figure 13 Effect of bridle wires on the longitudinal characteristics of the airplane.  $q \approx 3.26$ .

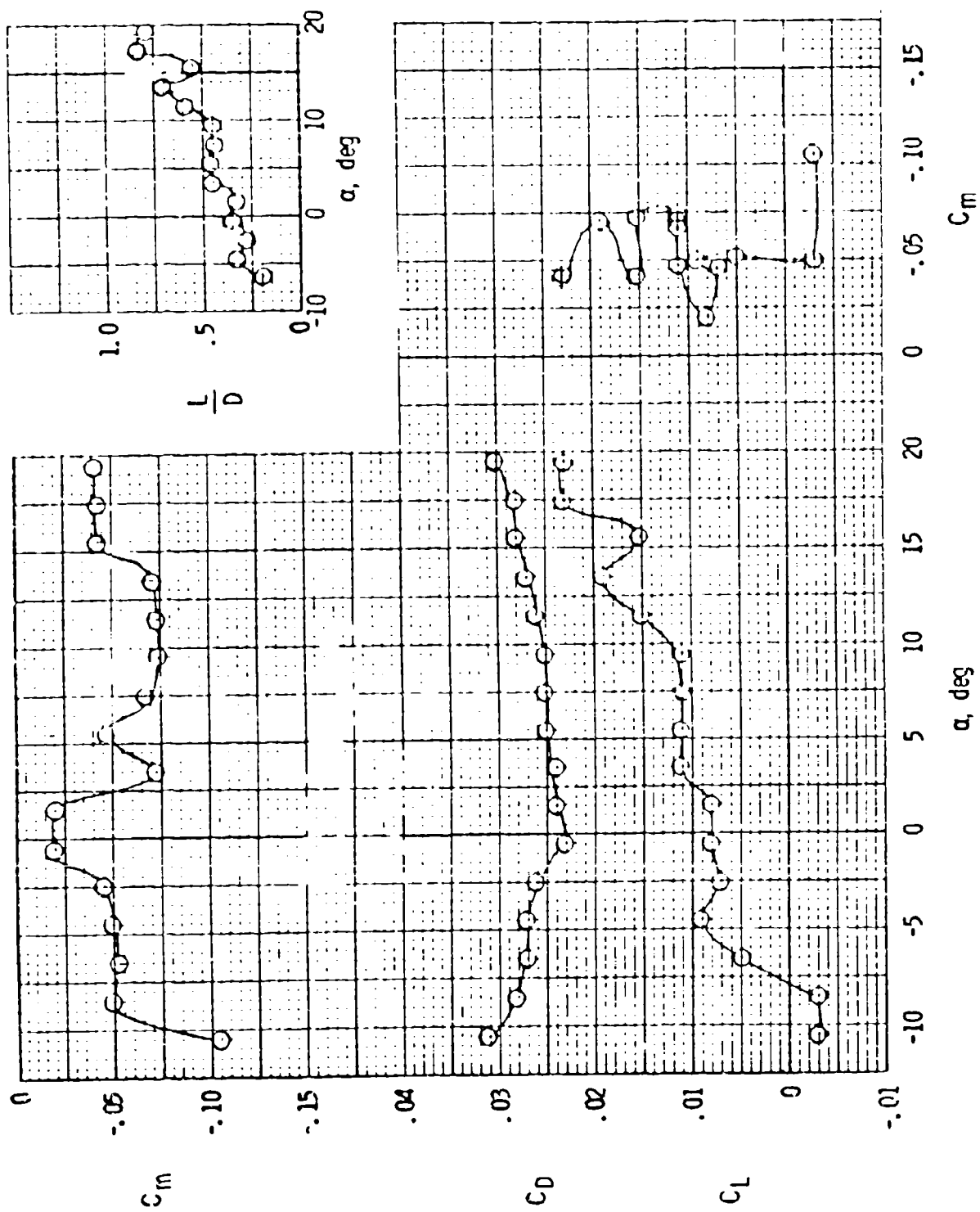
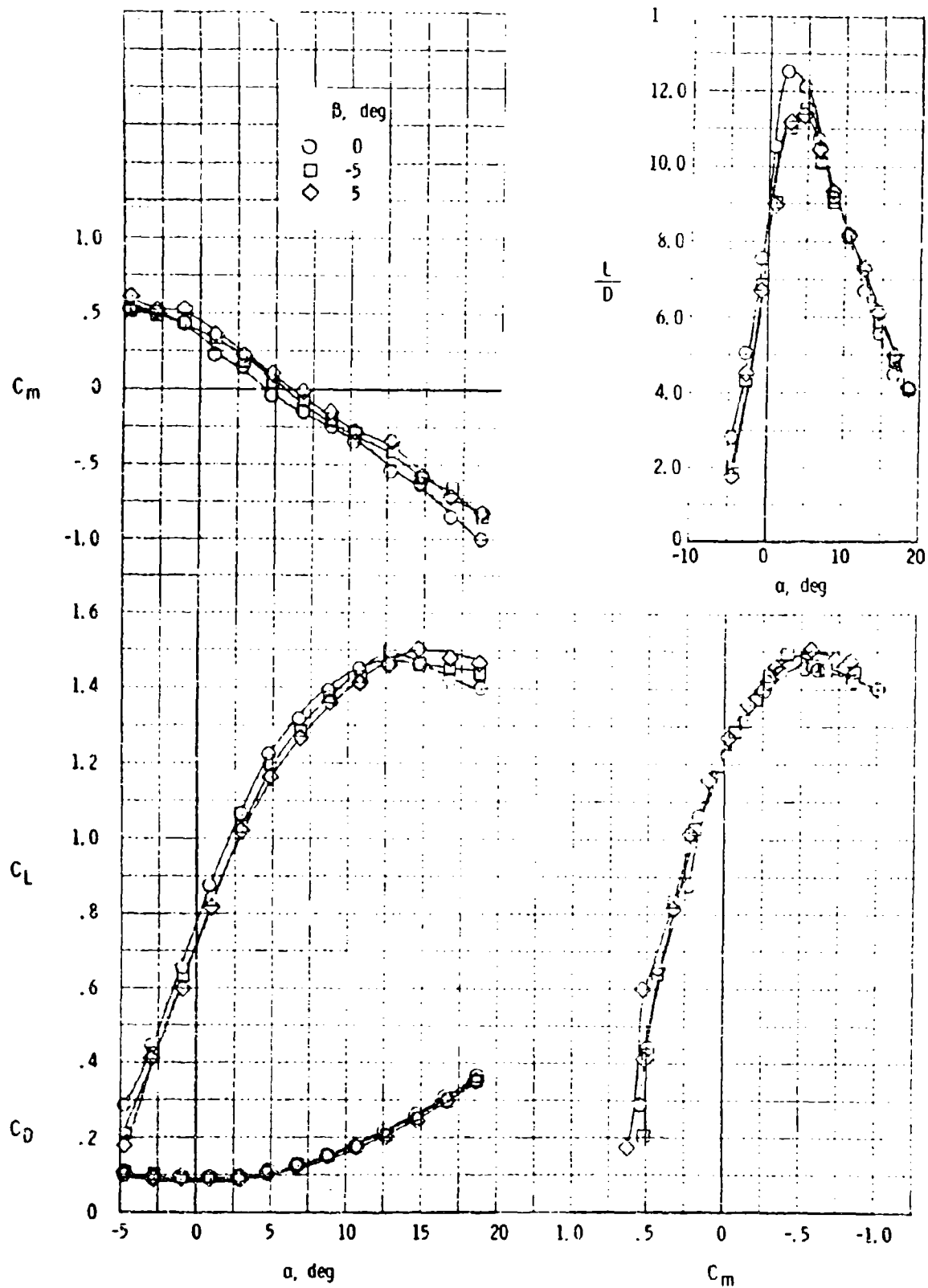
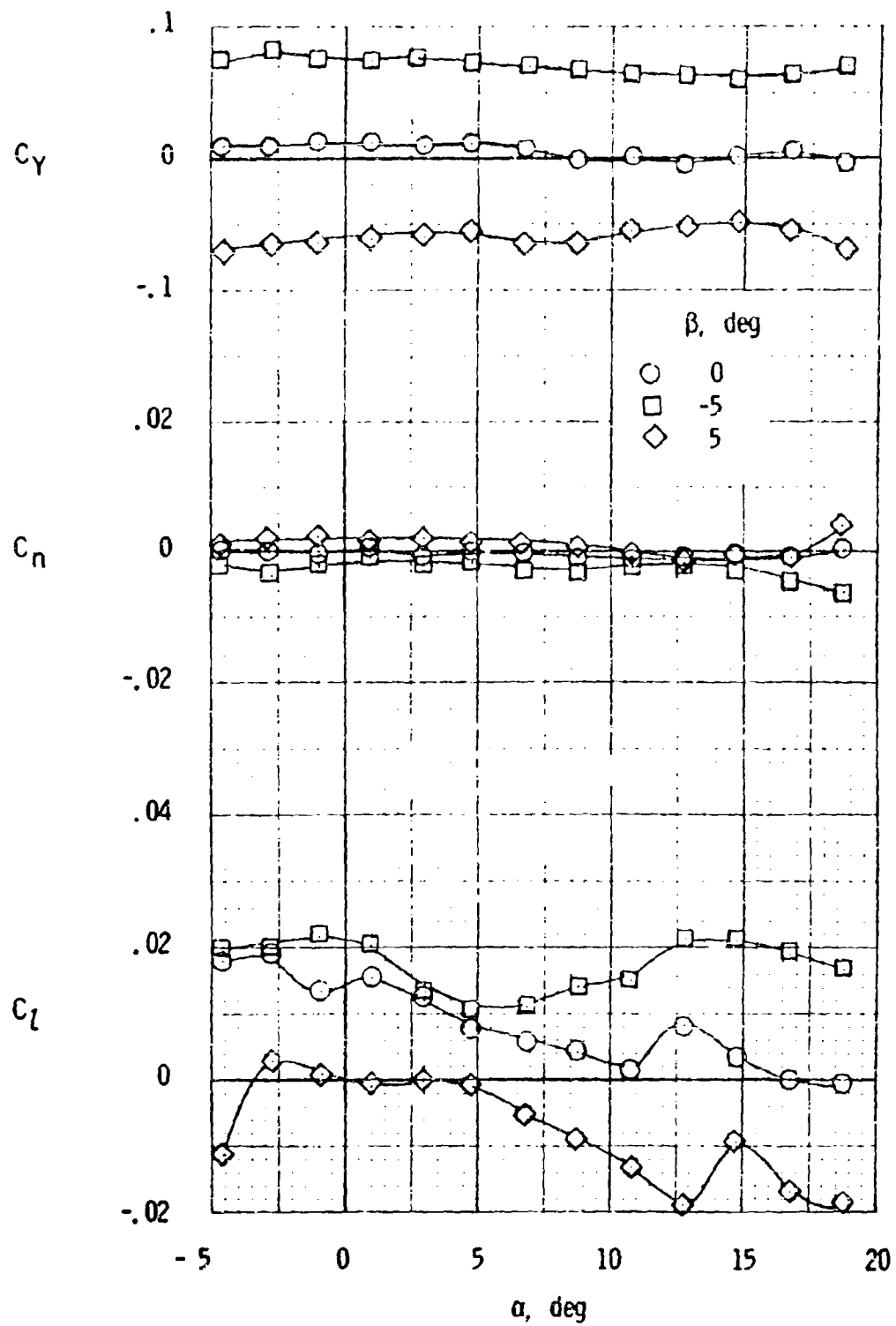


Figure 14 Longitudinal characteristics of the fuselage alone.  $q \approx 3.26$ .



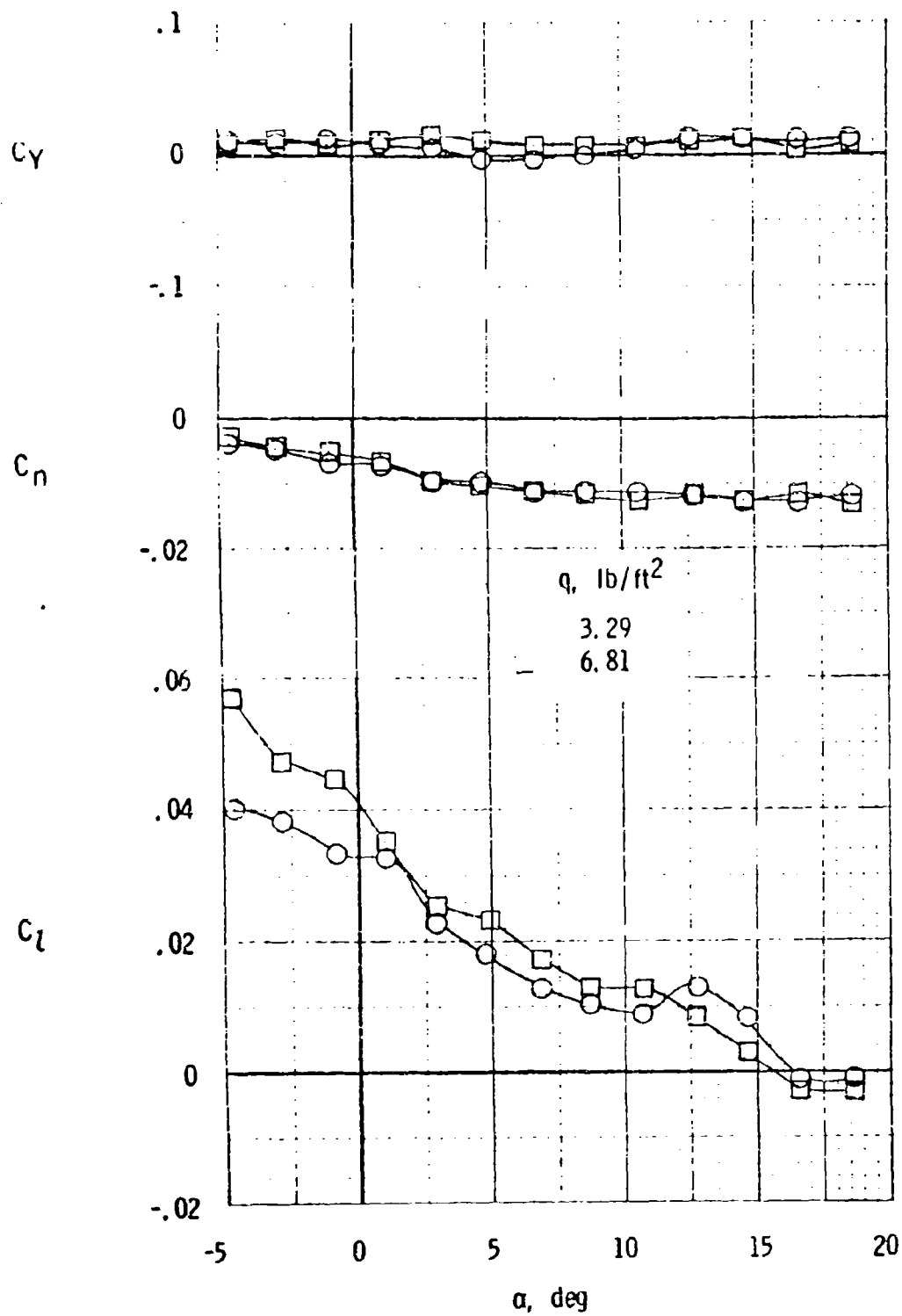
(a) Longitudinal characteristics.

Figure 15 Effect of sideslip on basic airplane configuration,  $q \approx 3.29$ .



(b) Lateral characteristics.

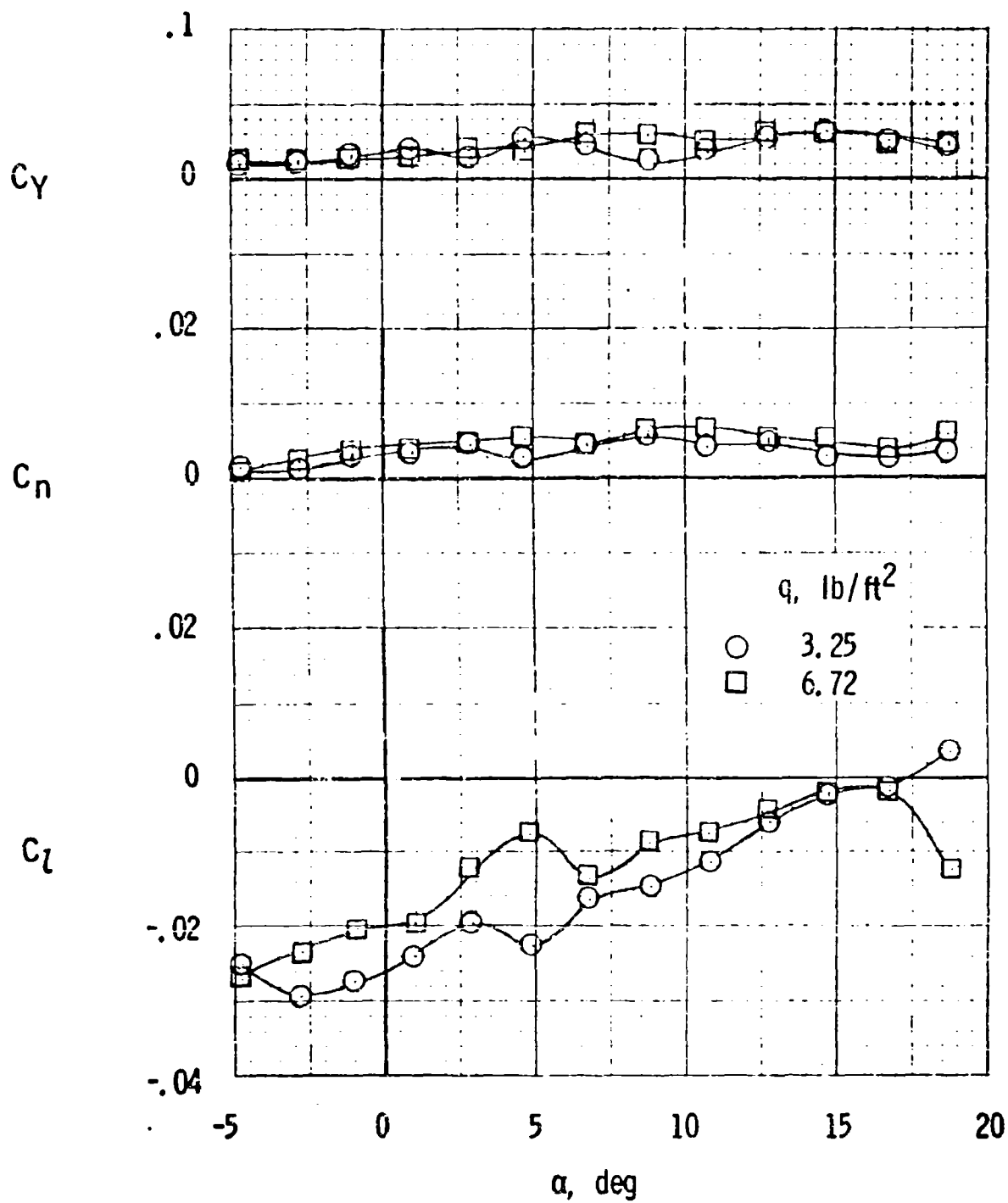
Figure 15 Concluded



(a)  $\delta_{aR} = -7.2^\circ$ ,  $\delta_{aL} = 8.2^\circ$ .

Figure 16 Effect of dynamic pressure on the lateral characteristics with ailerons deflected.





(b)  $\delta_{aR} = 7.4$ ,  $\delta_{aL} = -4.2$

Figure 16 Concluded

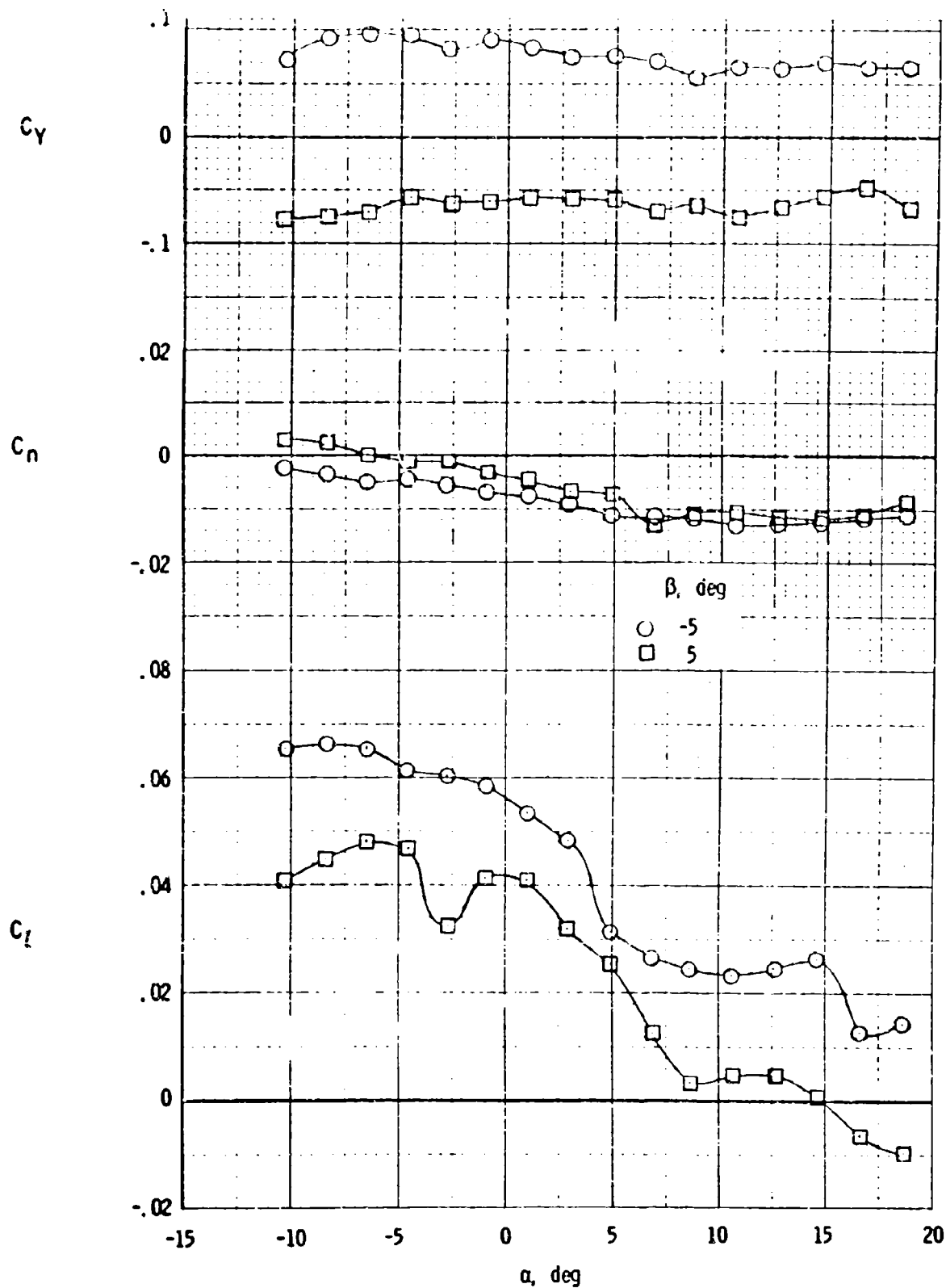


Figure 17 Effect of sideslip on the lateral characteristics of the airplane with allerons deflected.  $\delta_{aR} = -7.4^\circ$ ,  $\delta_{aL} = +8.9^\circ$ .  $q \approx 3.27$ .

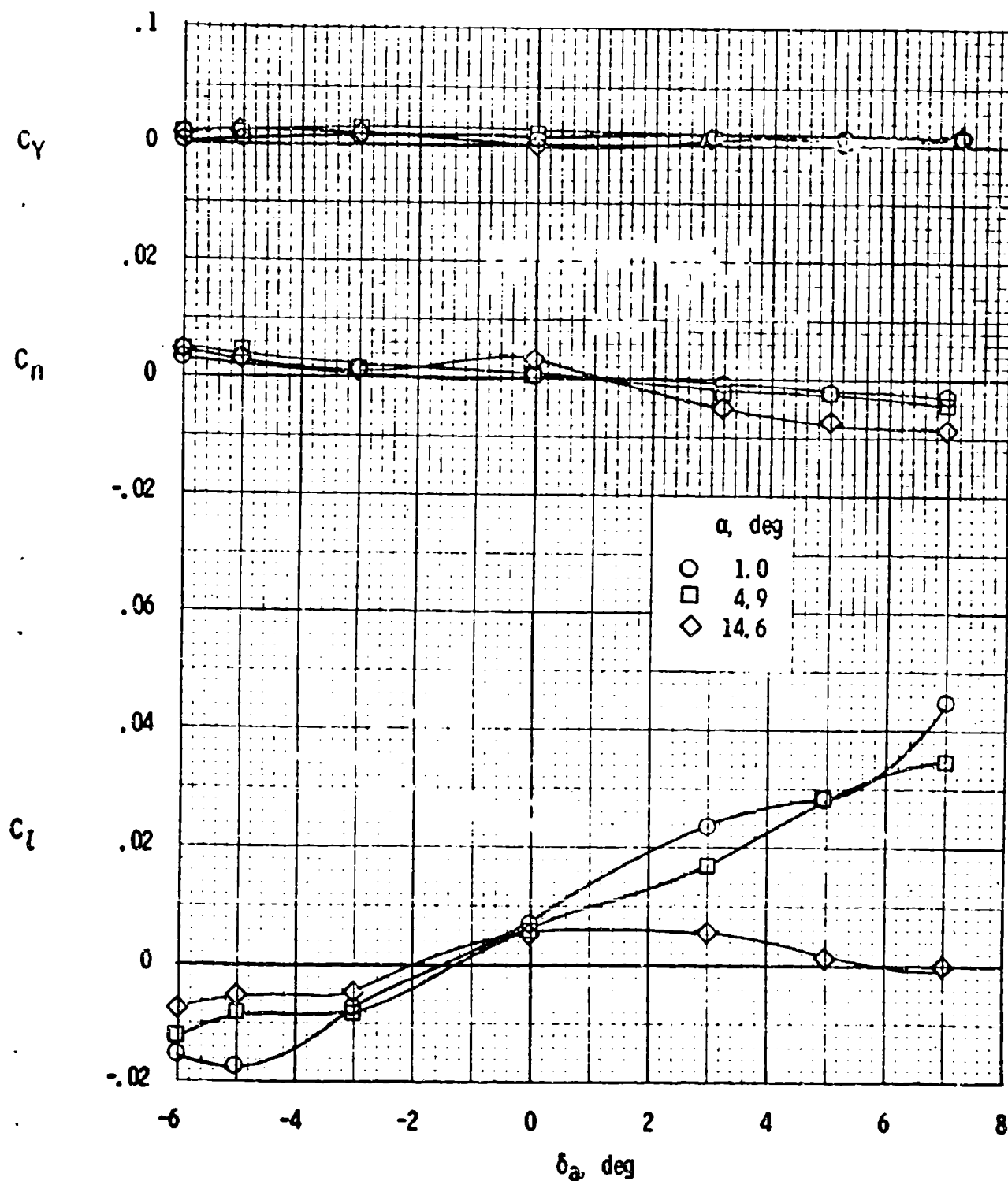


Figure 18 Aileron effectiveness on the lateral characteristics of the airplane at several angles of attack,  $q \approx 4.85$ .

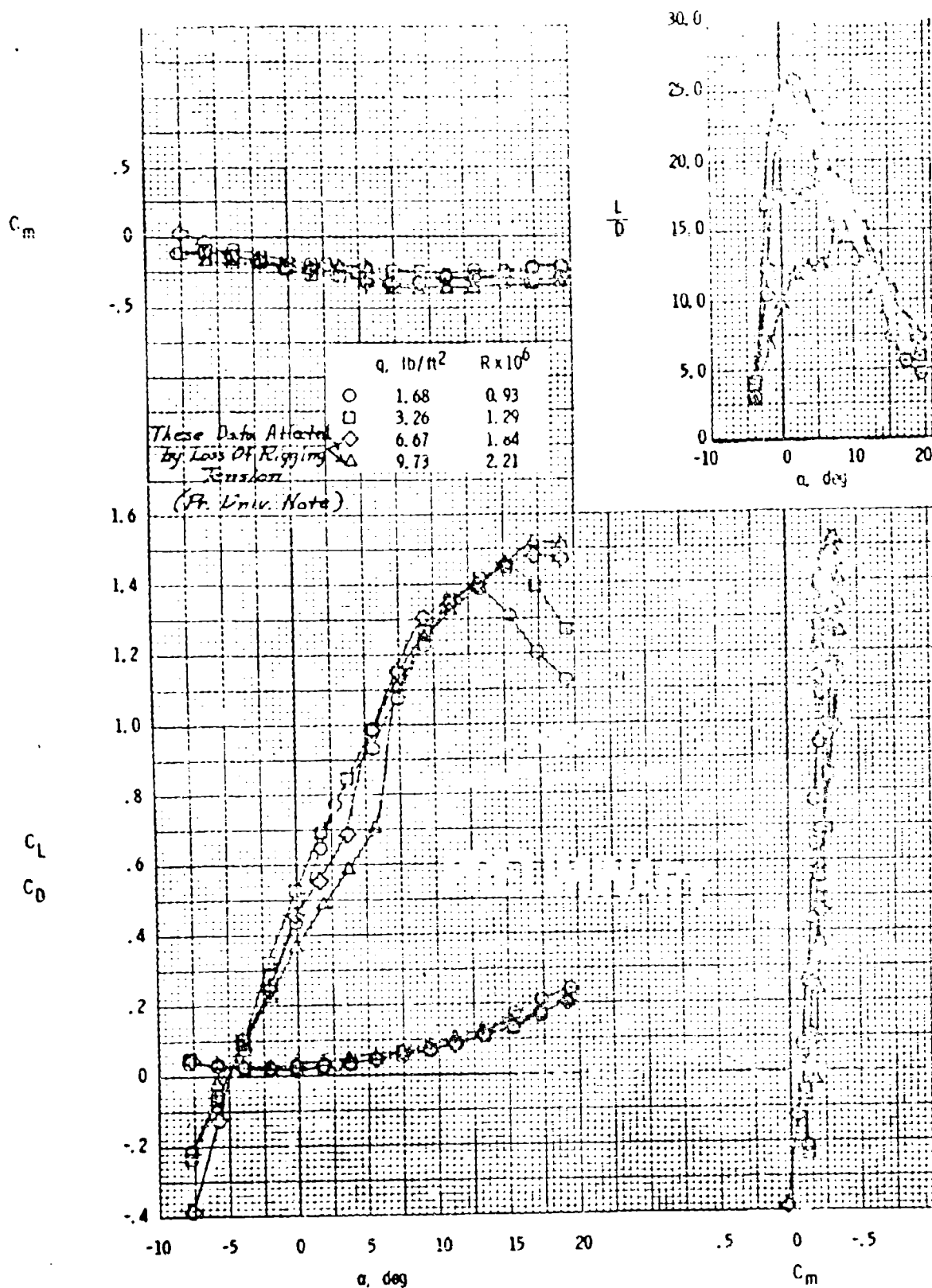
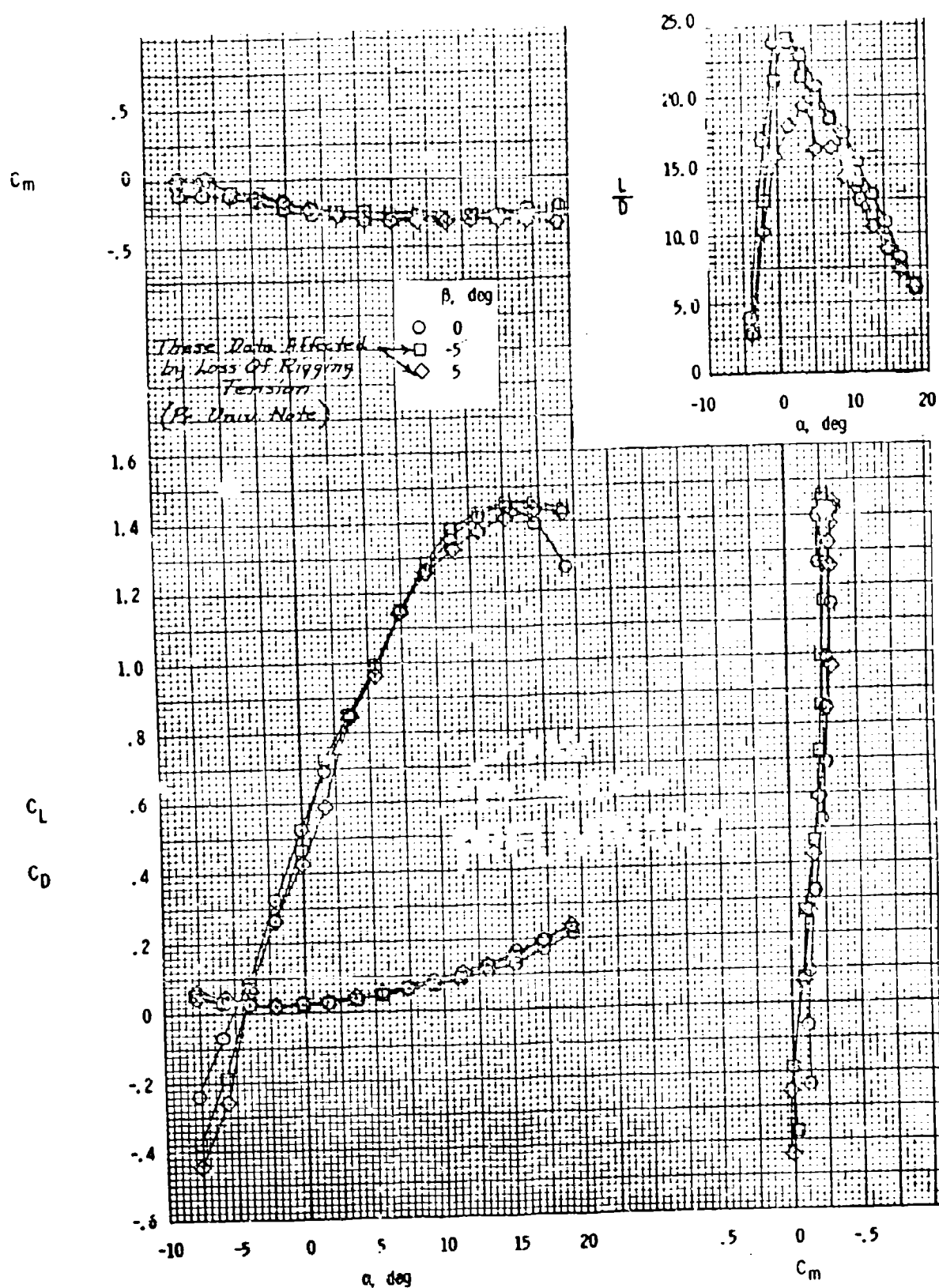
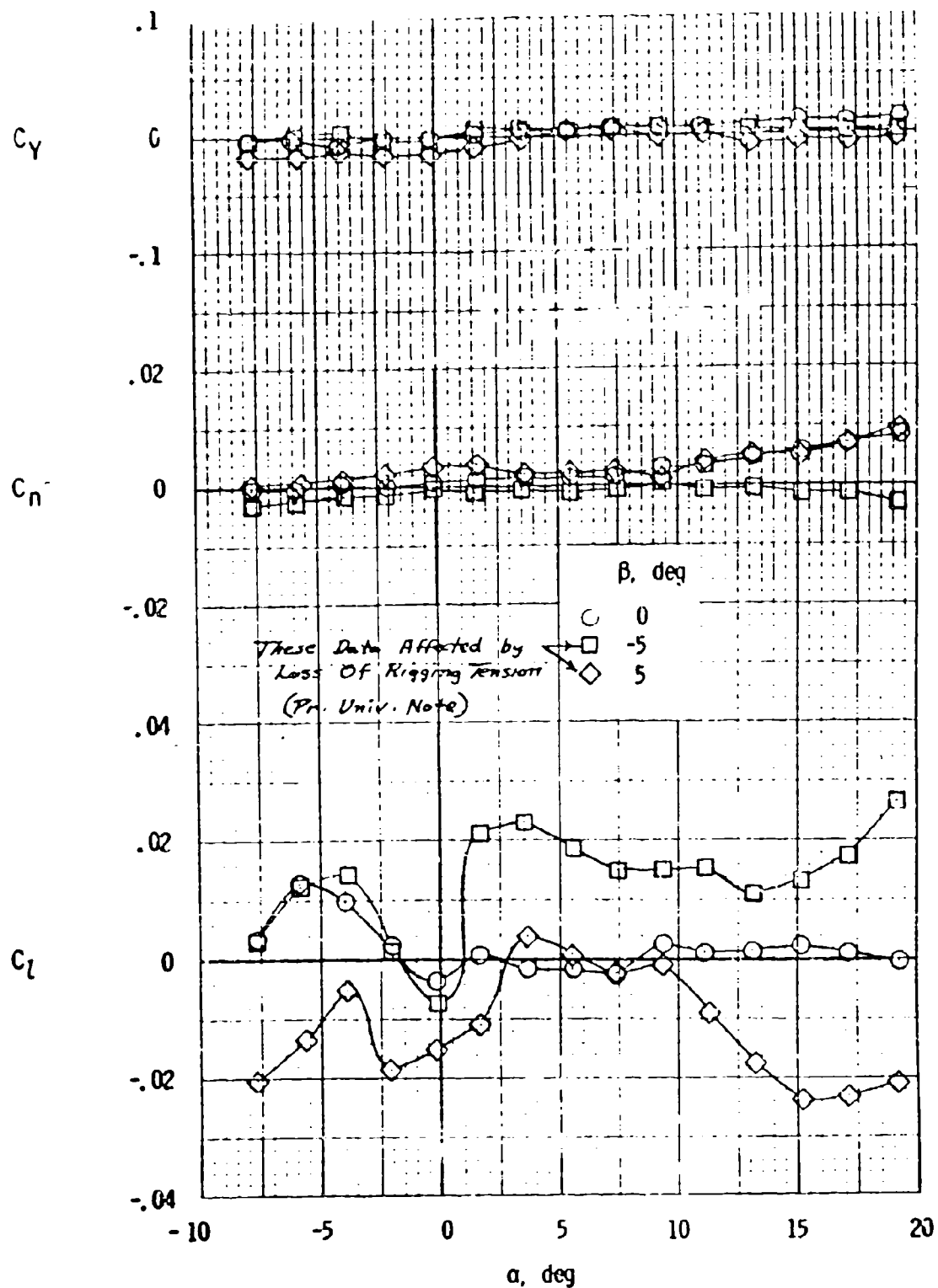


Figure 19 Effect of Reynolds number on the longitudinal characteristics of the wing with 5° dihedral.



(a) Longitudinal characteristics.

Figure 19 Continued Effect of sideslip on the characteristics of the wing with 5° dihedral.  $q \approx 3.25$ .



(b) Lateral characteristics.

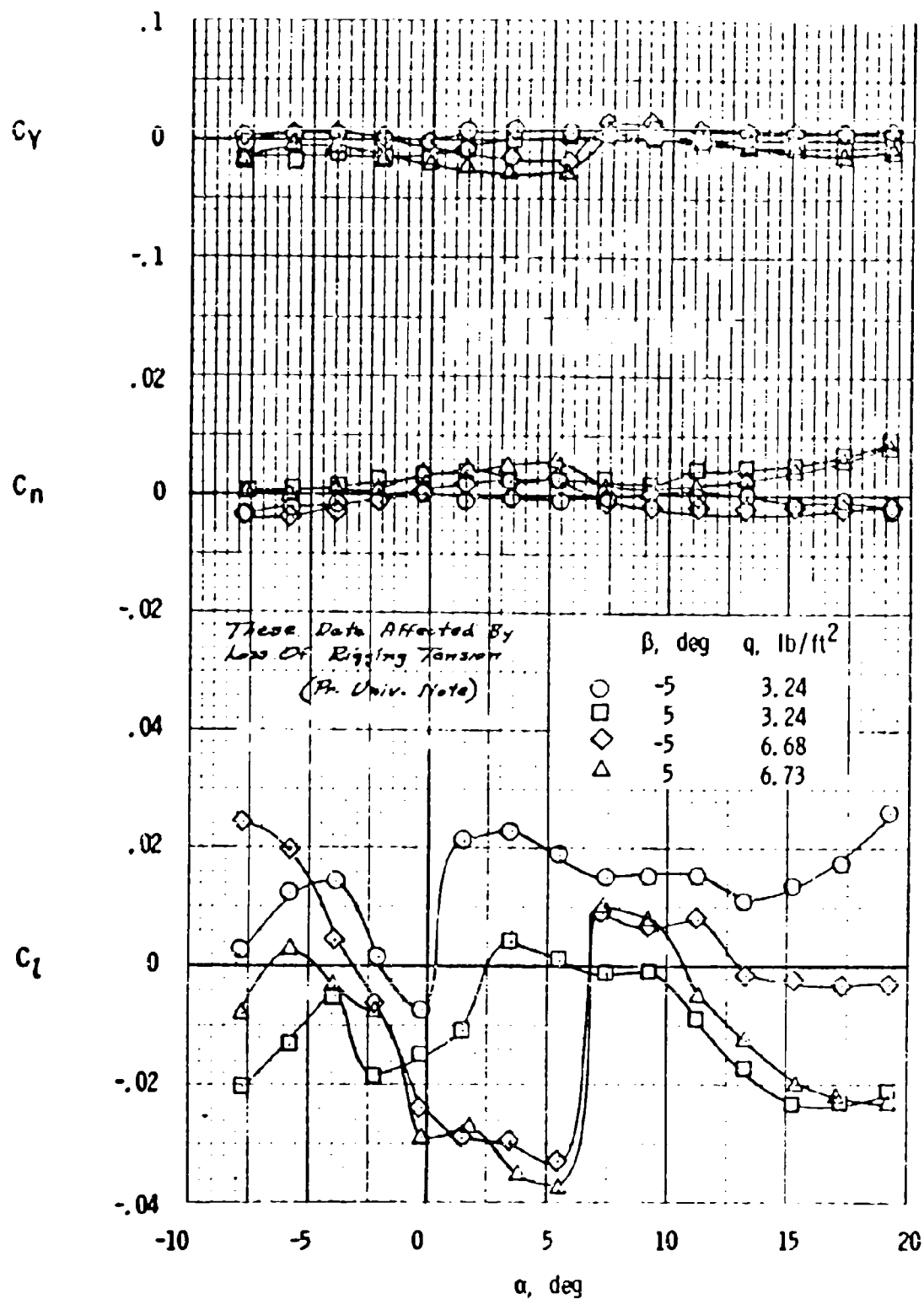


Figure 20 Effect of dynamic pressure on the lateral characteristics of the wing with sideslip for 5° dihedral.

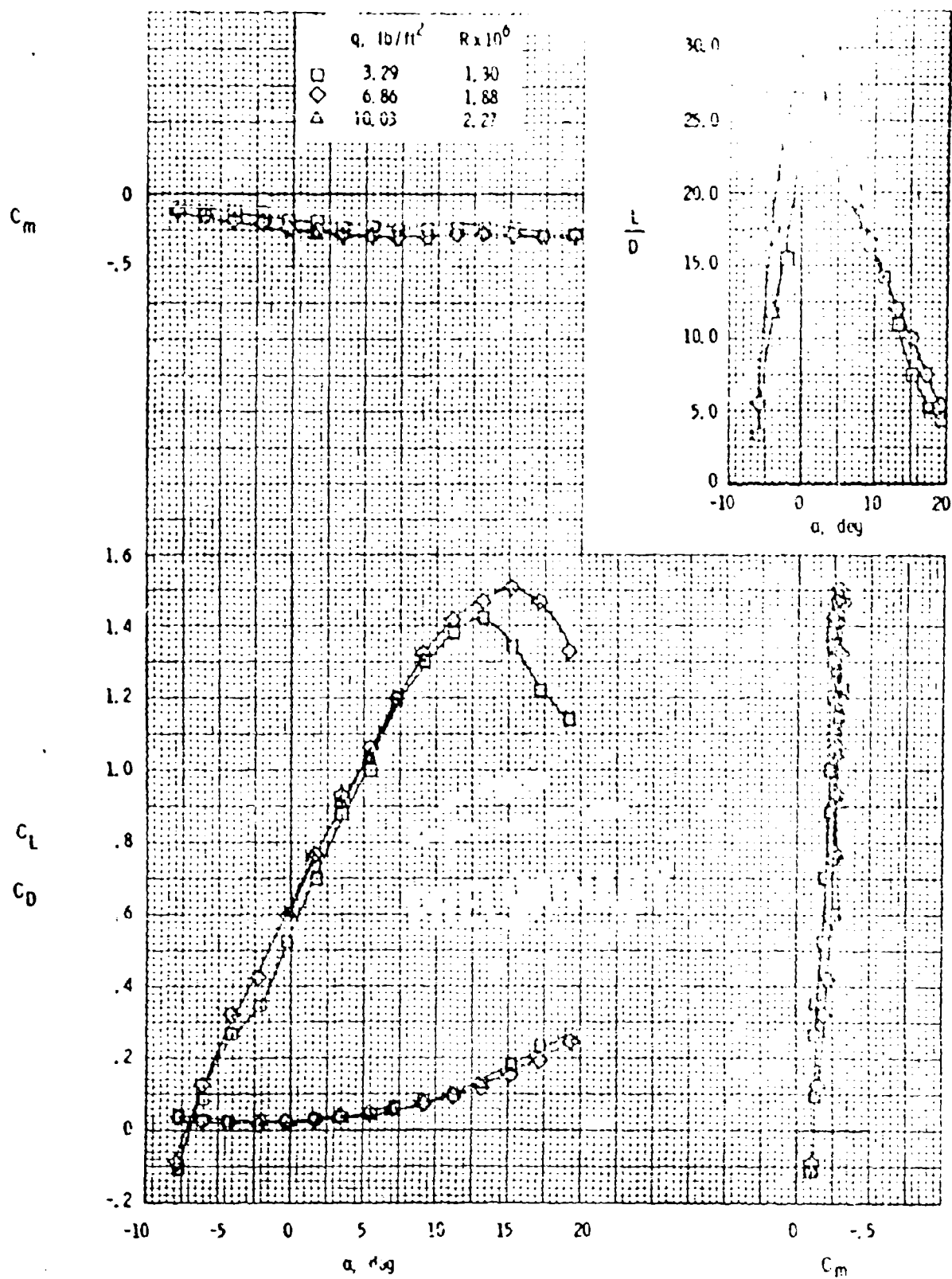
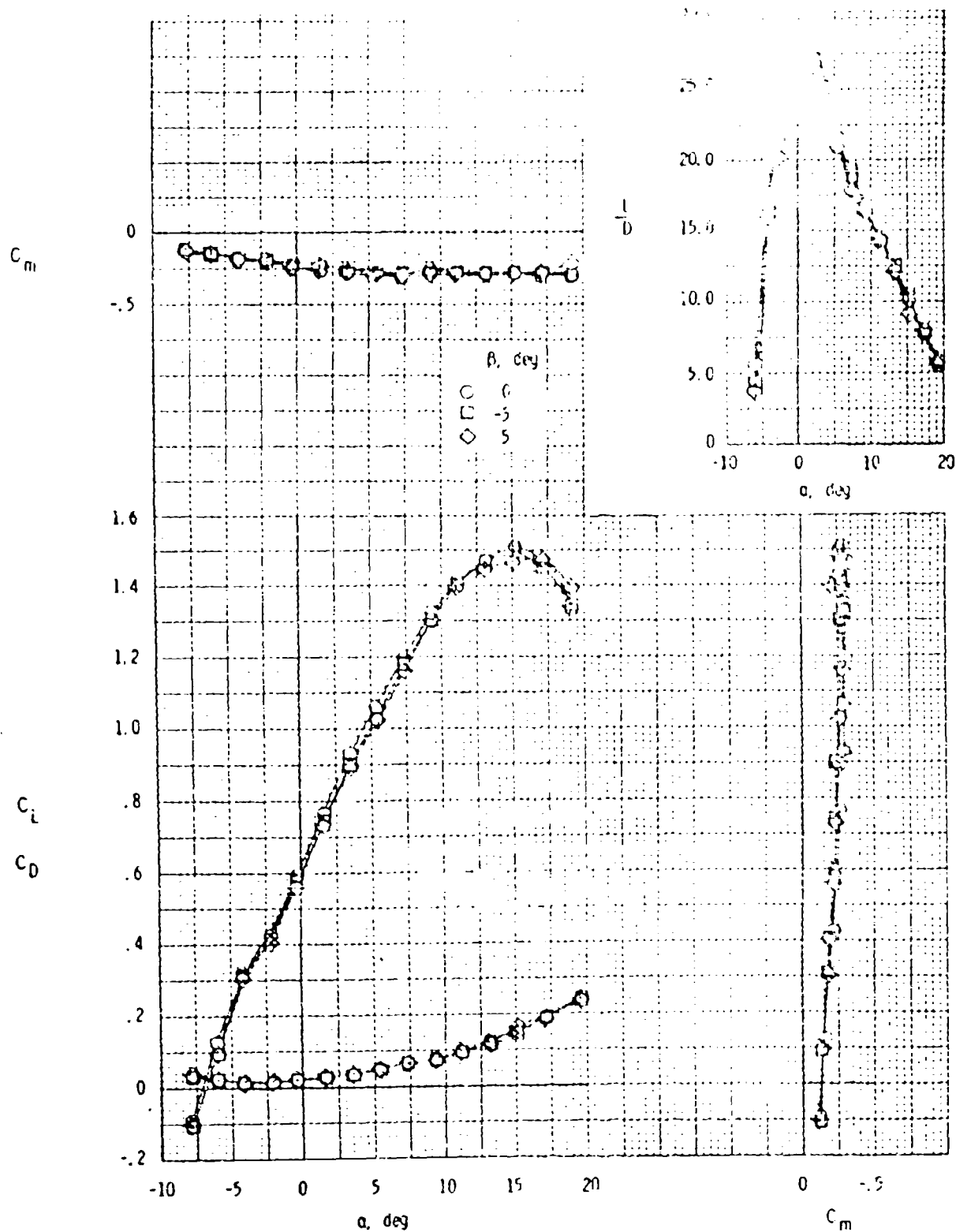


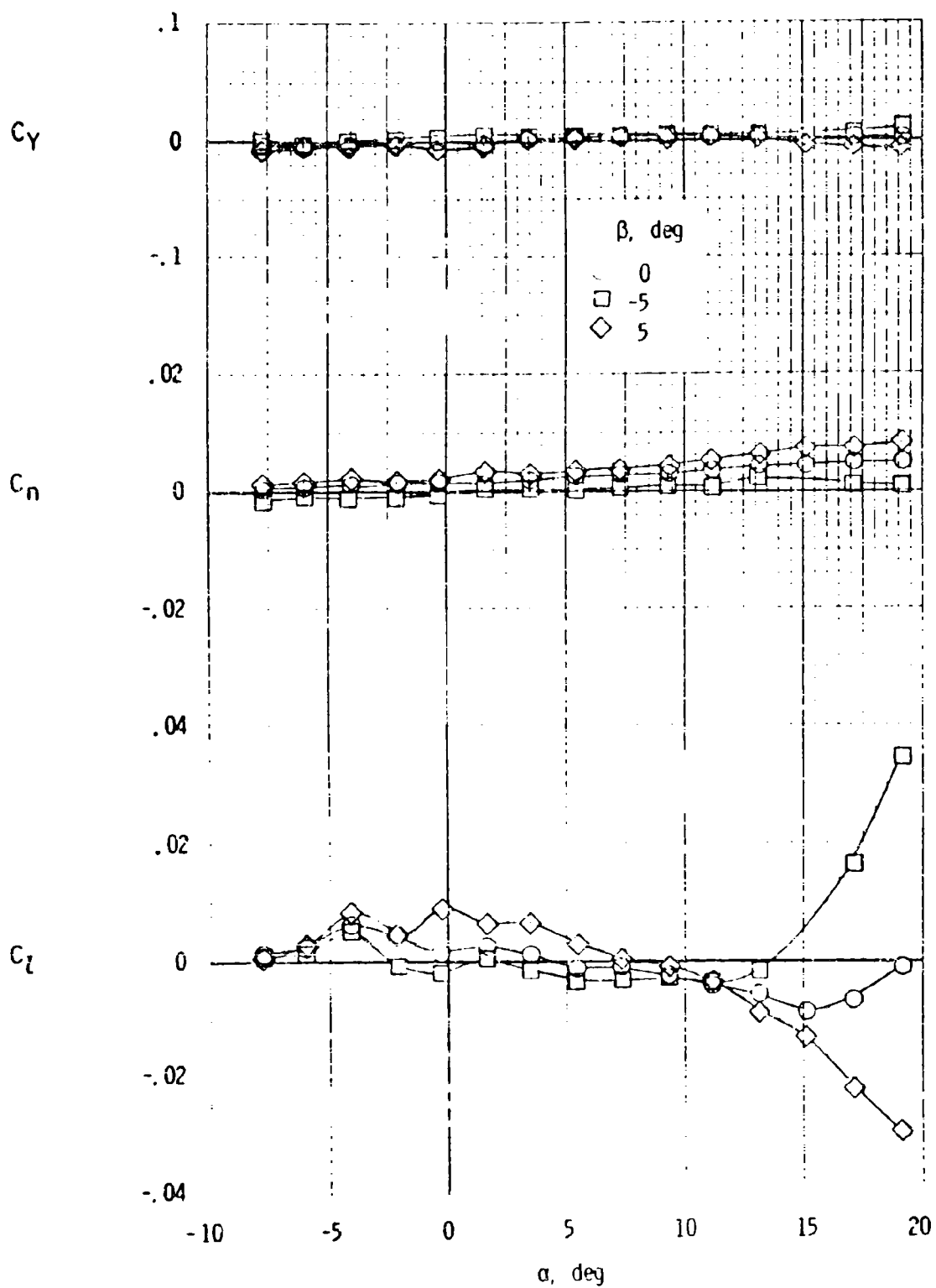
Figure 21 - Effect of Reynolds number on the longitudinal characteristics of the wing, with 0° dihedral.



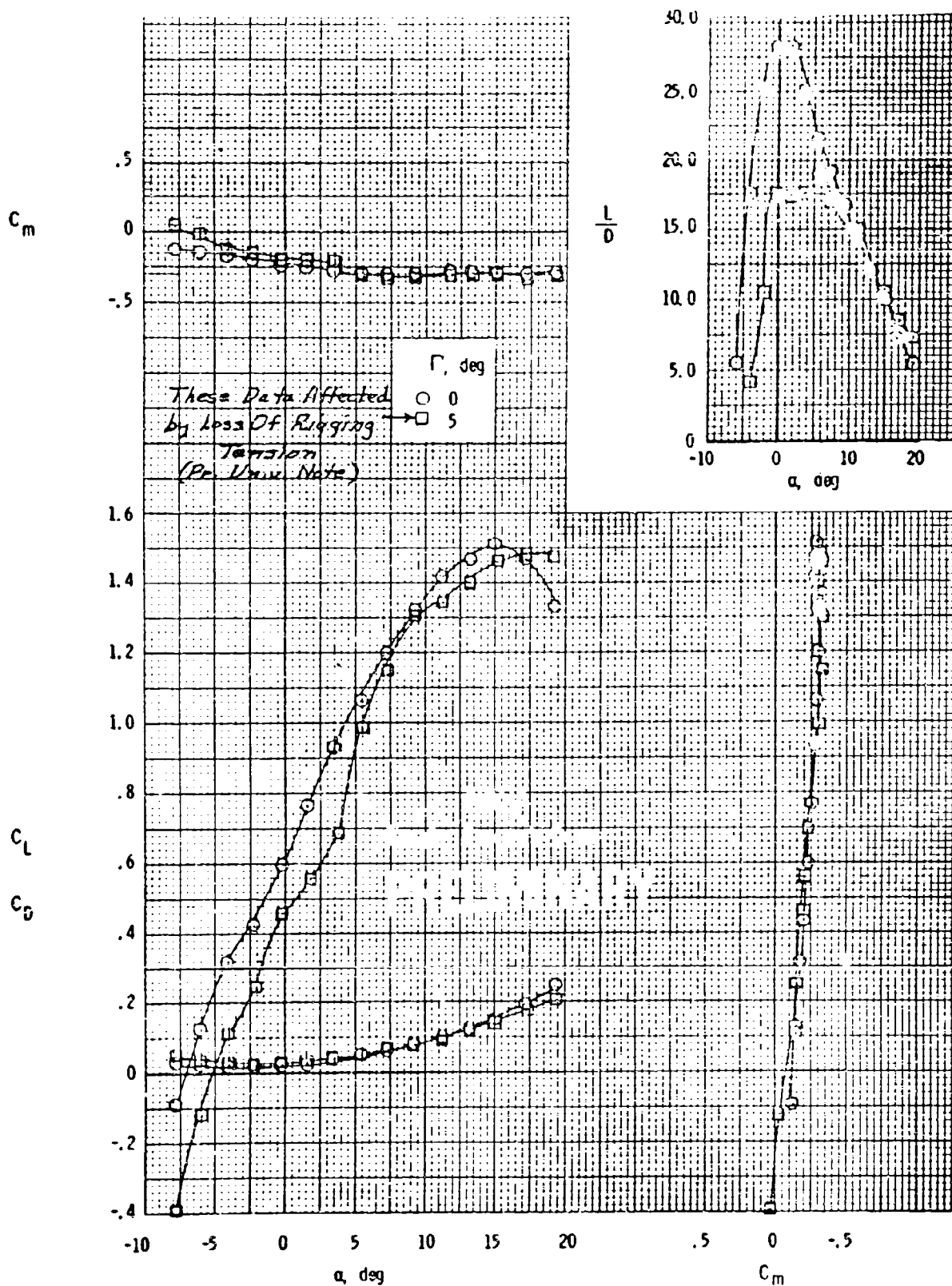


(a) Longitudinal characteristics.

Figure 22 Effect of sideslip on the characteristics of the wing with  $0^\circ$  dihedral.  $q \approx 6.88$ .

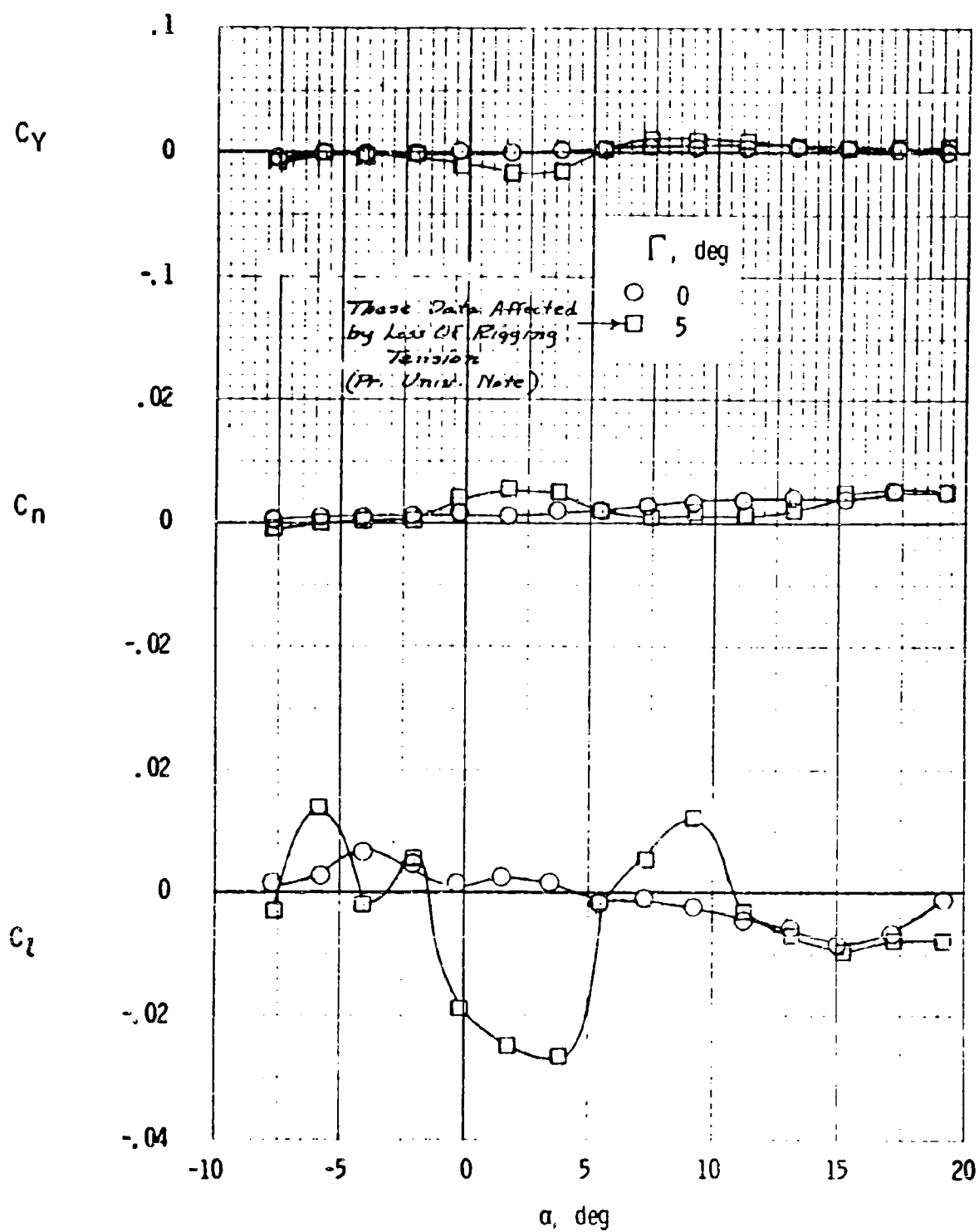


(b) Lateral characteristics.



(a) Longitudinal characteristics.

Figure 23 Effect of dihedral on the characteristics of the wing for  $\beta = 0^\circ$ ,  $q \approx 6.77$ .



(b) Lateral characteristics.

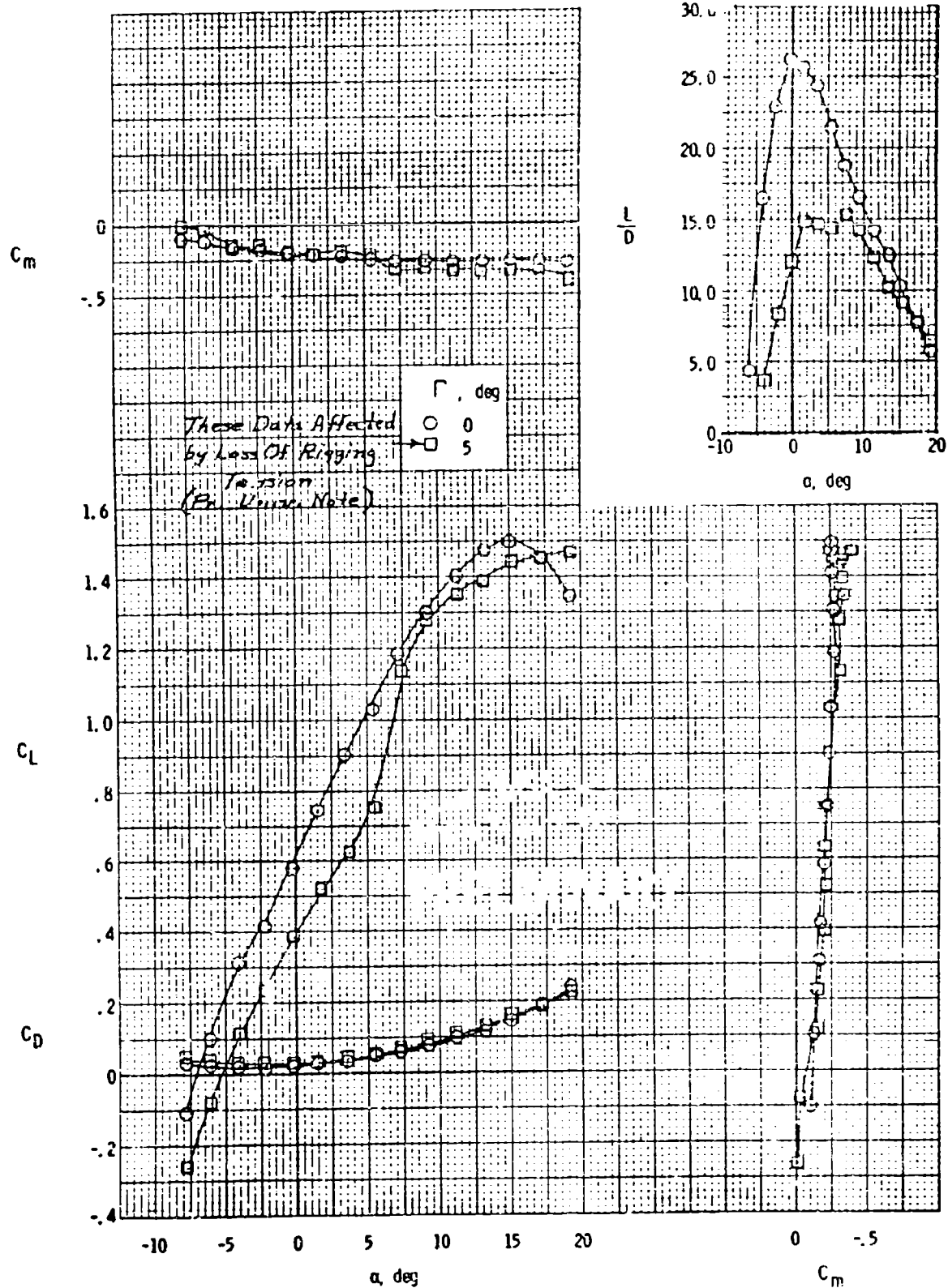
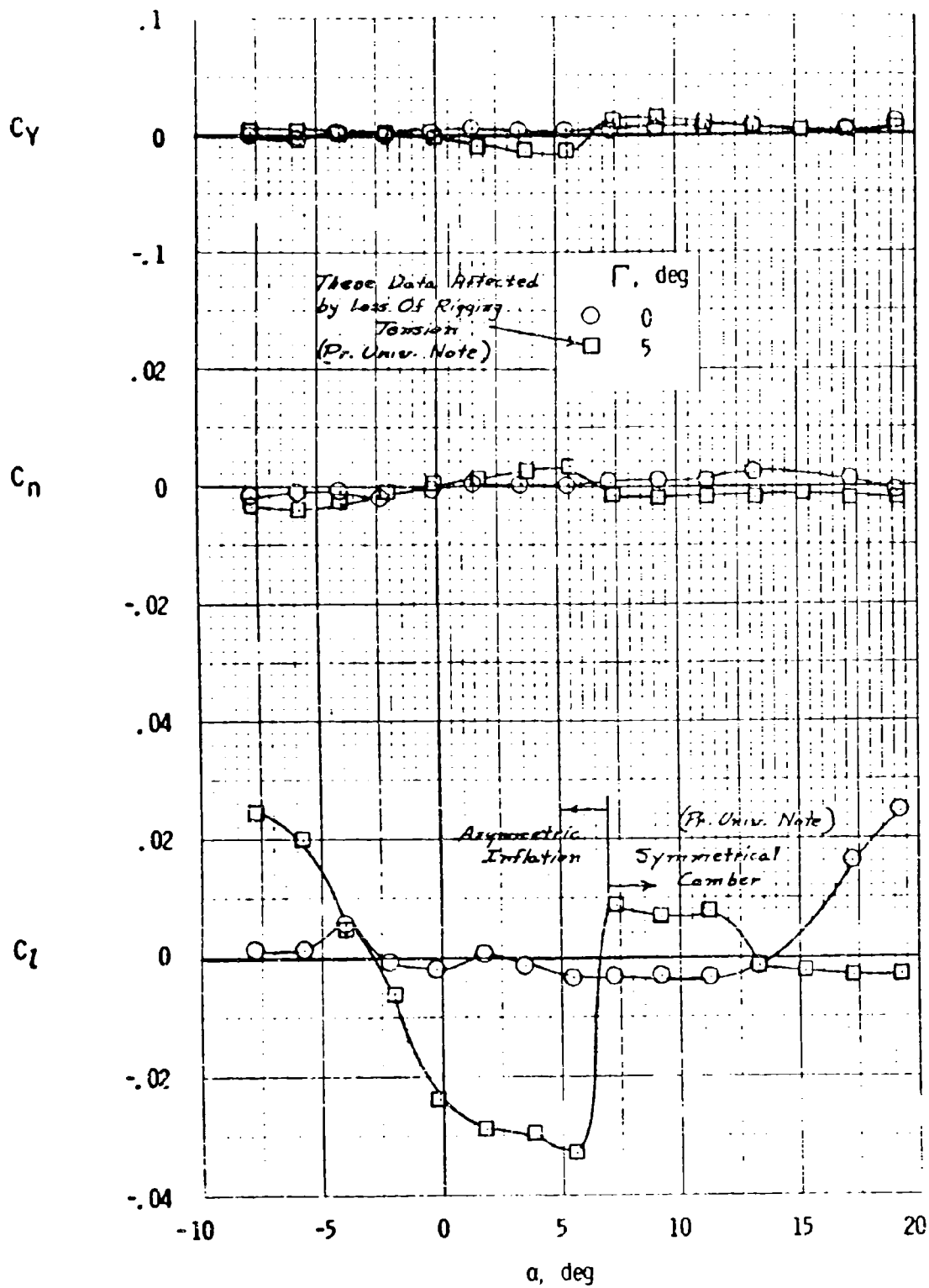
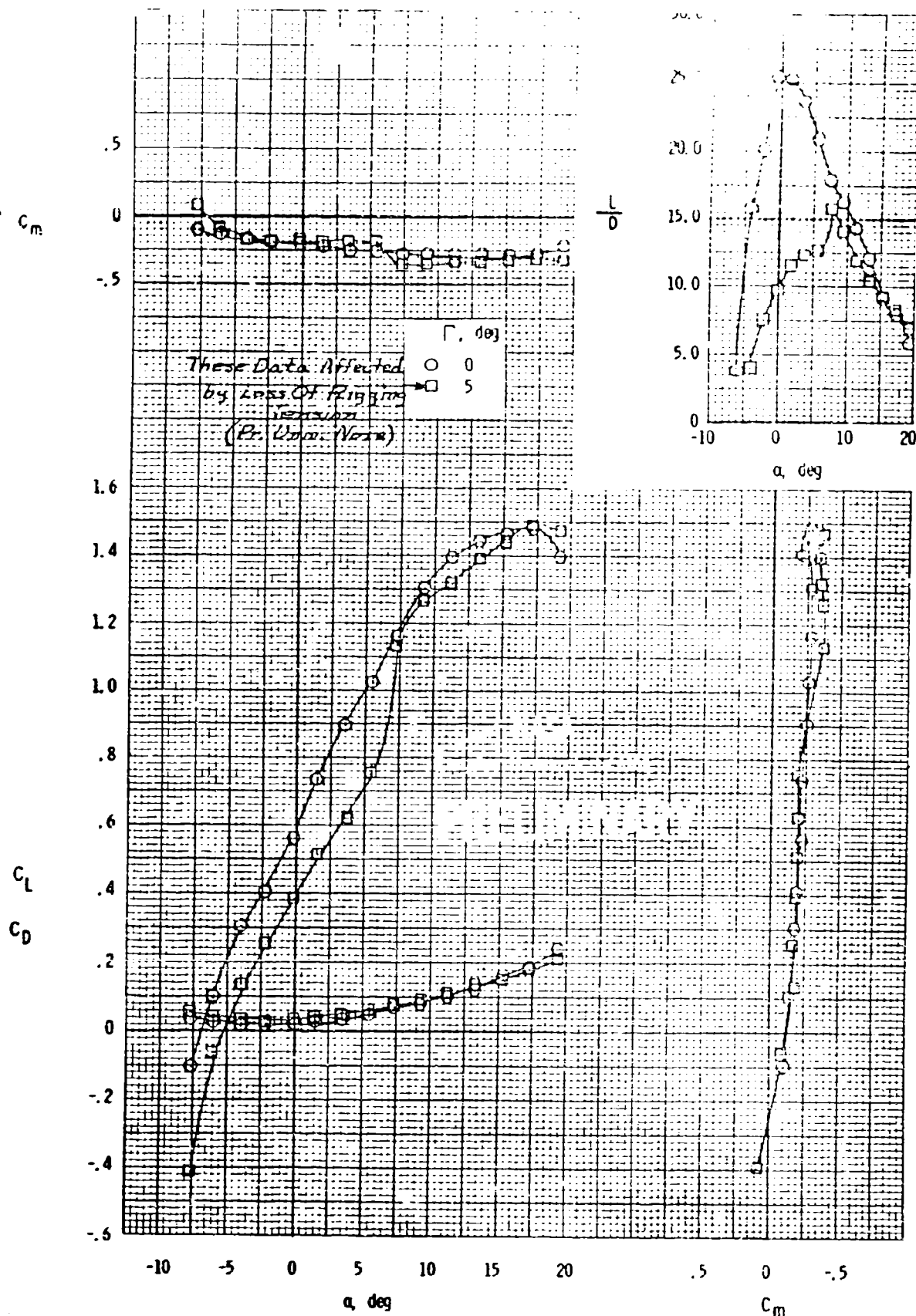


Figure 24 Effect of dihedral on the characteristics of the wing for  $\beta = -5^\circ$ ,  $q \approx 6.78$

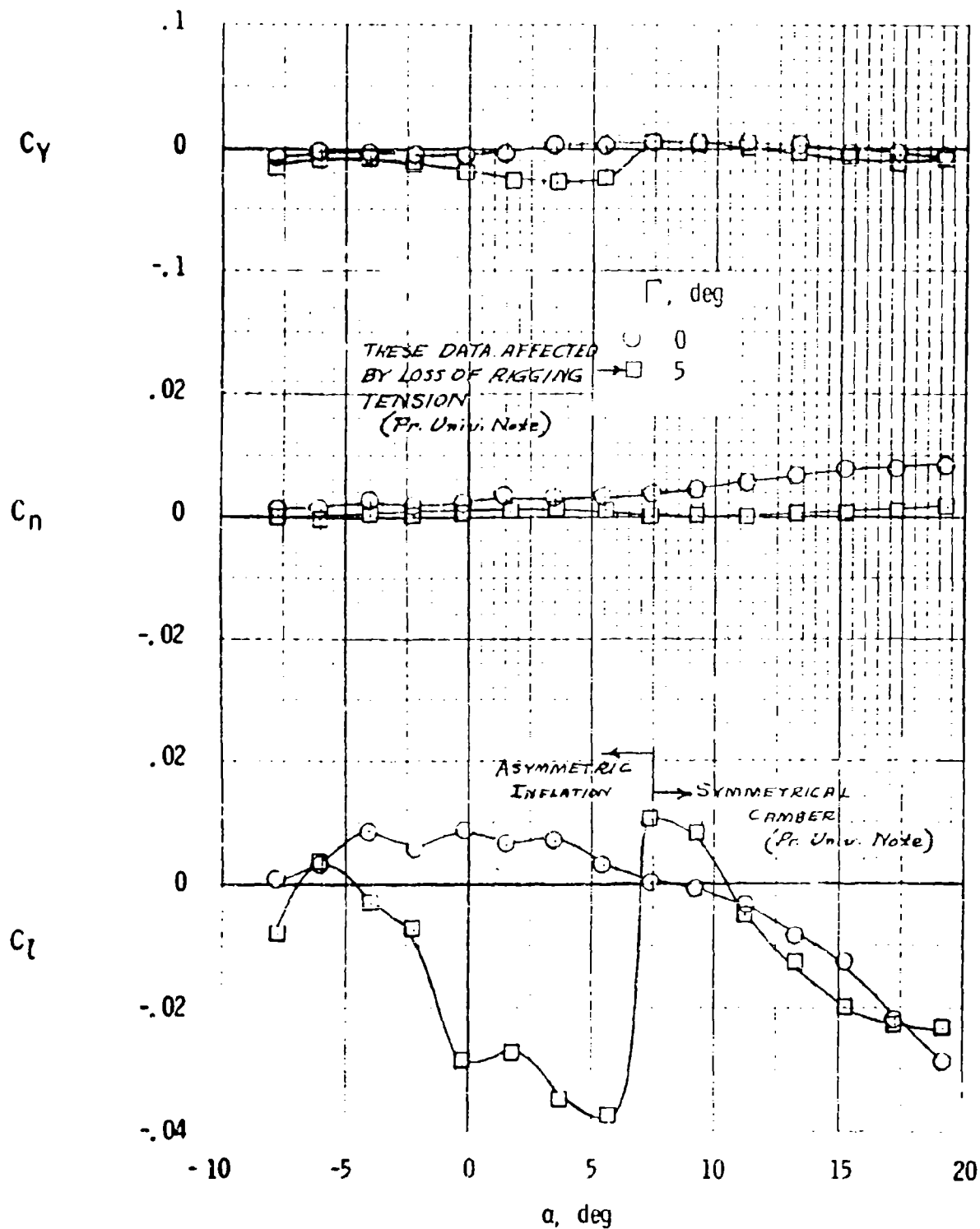


(b) Lateral characteristics.



(a) Longitudinal characteristics.

Figure 25 Effect of dihedral on the characteristics of the wing for  $\beta = 5^\circ$ ,  $u \approx 6.81$ .



(b) Lateral characteristics.



FIGURE 26 DRAG STRUT TENSION VERSUS  
ANGLE OF ATTACK



FIGURE 27 LIFT STRUT TENSION VERSUS  
ANGLE OF ATTACK

0 9 + 3.26  
0 0 + 5.83

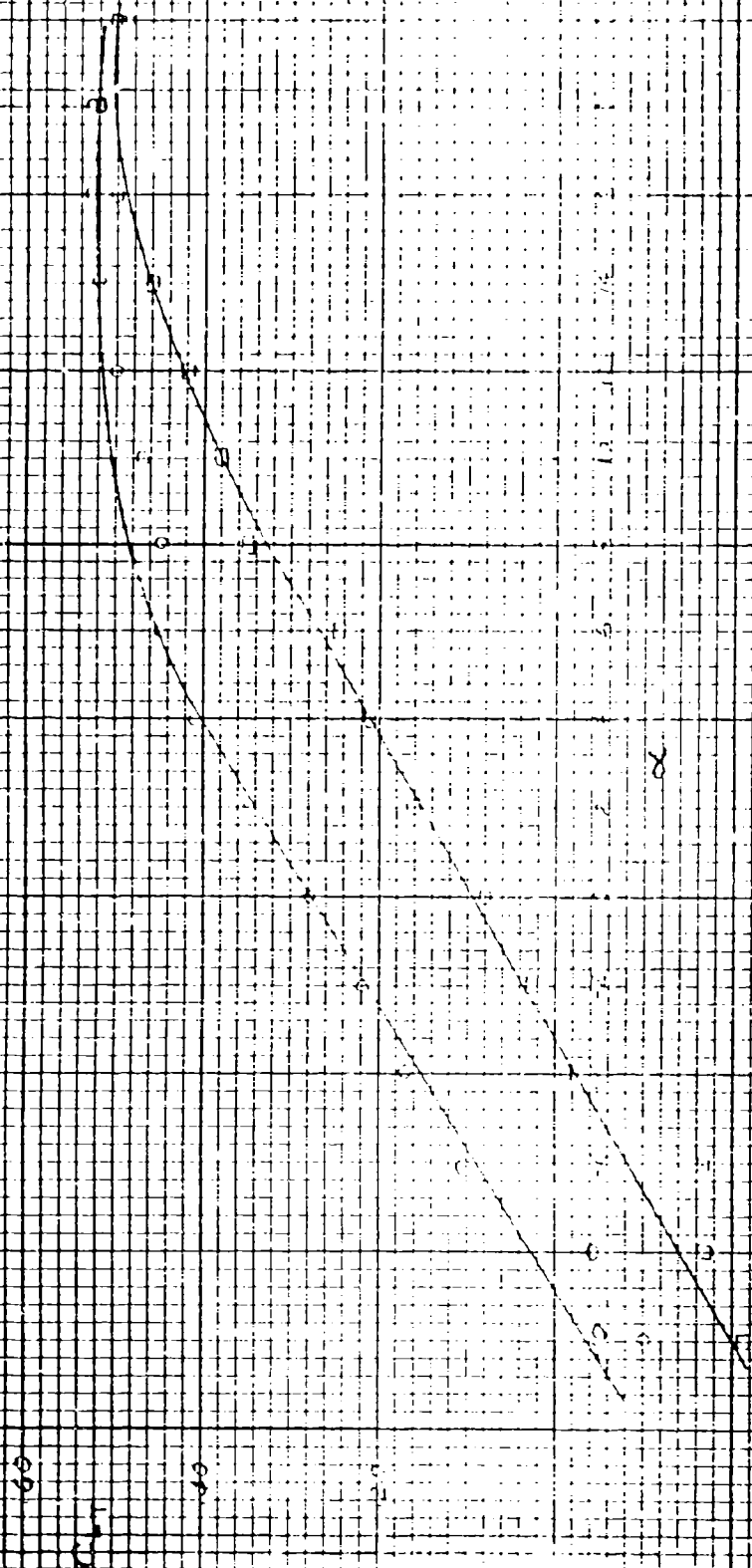


FIGURE 28 INBOARD BRIDLE TENSION VERSUS  
ANGLE OF ATTACK

$q = 3.26$

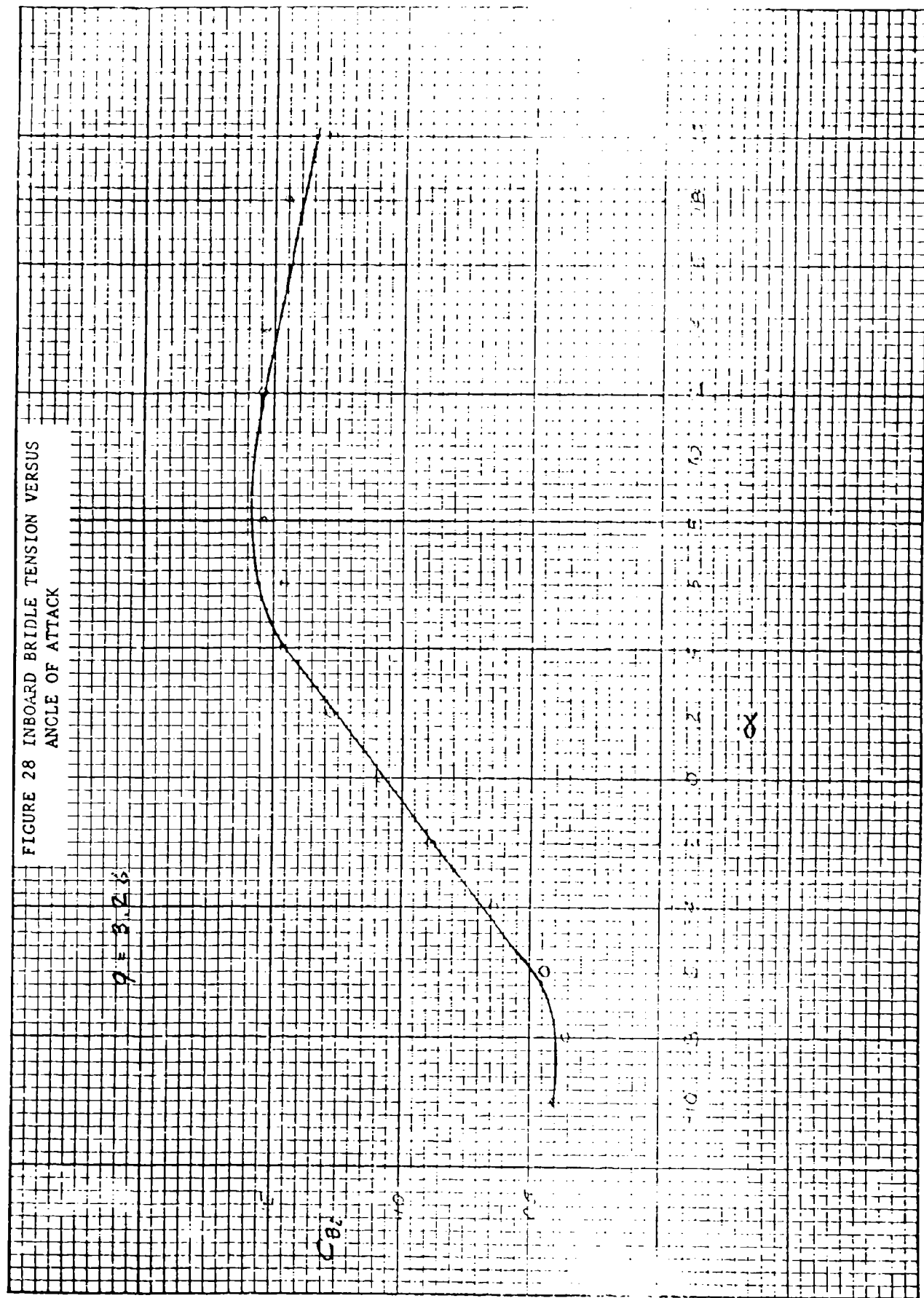


FIGURE 29 CENTER BRIDLE TENSION VERSUS

ANGLE OF ATTACK

ALL BRIDLES  
CENTER BRIDLE TENSION

$\gamma = 3.26$

0.05

0.10

0.15

0.20

$\alpha$

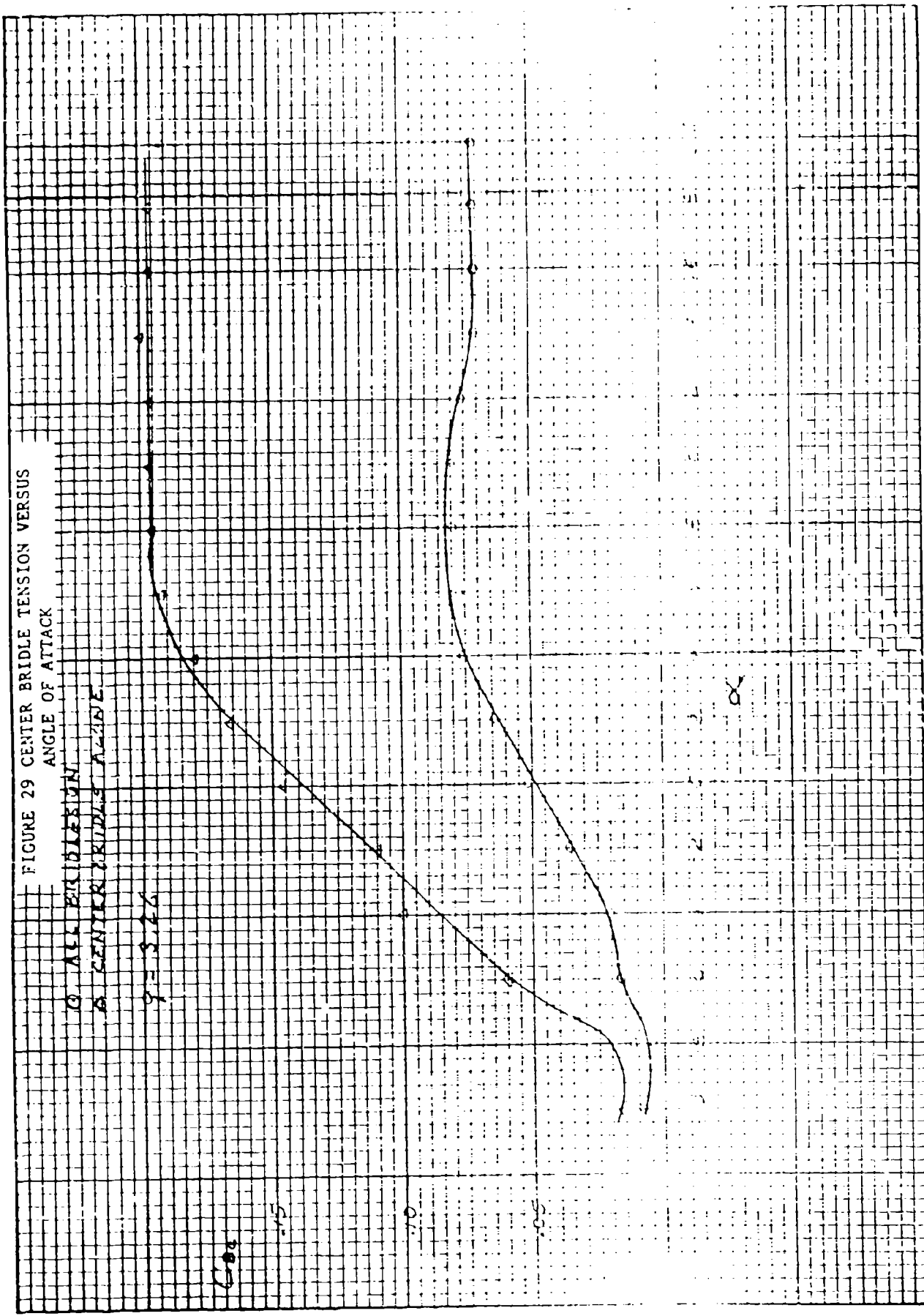




FIGURE 31 AILERON HINGE MOMENT VERSUS  
DEFLECTION ANGLE

$Q = 17.5$   
 $Q = 17.5$   
 $Q = 17.5$   
 $Q = 17.5$

$Q = 17.5$

0.00

0.00

0.00

0.00

0.00

$\delta_A$  (DOWN)

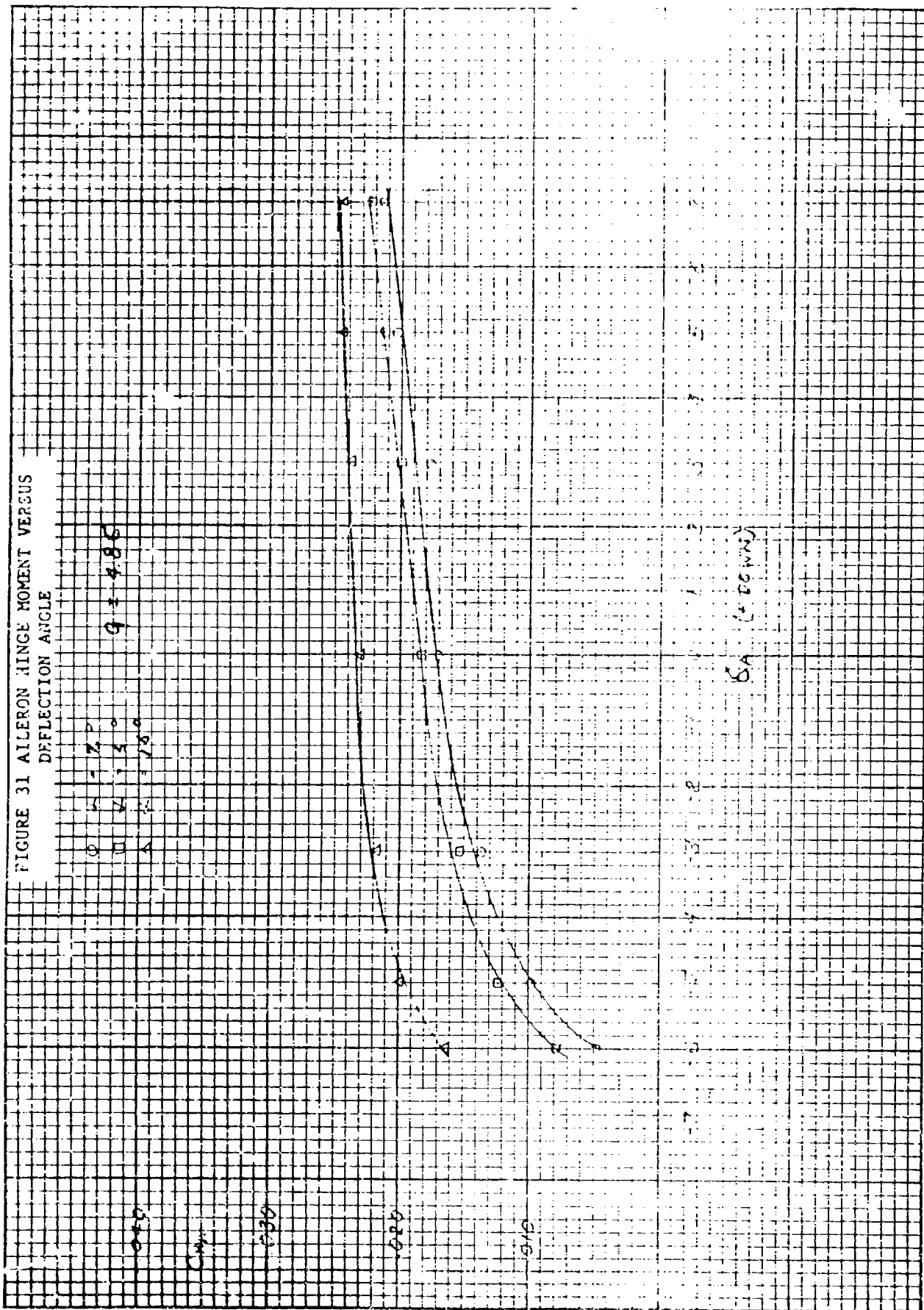


FIGURE 32 AILERON HINGE MOMENT VERSUS  
ANGLE OF ATTACK

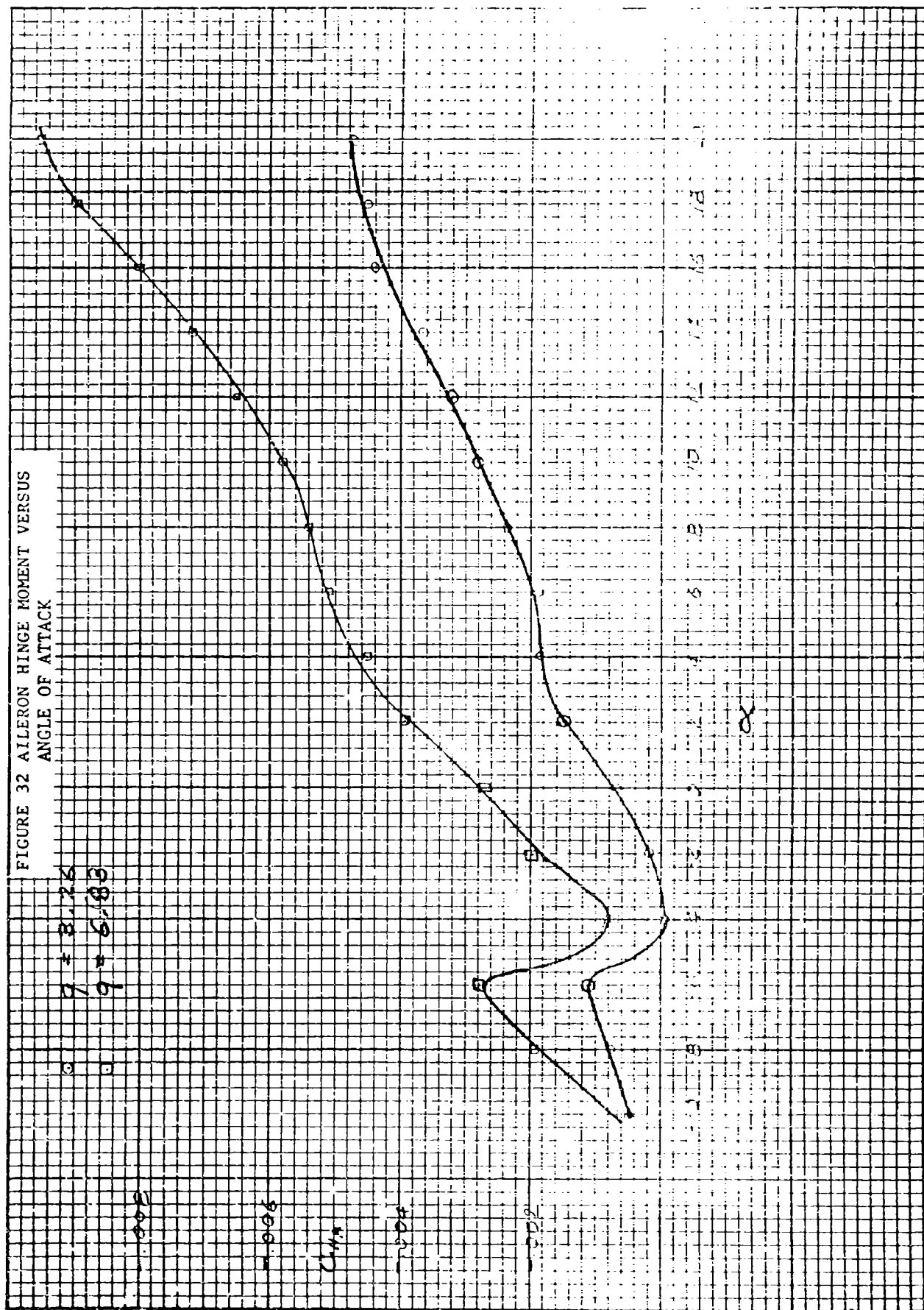


FIGURE 33 WIND OFF STATIC AILERON  
HINGE MOMENT HYSTERESIS

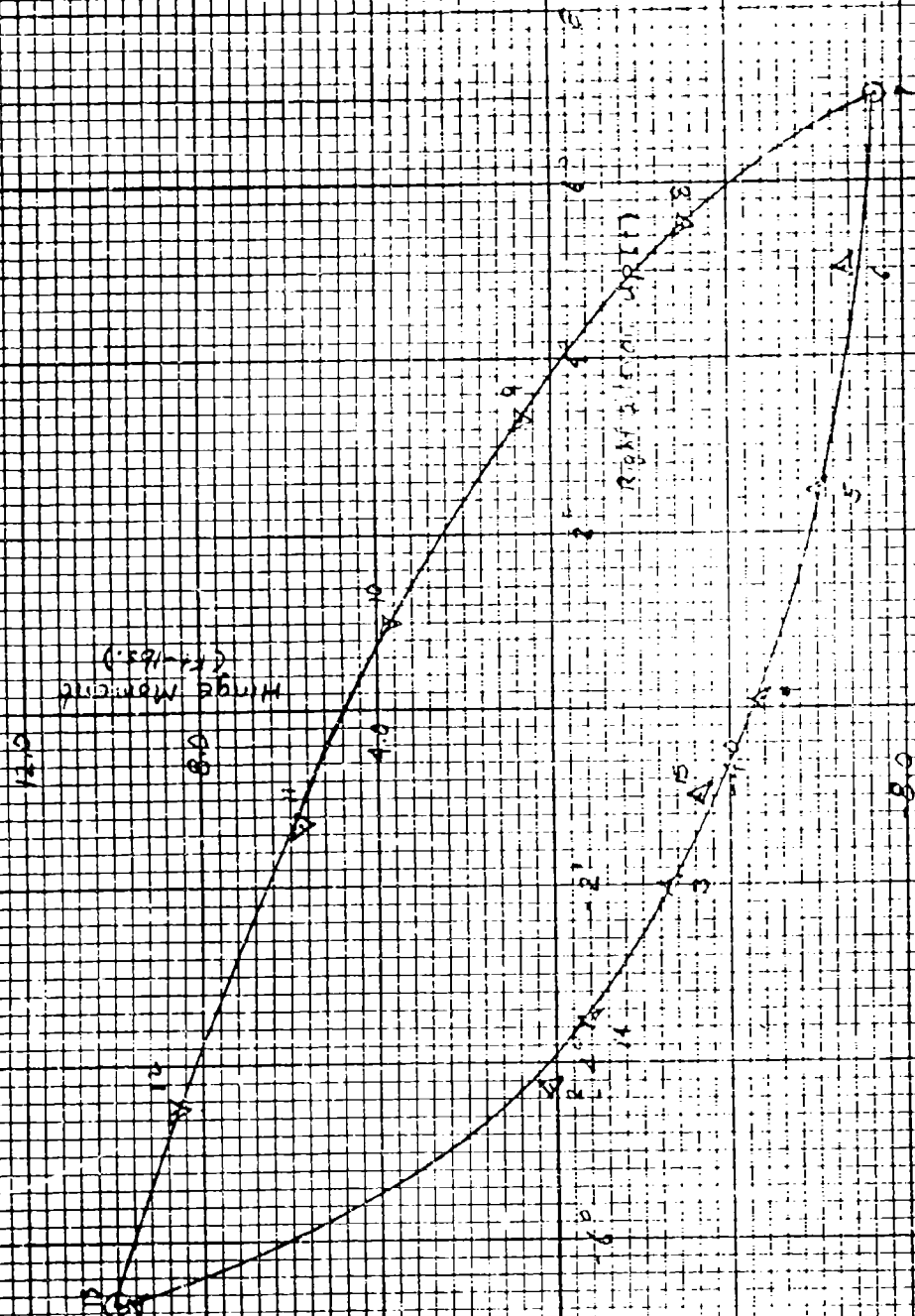




FIGURE 34 SPAR MOMENT VERSUS  
ANGLE OF ATTACK

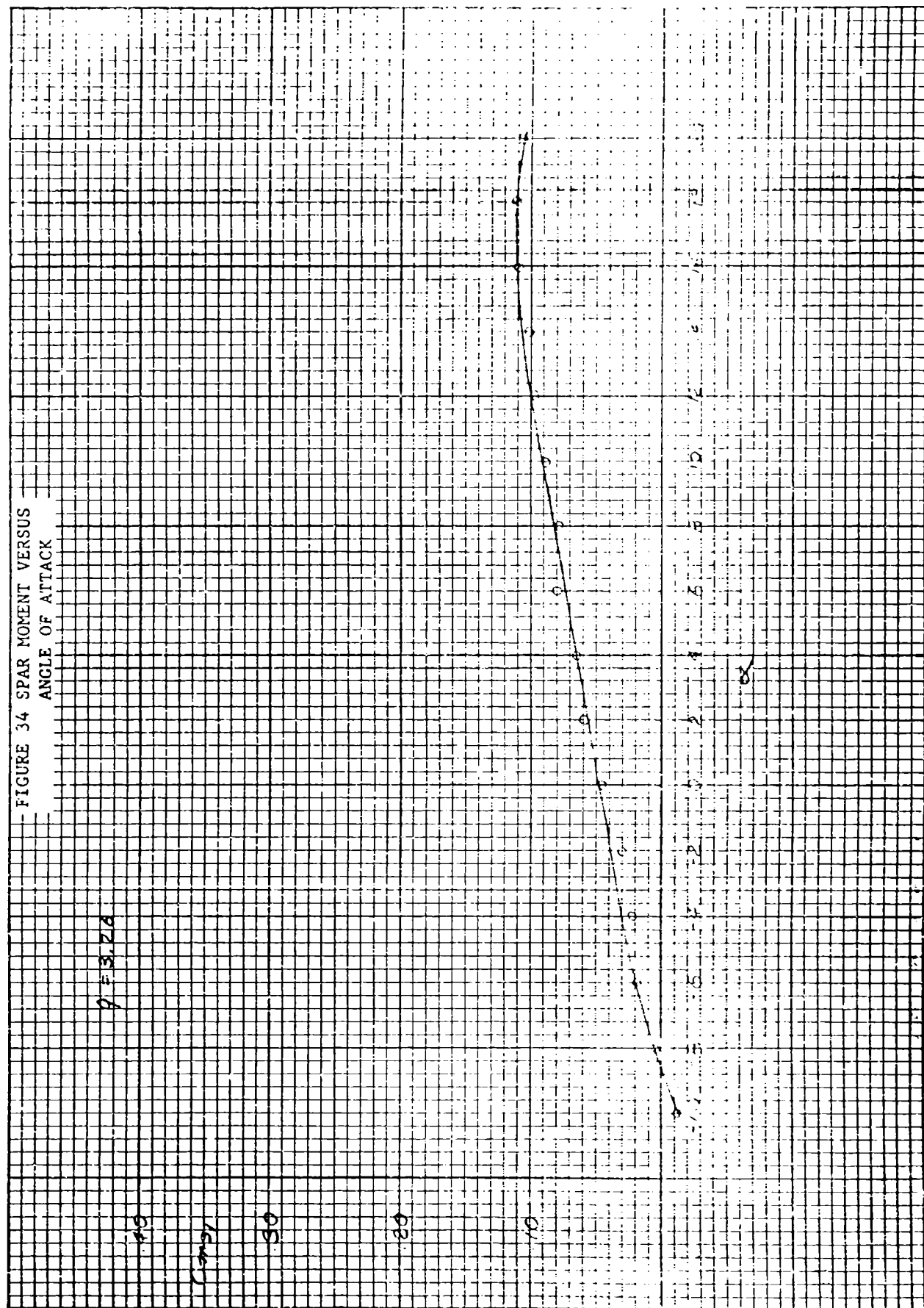


FIGURE 35 SPAR MOMENT VERSUS  
ANGLE OF ATTACK

$q = 32.6$

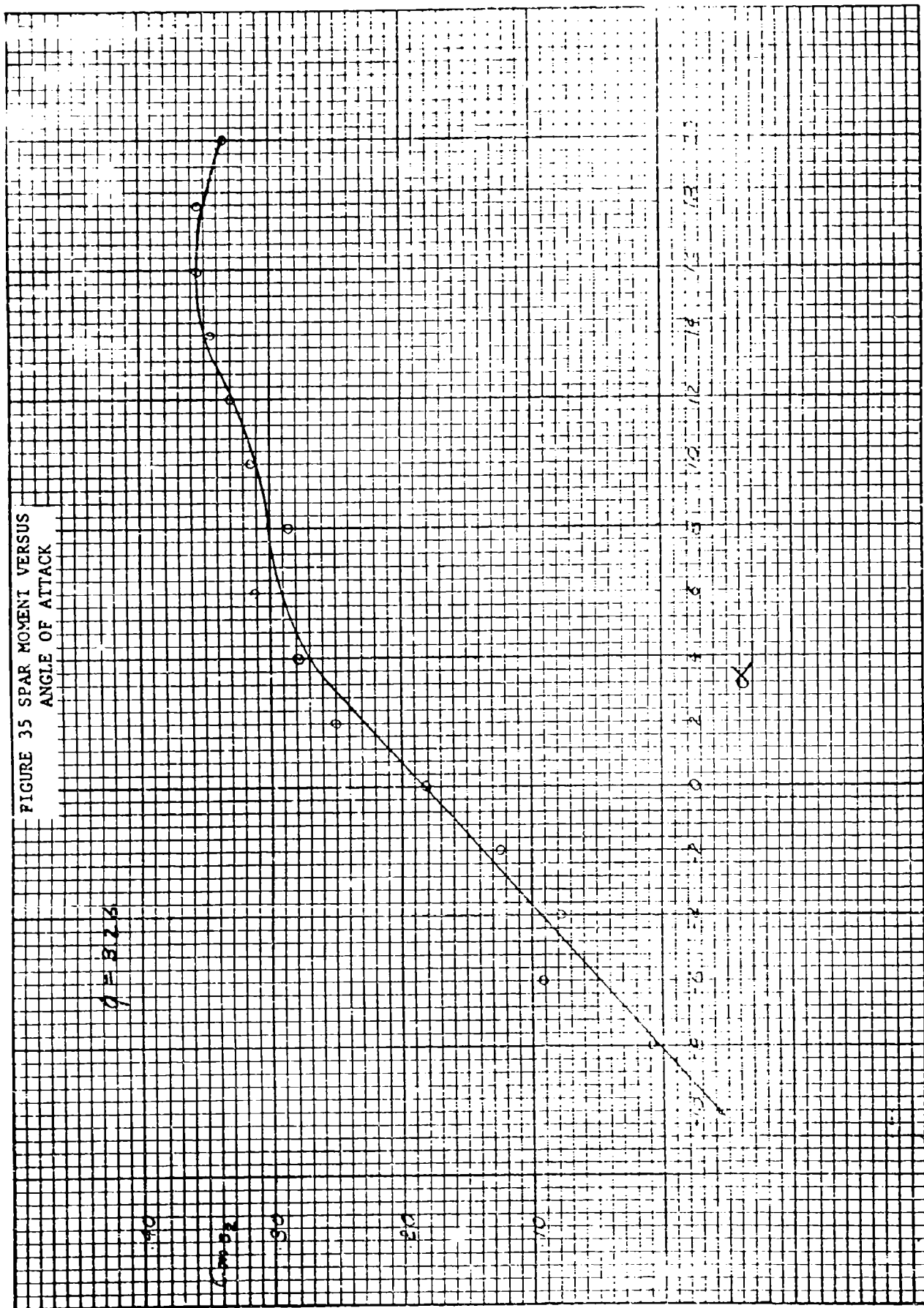


FIGURE 36 SPAR MOMENT VERSUS  
ANGLE OF ATTACK

$$q = 8.26$$

40

30

20

10

0

78

76

74

72

70

68

66

64

62

60

58

56

54

52

50

48

46

44

42

40

38

36

34

32

30

28

26

24

22

20

18

16

14

12

10

8

6

4

2

0

-2

-4

-6

-8

-10

-12

-14

-16

-18

-20

-22

-24

-26

-28

-30

-32

-34

-36

-38

-40

-42

-44

-46

-48

-50

-52

-54

-56

-58

-60

-62

-64

-66

-68

-70

-72

-74

-76

-78

-80

-82

-84

-86

-88

-90

-92

-94

-96

-98

-100

-102

-104

-106

-108

-110

-112

-114

-116

-118

-120

-122

-124

-126

-128

-130

-132

-134

-136

-138

-140

-142

-144

-146

-148

-150

-152

-154

-156

-158

-160

-162

-164

-166

-168

-170

-172

-174

-176

-178

-180

-182

-184

-186

-188

-190

-192

-194

-196

-198

-200

-202

-204

-206

-208

-210

-212

-214

-216

-218

-220

-222

-224

-226

-228

-230

-232

-234

-236

-238

-240

-242

-244

-246

-248

-250

-252

-254

-256

-258

-260

-262

-264

-266

-268

-270

-272

-274

-276

-278

-280

-282

-284

-286

-288

-290

-292

-294

-296

-298

-300

-302

-304

-306

-308

-310

-312

-314

-316

-318

-320

-322

-324

-326

-328

-330

-332

-334

-336

-338

-340

-342

-344

-346

-348

-350

-352

-354

-356

-358

-360

-362

-364

-366

-368

-370

-372

-374

-376

-378

-380

-382

-384

-386

-388

-390

-392

-394

-396

-398

-400

-402

-404

-406

-408

-410

-412

-414

-416

-418

-420

-422

-424

-426

-428

-430

-432

-434

-436

-438

-440

-442

-444

-446

-448

-450

-452

-454

-456

-458

-460

-462

-464

-466

-468

-470

-472

-474

-476

-478

-480

-482

-484

-486

-488

-490

-492

-494

-496

-498

-500

-502

FIGURE 37 SPAR MOMENT VERSUS  
ANGLE OF ATTACK

$q = 3.26$

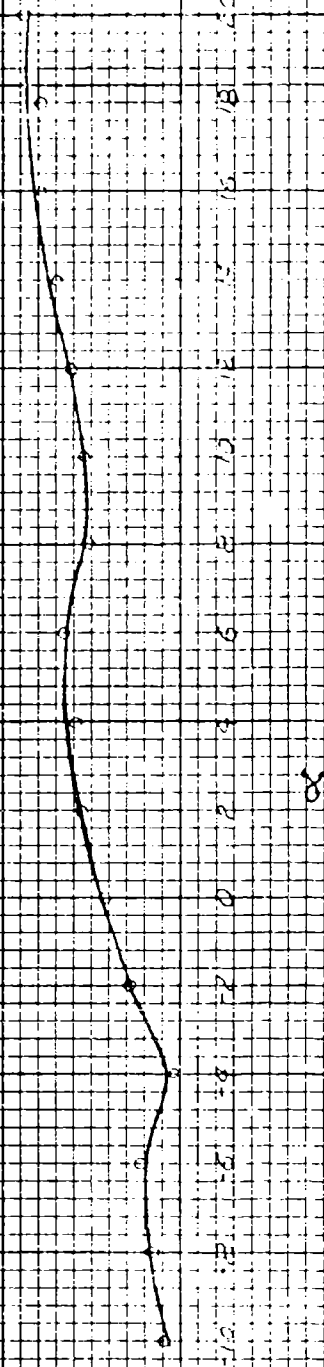
40

30

20

10

0



$\alpha$

FIGURE 38 MOMENT VERSUS STATION

$\phi = 3.26$   $\alpha = 0^\circ$

S.W. V BASIC

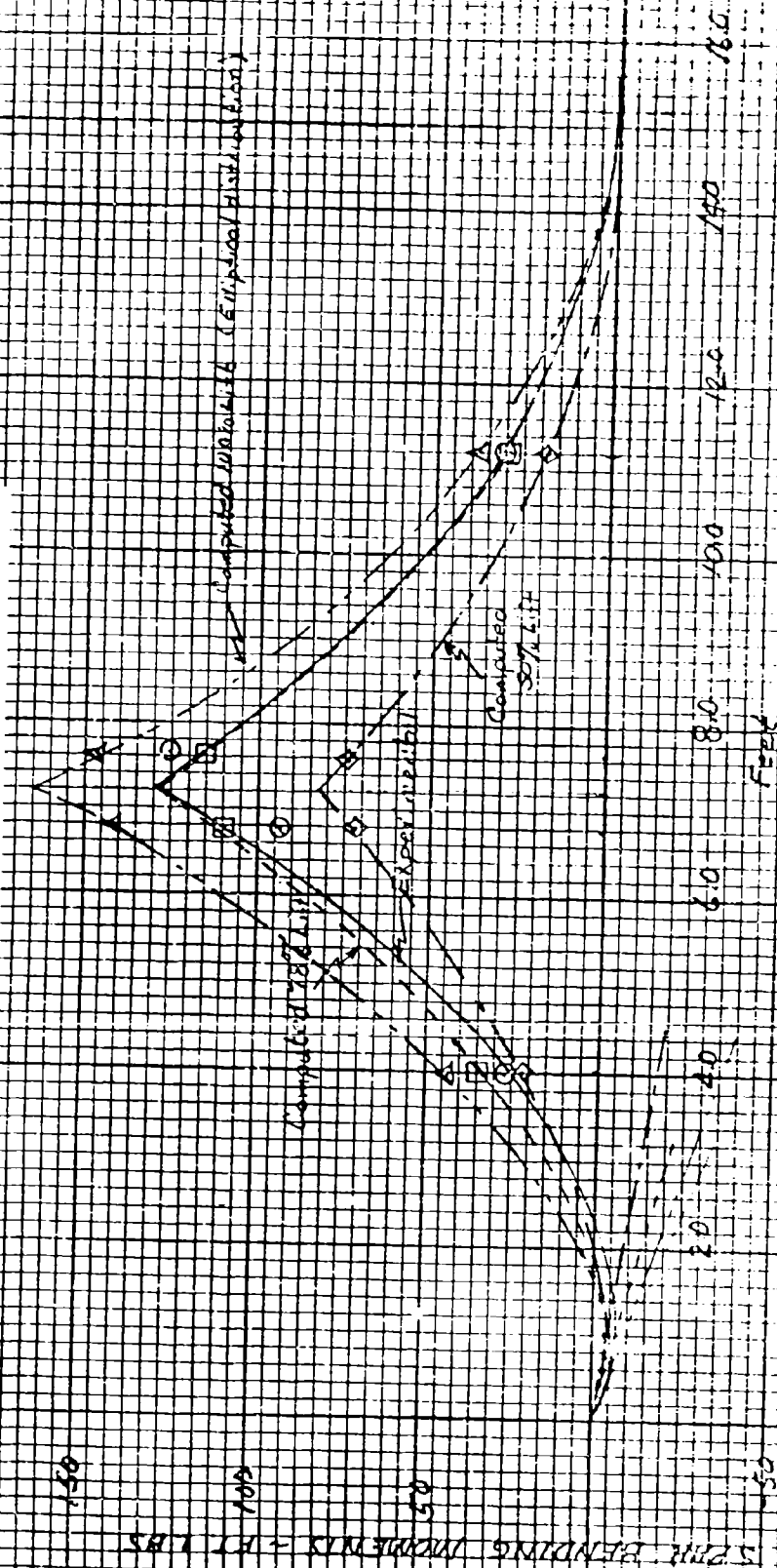


FIGURE 39 SPAR ROOT LIFT VERSUS  
ANGLE OF ATTACK

$q = 312.3$

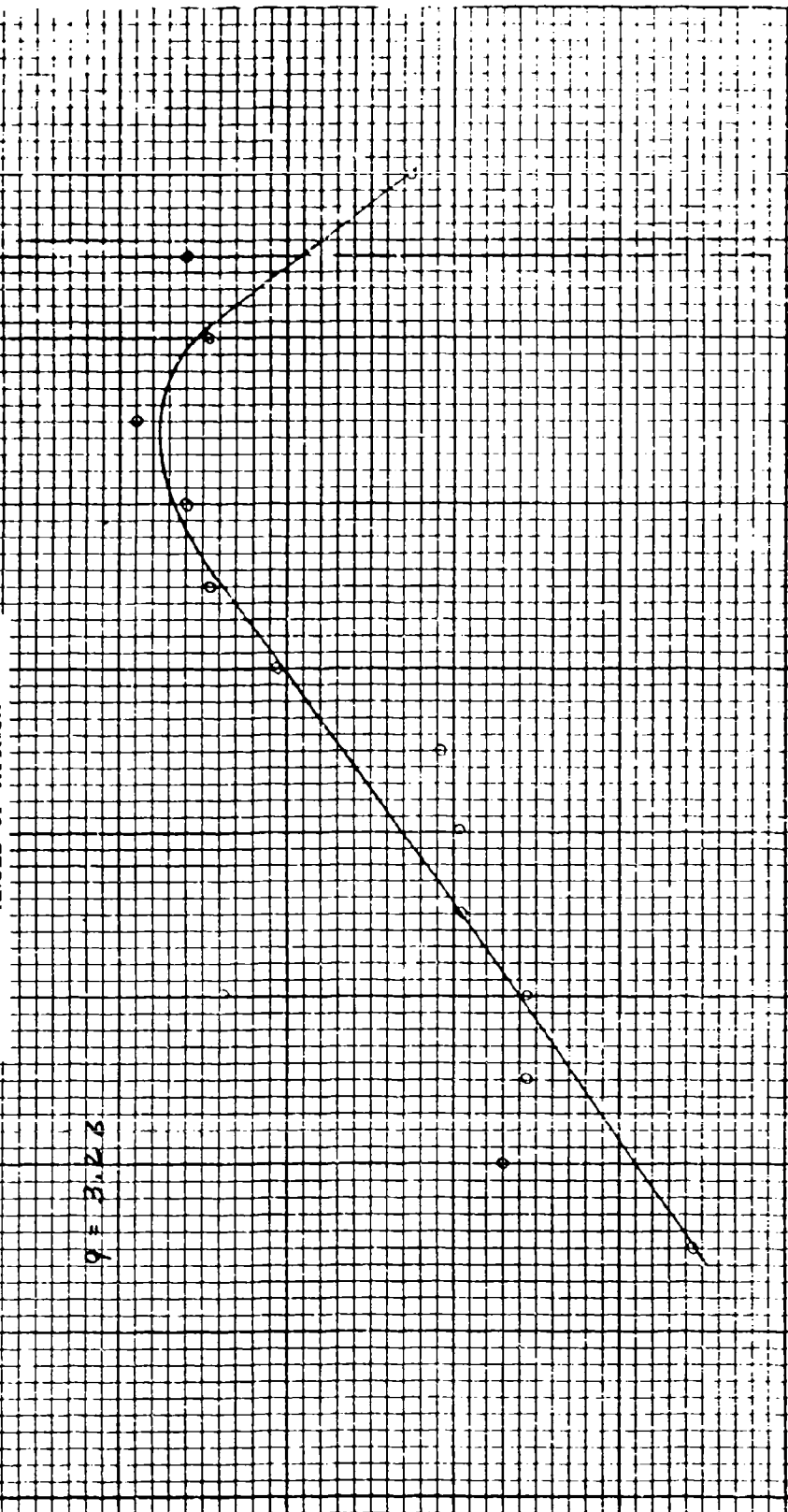
$C_{L1}$

0.9

0.8

0.7

0.6



0.6 0.7 0.8 0.9 1.0 1.1 1.2 1.3 1.4 1.5 1.6 1.7 1.8 1.9 2.0 2.1 2.2 2.3 2.4 2.5 2.6 2.7 2.8 2.9 3.0 3.1 3.2 3.3 3.4 3.5 3.6 3.7 3.8 3.9 4.0 4.1 4.2 4.3 4.4 4.5 4.6 4.7 4.8 4.9 5.0 5.1 5.2 5.3 5.4 5.5 5.6 5.7 5.8 5.9 6.0 6.1 6.2 6.3 6.4 6.5 6.6 6.7 6.8 6.9 7.0 7.1 7.2 7.3 7.4 7.5 7.6 7.7 7.8 7.9 8.0 8.1 8.2 8.3 8.4 8.5 8.6 8.7 8.8 8.9 9.0 9.1 9.2 9.3 9.4 9.5 9.6 9.7 9.8 9.9 10.0

$\alpha$

FIGURE 40 SPAR ROOT DRAG VERSUS  
ANGLE OF ATTACK

○ ALL BIRCHES D.N.  
○ ALL BIRCHES D.T.F.

$q = 326$

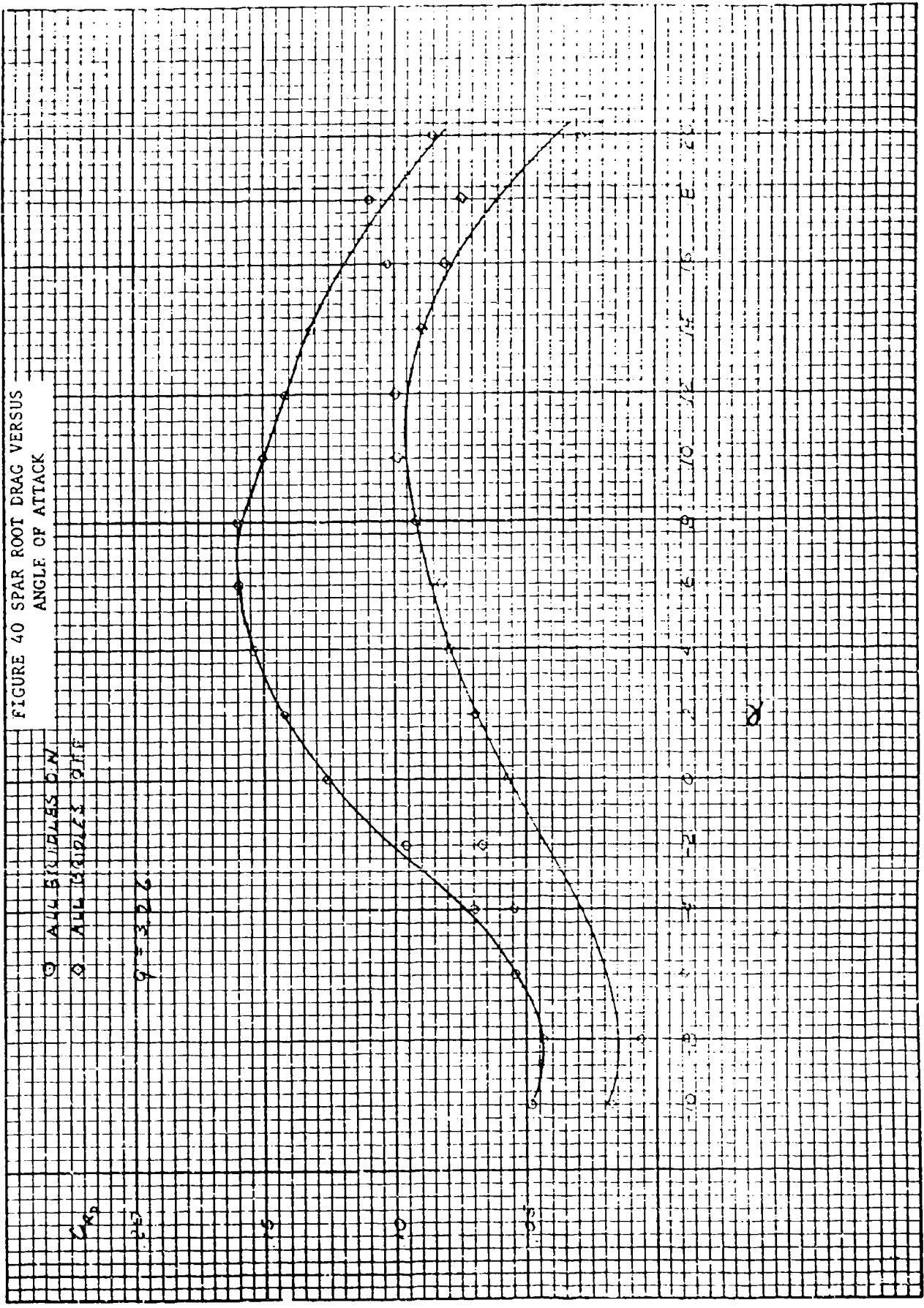


FIGURE 41 SPAR ROOT COMPRESSION FORCE  
VERSUS ANGLE OF ATTACK

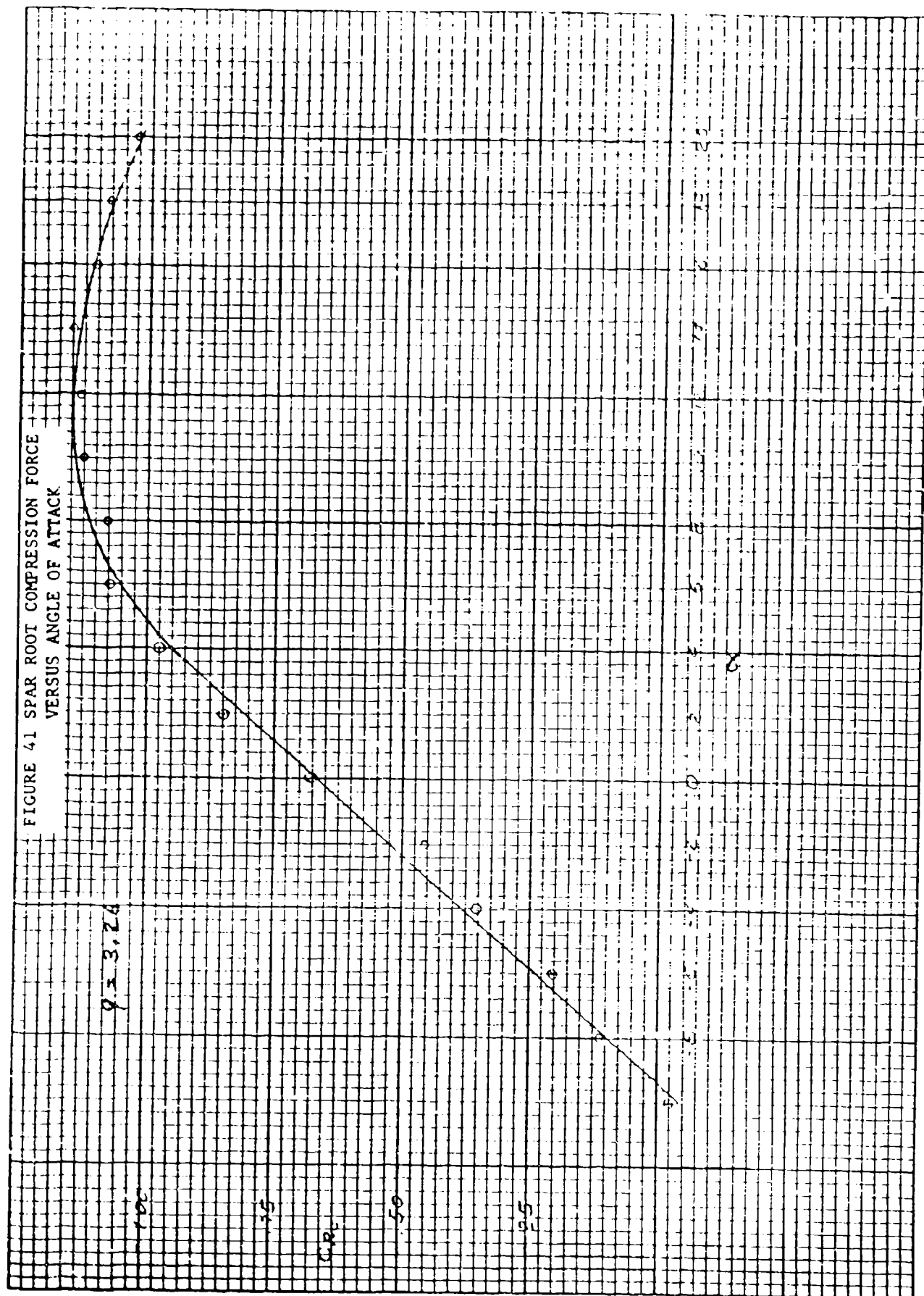




FIGURE 42 SPAR ROOT TORQUE VERSUS  
ANGLE OF ATTACK

$$q = 3.26$$

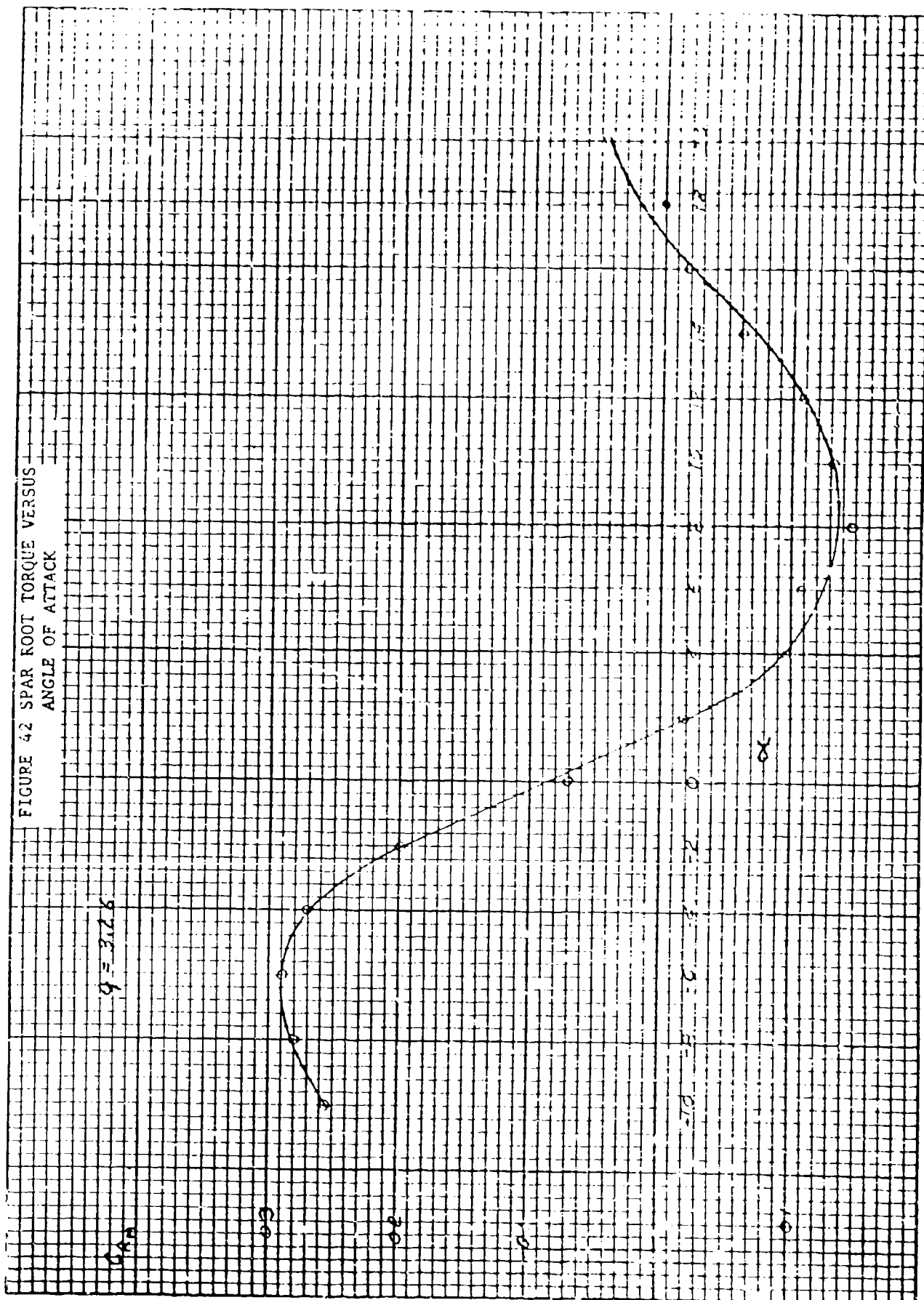


FIGURE 43 SPAR ROOT TORQUE VERSUS LIFT

$$q = 6.83$$

$C_{RM}$

0.02

0.01

0

-0.01

-0.02

-0.03

2

4

6

8

10

12

14

16

$C_L$

①

②

③

④

⑤

⑥

⑦

⑧

⑨

⑩

⑪

FIGURE 44 TRAILING WIRE TENSION VERSUS  
ANGLE OF ATTACK

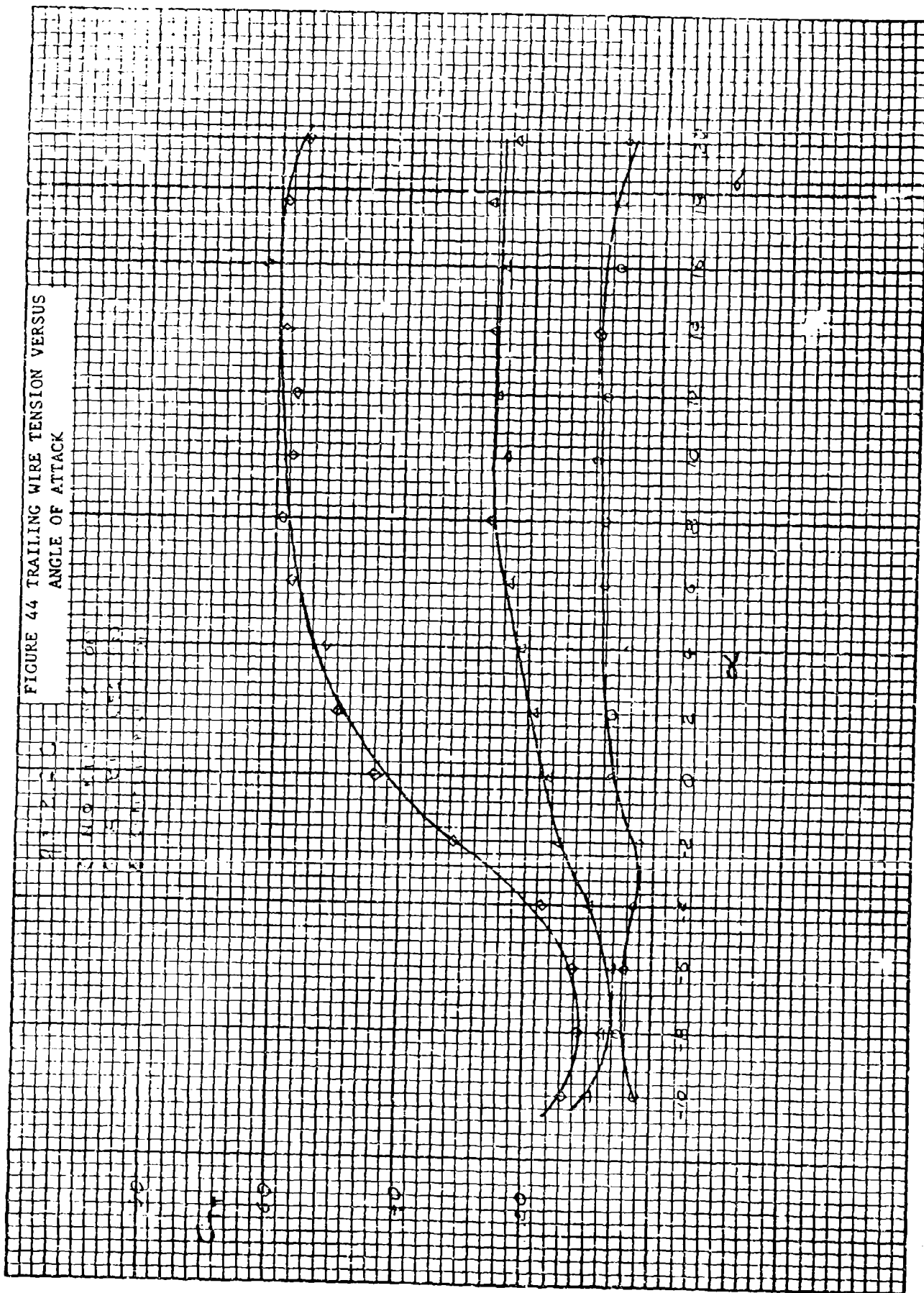


FIGURE 45 TRAILING EDGE X COMPONENT  
VERSUS ANGLE OF ATTACK

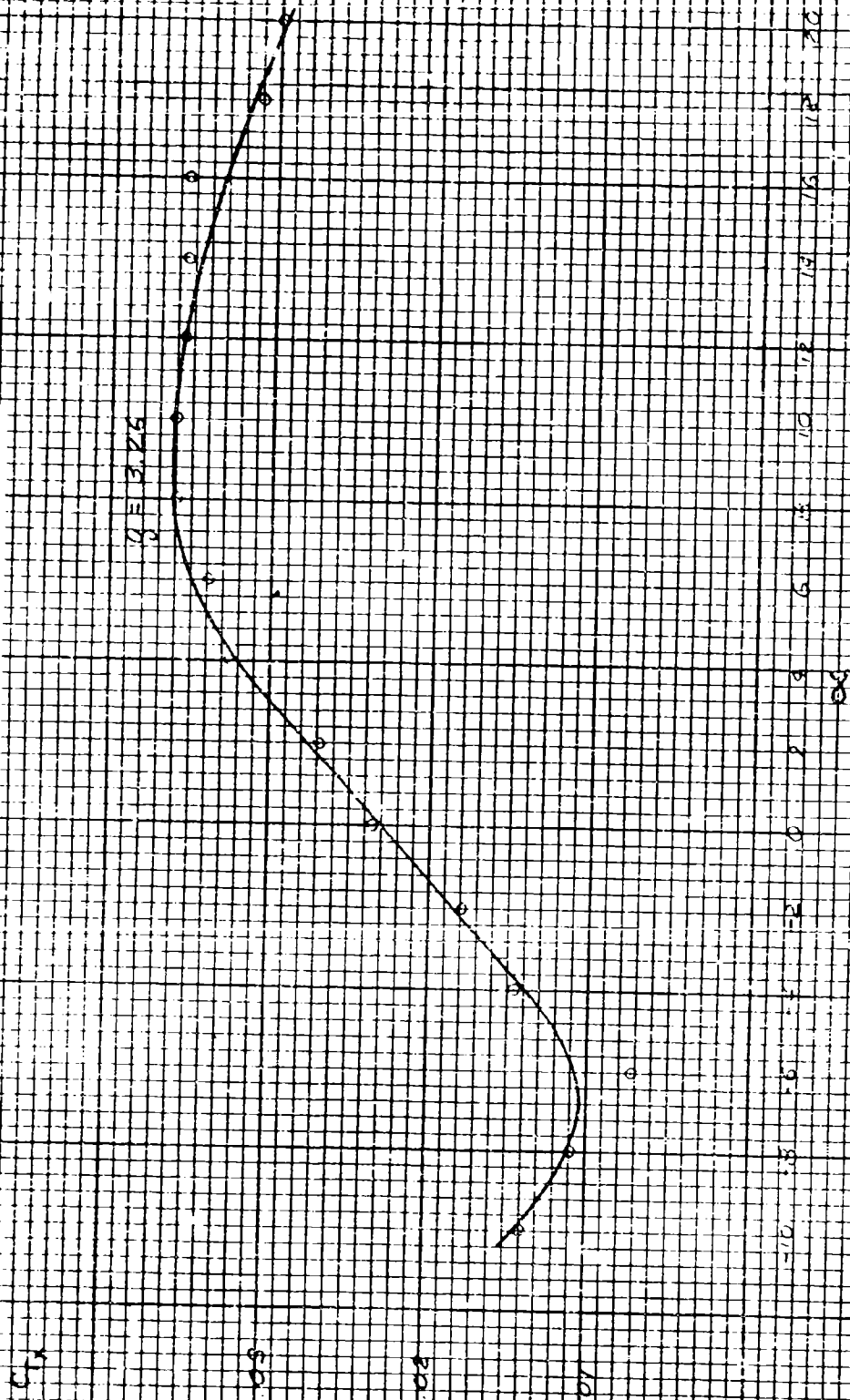




FIGURE 47 SAILWING V LINEARIZED DRAG POLARS  
AT 3.26 PSF DYNAMIC PRESSURE

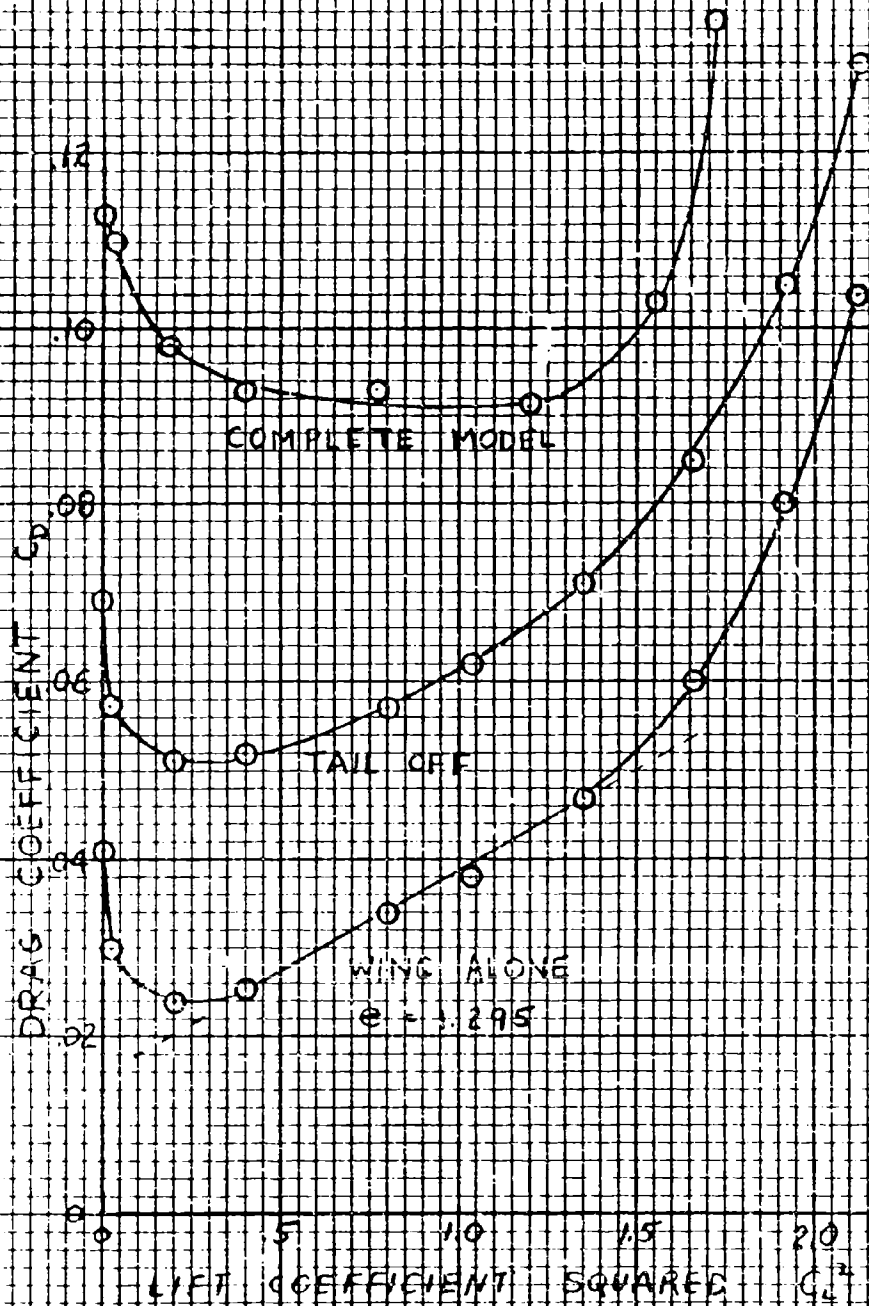


FIGURE 48 VARIATION OF MAXIMUM LIFT TO  
DRAG RATIO WITH DYNAMIC PRESSURE

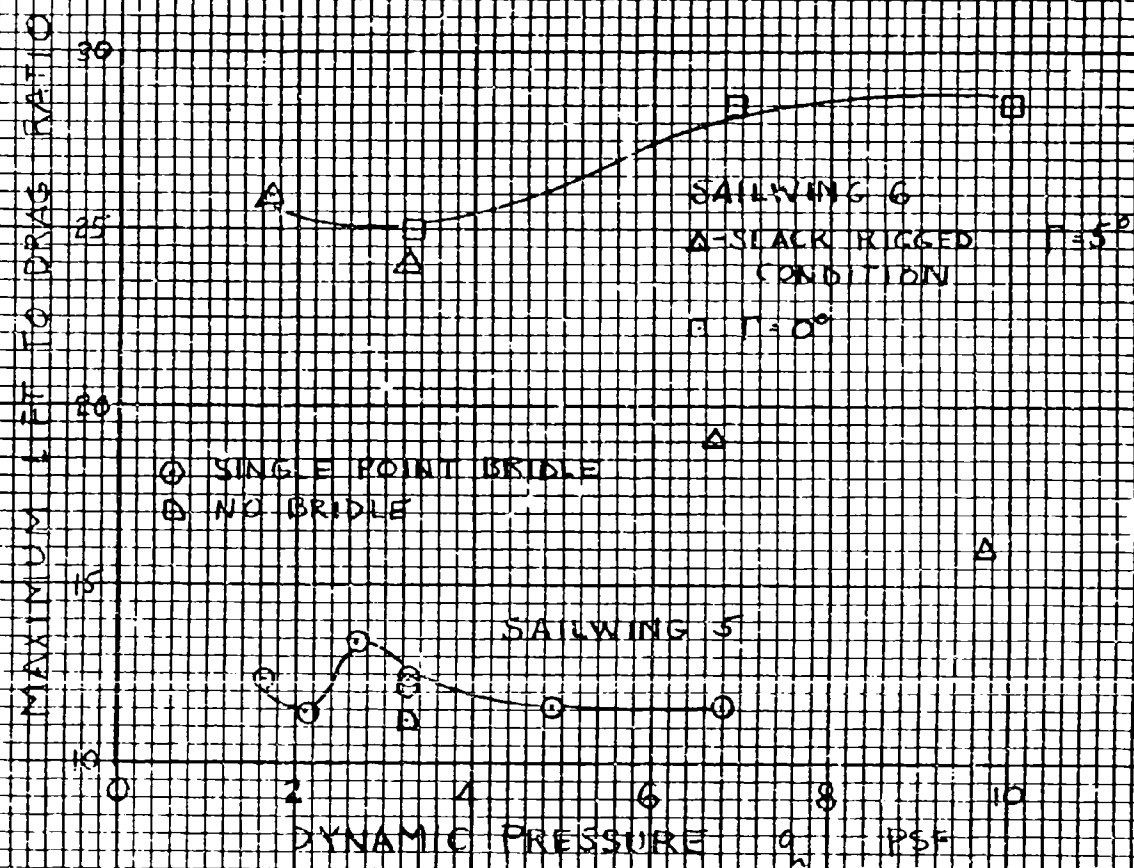




FIGURE 49 VARIATION OF MAXIMUM LIFT  
COEFFICIENT WITH DYNAMIC PRESSURE

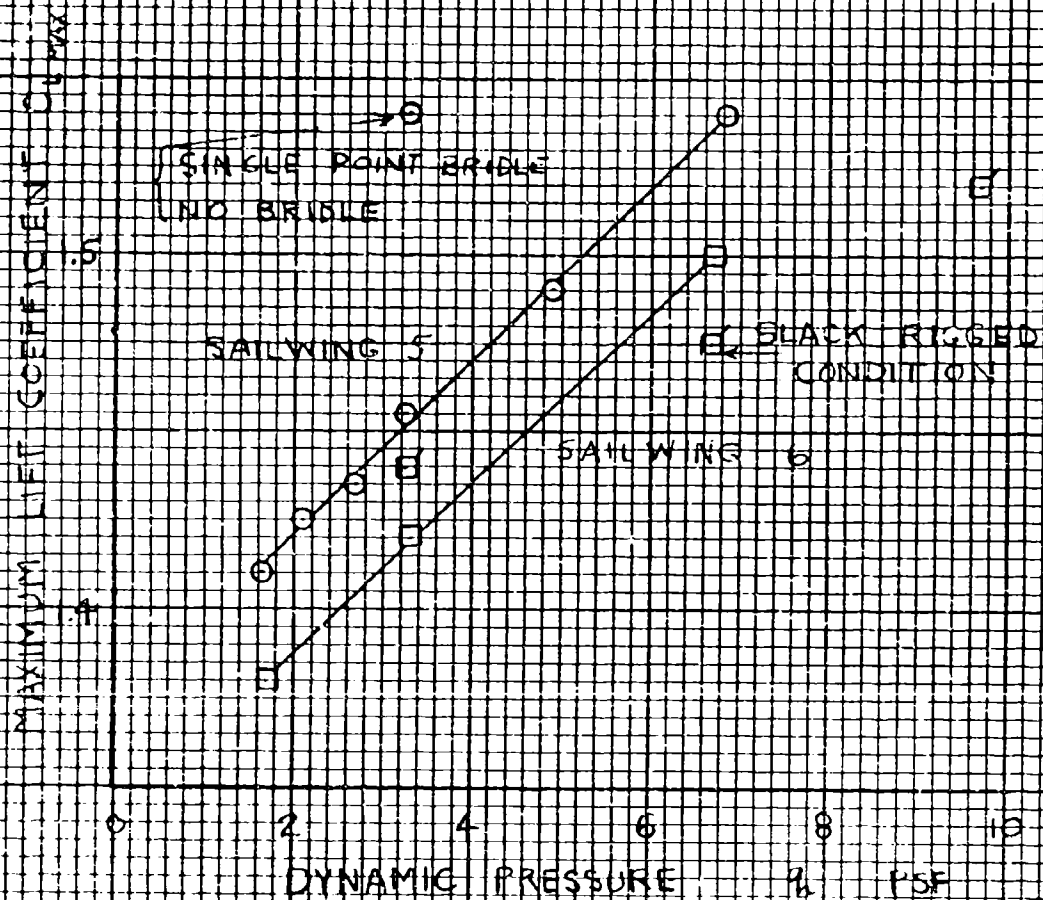




FIGURE 50 VARIATION OF LIFT CURVE  
SLOPE WITH DYNAMIC PRESSURE

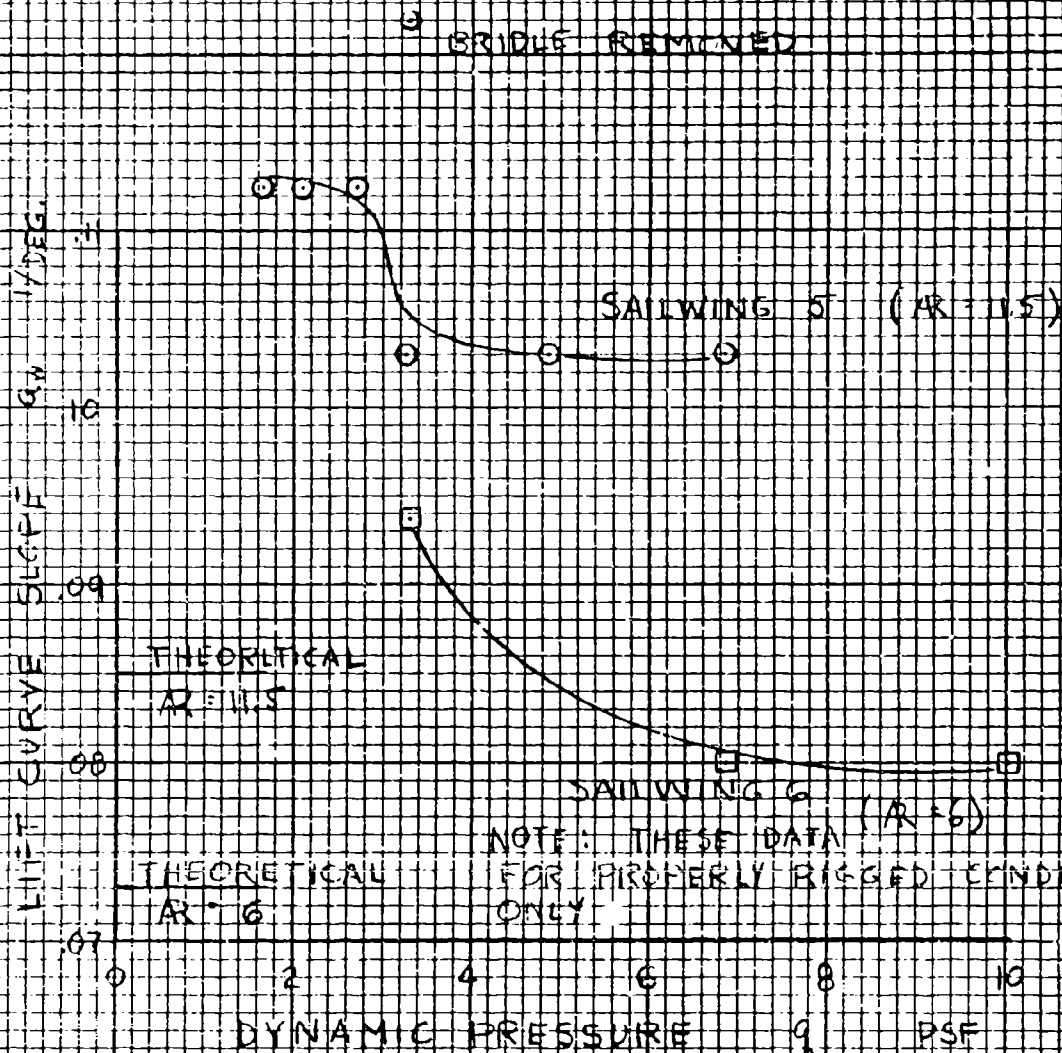


FIGURE 51 LONGITUDINAL STABILITY VARIATION  
WITH DYNAMIC PRESSURE

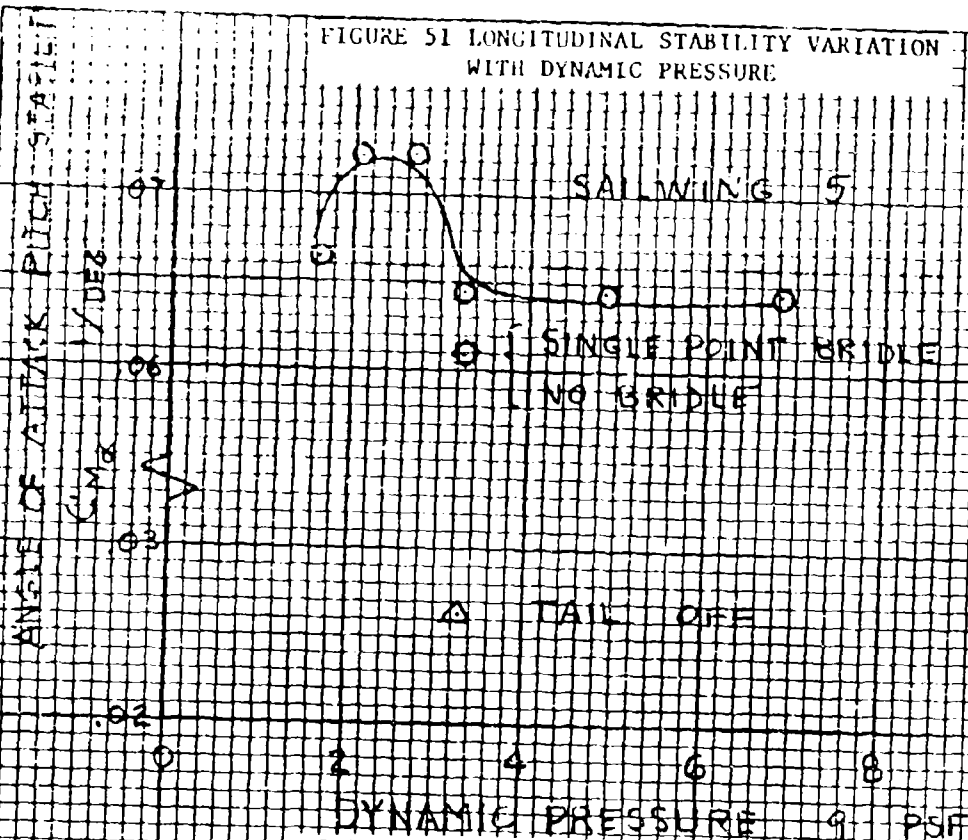


FIGURE 52 NEUTRAL POINT VARIATION  
WITH DYNAMIC PRESSURE

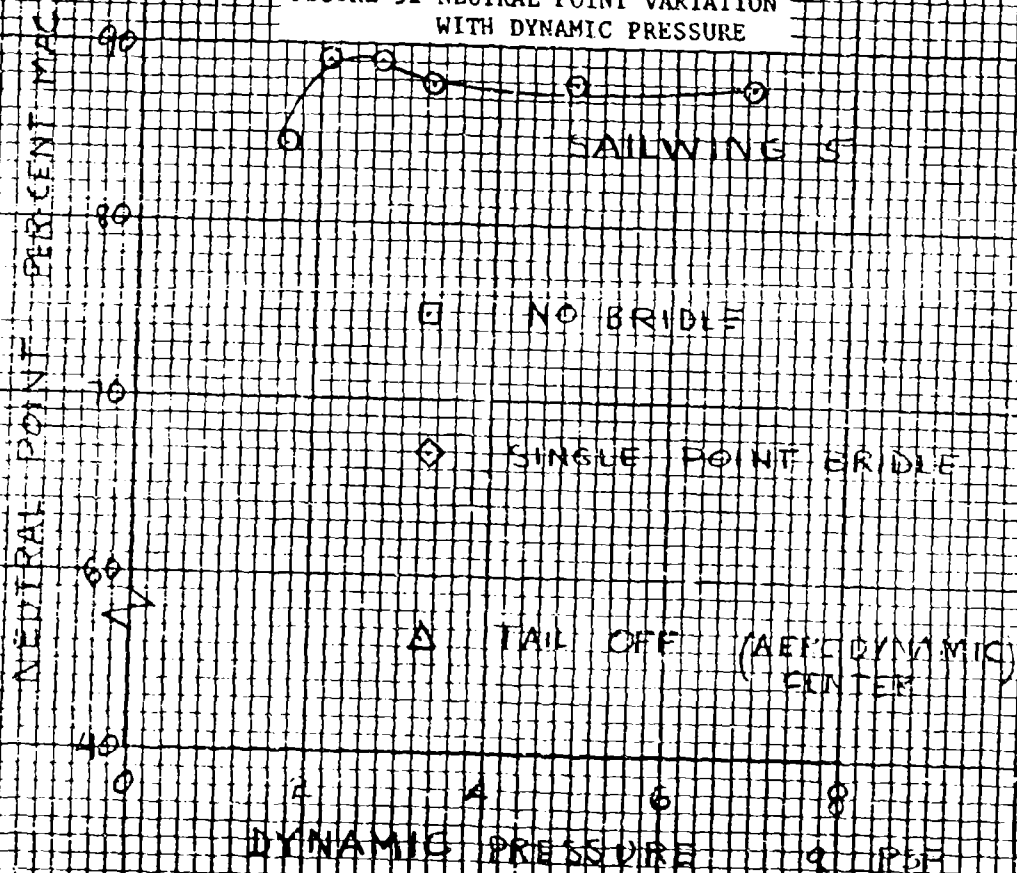
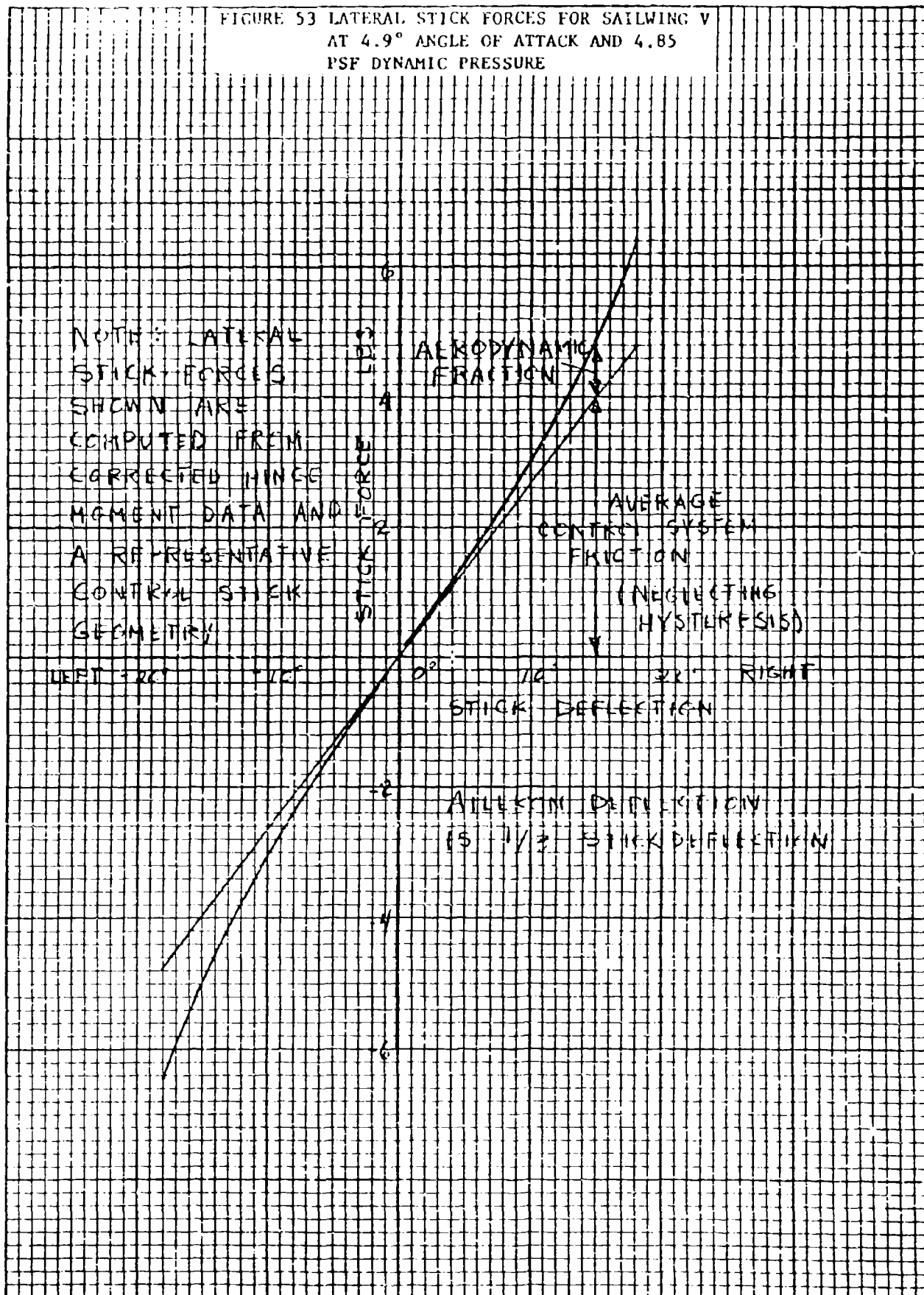


FIGURE 53 LATERAL STICK FORCES FOR SAILING V  
AT 4.9° ANGLE OF ATTACK AND 4.85  
PSF DYNAMIC PRESSURE



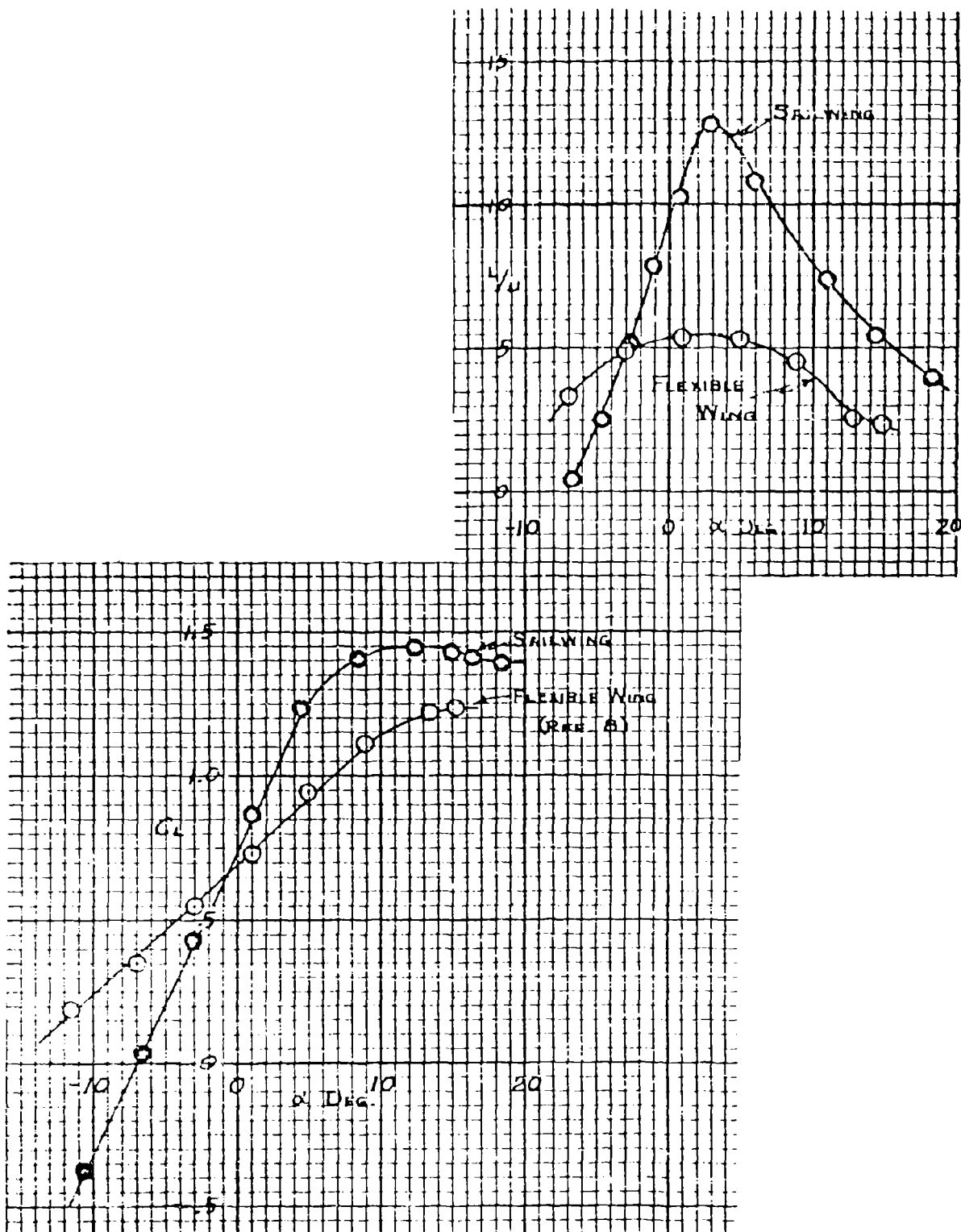


Figure 54 COMPARISON OF SAILWING AIRPLANE AND FLEXIBLE WING MANNED TEST VEHICLE

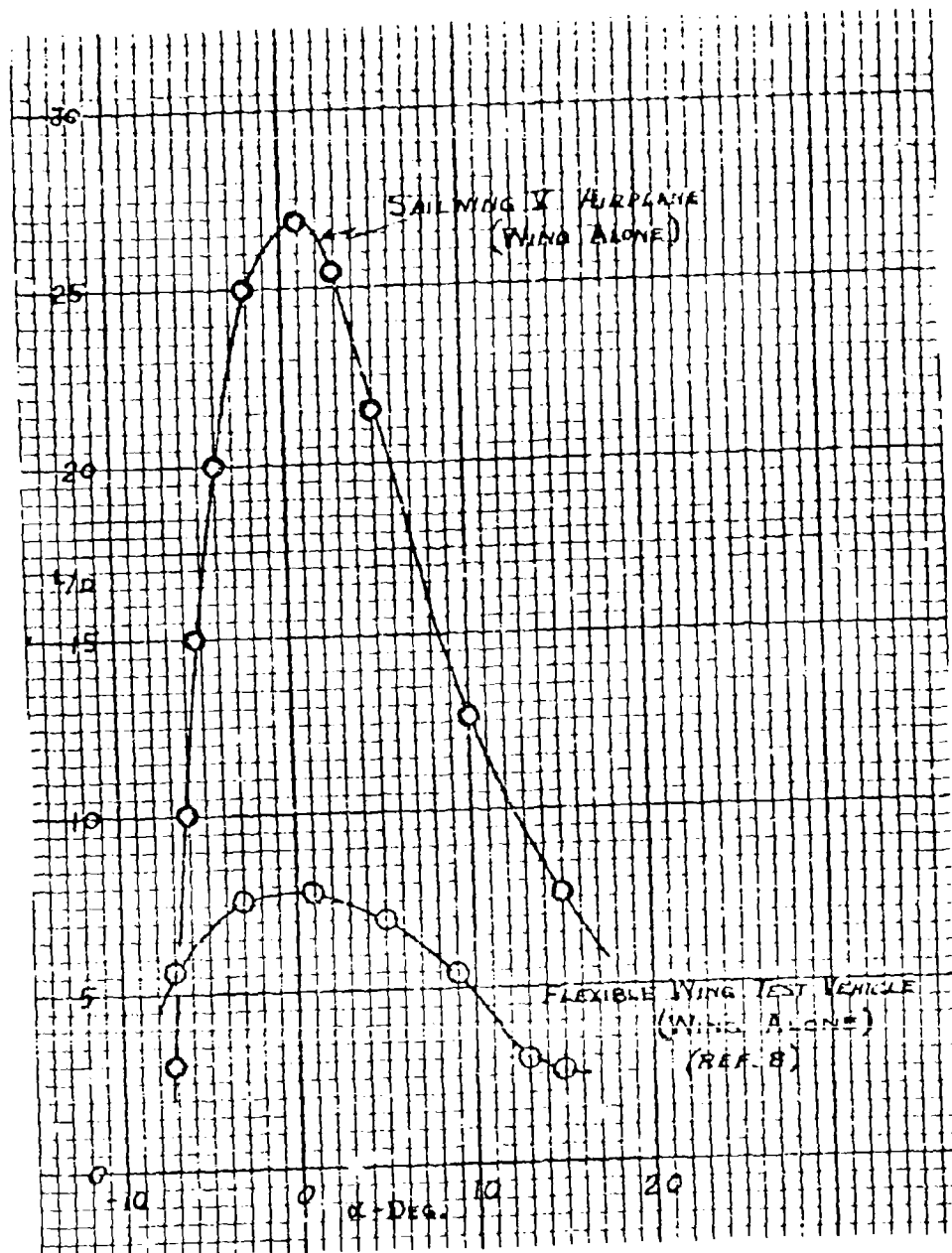


Figure 55 COMPARISON OF SAILWING V AIRPLANE (WING ALONE)  
WITH RYAN FLEX-WING TEST VEHICLE (WING ALONE)  
AND WITH

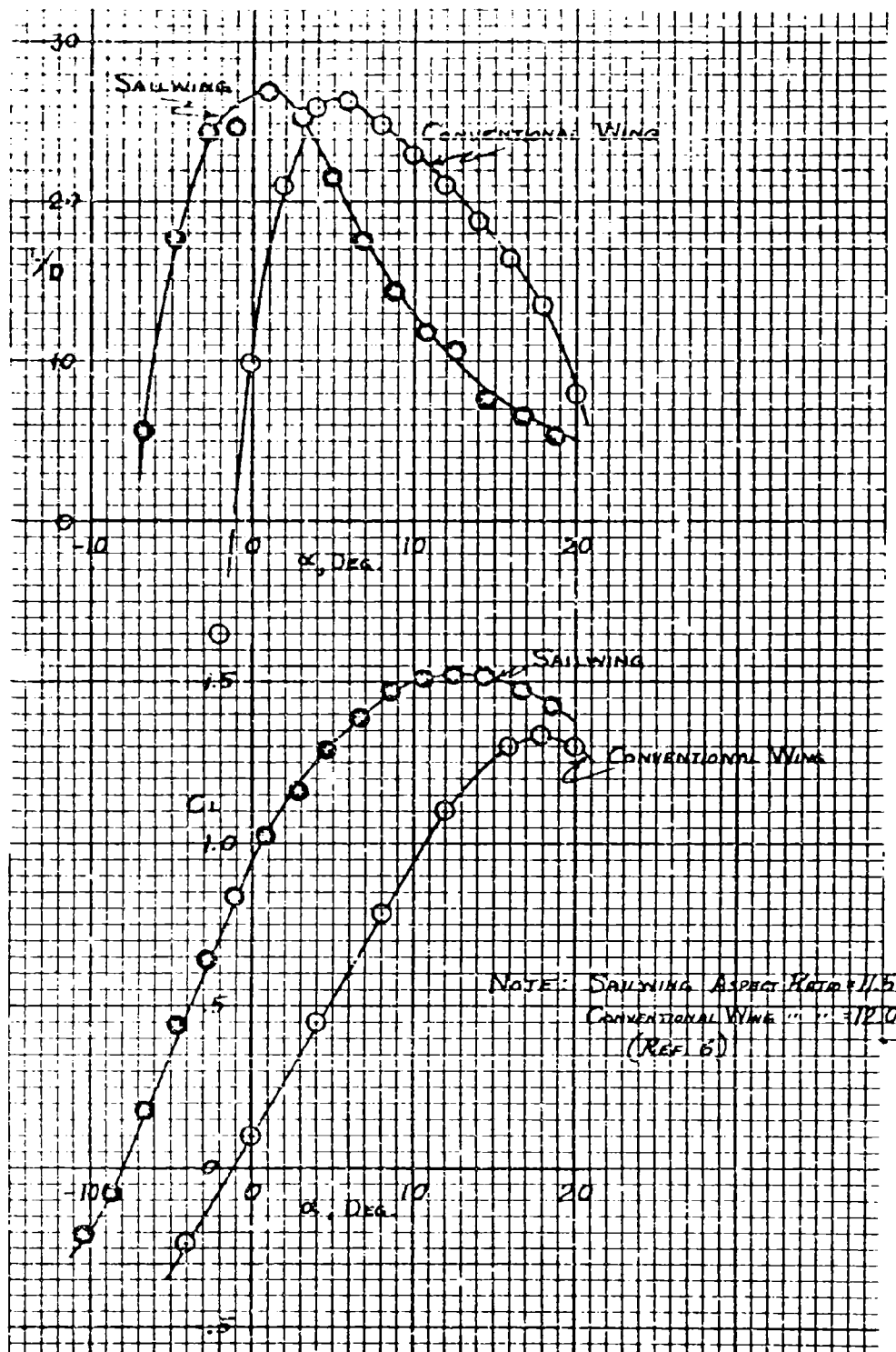


Figure 56 COMPARISON OF SAILWING V (WING-ALONE) WITH CONVENTIONAL WING OF SIMILAR GEOMETRY

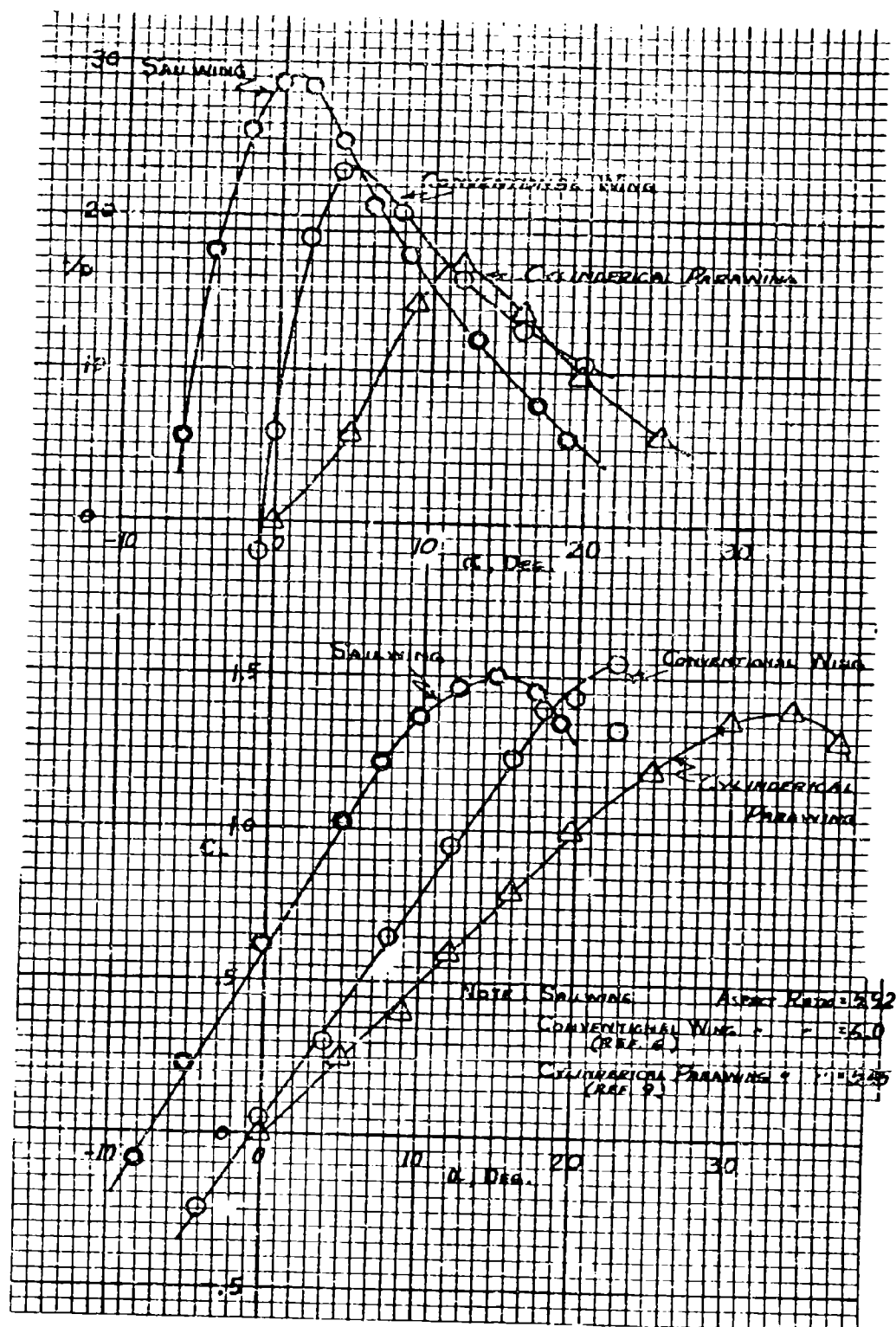


Figure 57 COMPARISON OF SAILWING VI WITH CONVENTIONAL WING OF SIMILAR GEOMETRY AND WITH CYLINDRICAL PARAWING

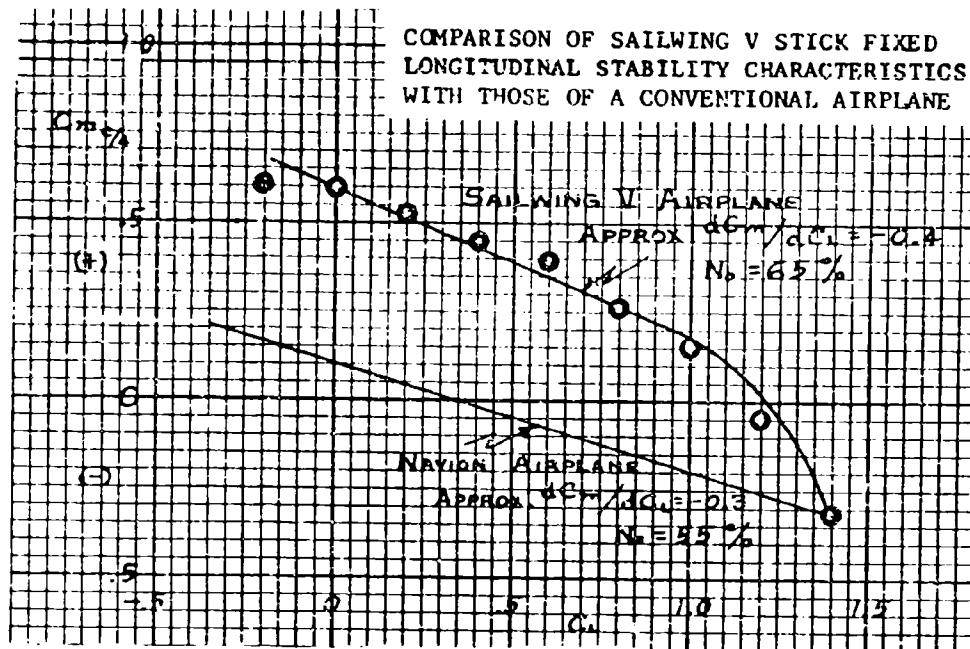


Figure 58

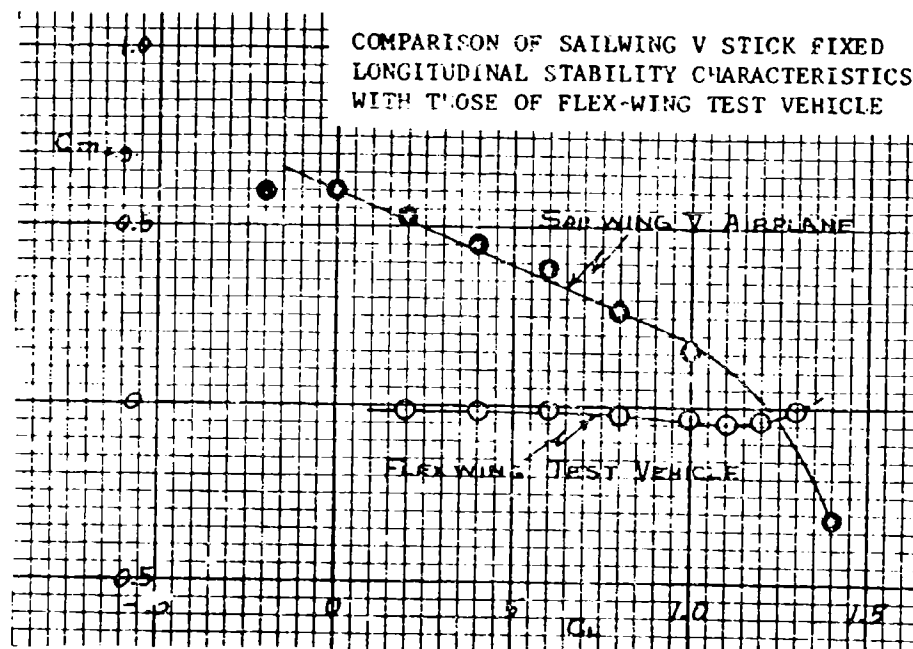


Figure 58 Concluded



*Report No. R540A-002 September 1966*

Each transmittal of this document outside  
the Department of Defense must have prior  
approval of ARPA/AGILE

**Addendum 1**

**FINAL TECHNICAL REPORT**

# **Sailwing Wind Tunnel Test Program**

**ARPA ORDER No. 879**

**Program Code No. 6G20(23)**

### INTRODUCTION

The results and conclusions of the Sailwing Wind Tunnel Test Program, ARPA Order No. 879, Program Code No. 6G20(23), are presented in the Final Technical Report, R540A-002, dated September 1966.

This document, which is Addendum No. 1 to the Final Technical Report, defines the follow-on program recommended by the Fairchild Hiller Corporation to advance the existing state of the art in Sailwing technology.

### RECOMMENDED FOLLOW-ON PROGRAM

In attempting to determine the most important areas for the expenditure of effort to further improve and refine the state of the art of Sailwing technology, it is first necessary to speculate on the types of application that will be made of the device.

For example: if it is desired to apply such a wing to a low speed drone, no future research and only minimal development need be done. It appears, in other words, to be immediately applicable.

If the wing is to be employed on a piloted (and particularly a passenger carrying) aircraft, then it is necessary to first gather a significant amount of flight test information. This would be more in the nature of a developmental program. While Princeton University/Fairchild Hiller research Sailwing aircraft have made more than two-hundred manned flights, these were practically all of a runway-skimming nature and only very gentle maneuvers were possible due to the proximity of the ground. One of the fundamental interests that prompted the full scale wind tunnel study was the possible application of the Sailwing to a simple, low-cost passenger/cargo type aircraft. For such an application it is highly desirable to

accumulate significant flight test time with the Sailwing mounted on a suitable fuselage - either one adapted from an existing airplane or one designed particularly for the purpose. These tests should include the examination of the Sailwing in maneuvers such as spins and spin recovery, high angle side and forward slips, and the general behavior of the wing in gusty air. Tests to determine the behavior of the wing if rigging tension is inadvertently lost (as occurred in one instance during the wind tunnel tests) should also be conducted. It appears that the Sailwing may be only this one step away from such an application, but this step is vital to a rational approach to a production aircraft.

For more sophisticated and unique applications such as for booster recovery systems and the variable geometry manned reentry vehicle, considerably more research as well as development is necessary. To name only the obvious gaps in existing technology, areas requiring research are: examination of the Sailwing behavior under values of dynamic pressure much higher than have so far been experienced, materials research, in-flight deployment techniques, configuration studies aimed at eliminating all external rigging, methods of longitudinal control for tailless configurations and additional lateral control studies.

A future purely research effort, one that is most promising insofar as performance and control improvement is concerned, is the study of ram-air inflation of the Sailwing. This would, in effect, provide a high degree of camber control and should improve L/D max in addition to providing the designer with a wide selection of lift curve slopes and maximum lift coefficients. A very important secondary result would be the asymmetric control of camber by this means which should yield a highly effective method of lateral control. Exploratory work to date has indicated that such a system is within relatively easy reach. The NASA wind tunnel tests, on the occasion of the inadvertent loss in rigging tension of Sailwing VI, also resulted in data promising to this concept.

In summary, based upon a deep conviction originating from flight research results and nurtured by the recent wind tunnel test findings, it is felt the Sailwing will become a vital part of future aeronautical art. Its exploitation and introduction into the work-a-day world should be as rapid as possible but consistent with logical step-by-step processes aimed at the most reasonable applications first. As the art continues to progress, the more sophisticated applications will probably occur in the manner mentioned above since basic aeronautical requirements to some extent, seem to be invariant with time.

It is, therefore, suggested that the two most important next objectives of the Sailwing Program should be:

1. The professional adaptation of a Sailwing to an existing professionally constructed airframe; the resultant product to be a truly flight test Sailwing Vehicle. This craft should be extensively tested and developed by the contractor, to be followed by a complete military flight test program suitable to the desired nature of the vehicle.
2. The continuation of basic research examining the performance and control gains associated with the use of controlled ram-air inflation of the Sailwing.

The pursuit of the first of these two objectives is considered to be vital to the future of Sailwings. The second objective should also be pursued since the substantial improvements in performance and control that could result could only benefit the concept and could occur in a relatively short-time period.



DEFENSE ADVANCED RESEARCH PROJECTS AGENCY  
3701 NORTH FAIRFAX DRIVE  
ARLINGTON, VA 22203-1714

November 20, 2001

Ms. Kelly Akers  
Defense Technical Information Center  
8725 John J. Kingman Road  
Suite 0944  
Ft. Belvoir, VA 22060-6218

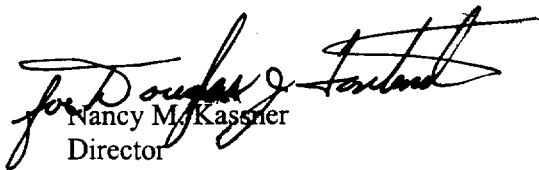
Dear Ms. Akers:

This is to advise you that the following documents have been reviewed and/or declassified and released under the Freedom of Information Act.

- Document Number: AD 803668  
Unclassified Title: Sailwing Wind Tunnel Test Program  
Report Date: September 30, 1966
- Document Number: AD 461202  
Unclassified Title: XV-8A Flexible Wing Aerial Utility Vehicle  
Report Date: February 1, 1965
- Document Number: AD 460405  
Unclassified Title: XV-8A Flexible Wing Aerial Utility Vehicle  
Report Date: February 1, 1965
- Document Number: AD 431128  
Unclassified Title: Operational Demonstration and Evaluation of the Flexible Wing Precision Drop Glider in Thailand  
Report Date: March-July 1963
- Document Number: AD 594 137L  
Unclassified Title: Communist China and Clandestine Nuclear Weapons-Input Substudies A-J, SRI Report  
Report Date: October 1970
- Document Number: AD B 176711  
Unclassified Title: Overlay and Grating Line Shape Metrology Using Optical Scatterometry  
Report Date: August 31, 1993

If you have any questions, please contact Mr. Fred Koether, our Declassification Specialist, at (703) 696-0176.

Sincerely,

  
Nancy M. Kassner  
Director

Security and Intelligence Directorate

TELCON, 4 DEC 2001;  
MR. KOETHER STATED  
THAT ABOVE DOCUMENTS  
ARE APPROVED FOR  
PUBLIC RELEASE  
J. J. Nowinski